FACULDADE DE ENGENHARIA DA UNIVERSIDADE DO PORTO

Extraction of Information Theory-Based Indices from Fetal-Maternal Heart Rate Simultaneous Signals

Ana Filipa Soeiro Gomes

Mestrado em Engenharia Biomédica

Supervisor: Dra. Luísa Castro

Second Supervisor: Dra. Teresa Henriques

July 19, 2023

Extraction of Information Theory-Based Indices from Fetal-Maternal Heart Rate Simultaneous Signals

Ana Filipa Soeiro Gomes

Mestrado em Engenharia Biomédica

Approved in oral examination by the committee:

Chair: Prof. João Tavares
External Examiner: Dra. Susana Brás
Supervisor: Dra. Luísa Castro

July 19, 2023

Abstract

Despite fetal acidemia having a low incidence in developed countries (lower than 0.6%), its quick diagnosis is essential to prevent irreversible neurological damage, morbidity, or even death. Before and during birth, the standard procedure for its diagnosis resorts to cardiotocography to assess the fetal heart rate (FHR) and uterine contractions. However, this method has limitations regarding its validity, reproducibility, and interpretation agreement.

The simultaneous analysis of the FHR and the maternal heart rate (MHR) has already been able to overcome one of the main problems described in the literature: the temporary capture of the MHR as that of the fetus. Linear and nonlinear methods have been studied to improve the analysis of FHR and MHR, having achieved promising results. Furthermore, previous research has sustained the possibility of fetal acidemia prediction being improved by nonlinear indices.

The main goal of this work is to estimate quantities related to the causal statistical structure of coupled FHR–MHR dynamic processes and evaluate their discriminant capacity for the diagnosis of fetal acidemia. In order to achieve it, several entropy-based measures were implemented, resorting to EntropyHub and ITS Toolkit, in a real database with the simultaneous MHR–FHR signals from the last two hours before birth to quantify their coupling. The MHR signal was acquired by electrocardiography (ECG) and the FHR by ultrasound, and they were both already pre-processed. The database records were divided into two groups: non-acidemic and acidemic fetuses, defining a threshold of 7.15 for the umbilical artery blood pH.

A correlation analysis supported the reliability of the entropy indices computed by verifying the expected relationships between them according to their theoretical formulation. Some new interesting associations were found but need further exploration to be validated. Sample Entropy and Transfer Entropy were found to be able to discriminate between non-acidemic and acidemic fetuses (p-value < 0.05) in the penultimate 10 minutes before birth by resorting to the Mann-Whitney test, supporting the capacity of information theory-based indices in improving fetal acidemia detection. Finally, the discriminant capacity of the indices for fetal acidemia considering the influence of time was assessed with Generalised Linear Mixed Models. However, no statistically significant results were found (p-value > 0.05).

Despite the low sample size (especially the low number of acidemic fetuses), evidence of both associations between FHR and MHR and the capacity of entropy indices to distinguish acidemic fetuses were found. Future studies with larger sample sizes would be needed to validate these findings and possibly recommend the MHR collection in clinical practice, which is done in a simple and non-invasive way, to improve fetal monitoring.

Keywords: fetal heart rate, maternal heart rate, fetal acidemia, entropy, simultaneous monitoring

Resumo

Apesar de a acidemia fetal apresentar baixa incidência em países desenvolvidos (inferior a 0,6%), o seu diagnóstico rápido é essencial para evitar danos neurológicos irreversíveis, morbidade ou morte. O procedimento padrão para o diagnóstico, antes e durante o parto, recorre à cardiotocografia para avaliar a frequência cardíaca fetal (FCF) e contrações uterinas. No entanto, este método apresenta limitações quanto à sua validade, reprodutibilidade e concordância de interpretação.

A análise simultânea da FCF e da frequência cardíaca materna (FCM) já conseguiu superar um dos principais problemas descritos na literatura: a captura temporária da FCM como a do feto. Métodos lineares e não lineares têm sido estudados com o intuito de melhorar a análise da FCF e FCM tendo alcançando resultados promissores. Além disso, pesquisas anteriores têm sustentado a possibilidade de a previsão da acidemia fetal ser melhorada por índices não lineares.

O principal objetivo deste trabalho é estimar quantidades relacionadas com a estrutura estatística causal do processo dinâmico simultâneo FCF–FCM e avaliar a sua capacidade discriminante para o diagnóstico da acidemia fetal. Para tal, foram implementadas várias medidas baseadas em entropia, recorrendo ao *EntropyHub* e *ITS Toolkit*, numa base de dados real com os sinais FCM-FFC simultâneos das últimas duas horas antes do nascimento, para quantificar o seu vínculo. O sinal de FCM foi adquirido por eletrocardiografia (ECG) e o de FCF por ultrassom, e ambos já estavam pré-processados. Os registos da base de dados foram divididos em dois grupos: fetos não acidémicos e fetos acidémicos, a partir da definição de um limiar de 7,15 para o pH sanguíneo da artéria umbilical.

Uma análise de correlação apoiou a confiabilidade dos índices de entropia calculados, verificando as relações esperadas entre eles de acordo com sua formulação teórica. Algumas novas associações interessantes foram encontradas, mas precisam de ser exploradas para serem validadas. A *Sample Entropy* e a *Transfer Entropy* mostraram-se capazes de discriminar entre fetos não acidémicos e acidémicos (valor de prova $< 0{,}05$) nos penúltimos 10 minutos antes do nascimento por meio do teste de *Mann-Whitney*, suportando a capacidade dos índices baseados na teoria da informação para melhorar a deteção da acidemia fetal. Finalmente, a capacidade discriminante dos índices de acidemia fetal considerando a influência do tempo foi avaliada com *Generalised Linear Mixed Models*. No entanto, não foram encontrados resultados estatisticamente significativos (valor de prova $> 0{,}05$).

Apesar do pequeno tamanho da amostra (especialmente o baixo número de fetos acidémicos), foram encontradas evidências de associações entre FCF e FCM e da capacidade dos índices de entropia de distinguir fetos acidémicos. Estudos futuros com amostras maiores seriam necessários para validar as conclusões e possivelmente recomendar a aquisição da FCM na prática clínica, que é feita de forma simples e não invasiva, para melhorar a monitorização fetal.

Palavras-chave: frequência cardíaca fetal, frequência cardíaca materna, acidemia fetal, entropia, monitorização simultânea

Acknowledgements

First, I would like to thank my supervisors, Prof. Luísa and Teresa, for having me on this thesis. Their help and guidance throughout this work were essential to tackle the goals we set to achieve.

To my family, particularly my parents and brother, who have always supported me and never let me demoralise in the most critical phases of my academic journey. None of it would be possible without them. A special thanks to my uncle, who was always available to help me whenever needed, and to my grandparents for their love and care.

To Rúben, for his unwavering encouragement, understanding and belief in me that kept me motivated and focused throughout this challenging academic endeavour and always encourages me to pursue new and ambitious goals.

Lastly, to my friends, for their unique friendship and motivation. Without them, this journey would not have been as easy or fun.

Filipa Gomes

"The important thing is not to stop questioning.
Curiosity has its own reason for existing."

Albert Einstein

Contents

List of Figures

List of Tables

Abbreviations

AIC	Akaike Information Criterion
ApEn	Approximate Entropy
AttnEn	Attention Entropy
BIC	Bayesian Information Criterion
BubbEn	Bubble Entropy
(c)CondEn	(corrected) Conditional Entropy
Ci	Complexity index
CondPermEn	Conditional Permutation Entropy
CondRenPermEn	Conditional Rényi Permutation Entropy
CTG	Cardiotocography
DispEn	Dispersion Entropy
ECG	Electrocardiography
EEG	Electroencephalogram
EFM	Electronic Fetal Monitoring
FGR	Fetal Growth Restriction
FHR	Fetal Heart Rate
FMCG	Fetal Magnetocardiography
(F)PPG	(Fetal) Photoplethysmography
FuzzEn	Fuzzy Entropy
GLMM	Generalised Linear Mixed Model
HRV	Heart Rate Variability
IS	Information Storage
IT	Information Transfer
MHR	Maternal Heart Rate
MI	Mutual Information
MSE	Multiscale Entropy
PermEn	Permutation Entropy
RankEn	Rank Entropy
RenPermEn	Rényi Permutation Entropy
RV	Respiration Variability
SampEn	Sample Entropy
SE	Self-Entropy
ShEn	Shannon Entropy
TE	Transfer Entropy
UAB	Umbilical Artery Blood
XApEn	Cross-Approximate Entropy
XCondEn	Cross-Cond Entropy
XFuzzEn	Cross-Fuzzy Entropy
XPermEn	Cross-Permutation Entropy
XSampEn	Cross-Sample Entropy

Chapter 1

Introduction

1.1 Motivation

Although fetal acidemia has a low incidence in developed countries (lower than 0.6%), cases that last more than a few hours are usually related to irreversible neurological damage, morbidity, or death [105], making the early diagnosis essential. Intrapartum fetal monitoring resorting to cardiotocography (CTG) assesses the fetal heart rate (FHR) – usually with a Doppler ultrasound – and uterine contractions, and is the standard procedure for its diagnosis before and during birth. However, it has limitations in its validity, reproducibility, and interpretation agreement [9, 28].

Regarding the FHR signal acquisition, one of the main problems is the temporary capture of the maternal heart rate (MHR) as that of the fetus, which has been reported to happen in 90% of the cases where external monitoring is used leading to miss diagnoses of fetal acidemia and fetal death [63, 121]. Simultaneous analysis of the MHR and FHR has been proposed as a method to eliminate the MHR–FHR ambiguities and showed an improvement in fetal acidemia detection, especially in the last hour of labour [63]. Nevertheless, only some studies have assessed the relationship between MHR and FHR during labour, and MHR tracings analysis also suffers from reliability problems due to its complexity [18].

Thus, there is an obvious necessity to explore the relationship between FHR and MHR, using algorithms able to overcome the subjectivity of their analysis interpretation.

1.2 Context

Linear and nonlinear methods have been studied to improve the MHR and FHR analysis, namely to overcome the subjectivity of common visual analysis [65, 79, 80, 81, 98, 99]. These methods have been mainly applied to FHR analysis achieving promising results in distinguishing different thresholds of pH values [28, 65].

Moreover, research aiming to assess the relationship between MHR and FHR during labour and its capacity to help in the prediction of newborn acidemia has associated non-acidemic fetuses with a decrease in the MHR–FHR correlations, whereas acidemic fetuses were associated with an

increase in these correlations [120]. Suggesting that in fetal acidemia situations, the fetus loses its autonomy and there is an increase in the maternal–fetal attachment, which is usually related to stressful situations [5]. These findings indicate that it is possible to improve the capacity to predict fetal acidemia using combined MHR and FHR analysis.

Entropy-based methods have been successfully applied in heart rate studies. Cross entropy and information dynamic measures have been getting more attention in the study of bivariate cardiac systems, for example, to assess the synchronisation between electrocardiographic R–R intervals and pulse–pulse intervals [89, 151, 163]. Recent papers have started to use them to quantify the MHR–FHR coupling [7, 60, 99], e.g., in relation to fetal gender or gestational week.

MHR collection is not usual in clinical practice, hence, if the benefit of MHR analysis in detecting fetal pathologies is confirmed, this study may be one more in the sense of recommending the collection of this signal, which is done in a simple and non-invasive way, bringing performance improvements to fetal monitoring.

1.3 Objectives

The main goal of this dissertation is to estimate quantities related to the causal statistical structure of coupled FHR–MHR dynamic processes and evaluate their discriminant capacity for the diagnosis of fetal acidemia. This aim will be pursued by analysing several entropy-based measures chosen based on their current applications in heart rate studies. These will then be implemented in a dataset containing the simultaneous FHR and MHR real signals from the last two hours before birth to quantify their coupling. The results will allow a correlation analysis between the different measures. Finally, the computed indices ability to discriminate between acidotic and normal fetuses will be assessed.

This work is intended to not only explore the FHR–MHR relationship but also to aid clinicians in interpreting these coupled signals by providing a comprehensive analysis of the capacity of different entropy-based algorithms to extract information from these signals.

1.4 Outline

In addition to the introduction, this dissertation preparation contains five more chapters describing relevant information for the objective of this work, the methodology followed, the main results obtained and the conclusions drawn from these. Chapter 2 focuses on fetal acidemia (causes, consequences, diagnosis, and prevalence) and intrapartum fetal monitoring. For this last topic, several FHR and FHR–MHR systems and monitors are tackled. Chapter 3 explores entropy-based measures developed for univariate and bivariate systems and reviews their current applications on heart rate signals. Chapter 4 describes the implementation of the methods and the statistical analysis that will be conducted. Chapter 5 contains the data exploration and the main results achieved in the course of the work, as well as their significance. Chapter 6 concludes the dissertation with the main findings, limitations and suggested future work.

Chapter 2

Maternal and fetal heart rate monitoring in the detection of fetal acidemia

This chapter focuses on fetal acidemia and its early detection with intrapartum monitoring. It starts with how the normal mother and fetus exchange of substances occurs and how the disruption of the oxygen supply to the fetus can lead to fetal acidemia. The causes, consequences, and diagnosis of this disease are also explained. Then, fetal heart rate monitors are described and their potentiality to detect fetal acidemia is discussed. Finally, the analysis is extended for simultaneous maternal and fetal heart rate signals, and some current applications of these coupled signals are presented.

2.1 Fetal oxygen and nutrient supply

Proper fetal oxygenation ensures the viability and adequate development of the fetus. It is a process that takes place in the placenta and depends on the relationship between the fetus and the mother [51]. The placenta is the largest fetal organ, with about 22 centimetres by birth, has a flat, disc-like shape and is usually located along the back uterine wall [131].

The placenta has an essential role during the fetus's development, being the mean of communication between the mother and the fetus. It is also responsible for exchanging substances and gases, namely the supply of oxygen, water with electrolytes, hormones, and other nutrients, and the removal of carbon dioxide, water, urea, hormones, and other waste products. Furthermore, it protects against bacterial infections and specific diseases and contributes to the development of immunity [71, 78].

Regarding the placenta constitution, illustrated in Figure 2.1, it is divided into two major parts: the maternal, also called decidua basalis, which comes from the endometrium, and the fetal designated villous chorion (or chorionic plate), which is developed from the outermost embryonic

membrane [131]. Embedded in the decidua are the maternal blood vessels, which are continuous with the maternal circulation, rising from the uterine wall and ending in the intervillous space, also comprised in the decidua. Around the mid-first trimester, the maternal spiral arteries are remodelled to increase the blood supply to the placenta, becoming uteroplacental vessels by the trophoblast invasion – the outer layer cells of the blastocyst [162]. The chorion comprises the chorionic villi, which contain a network of fetal capillaries that provide maximum contact area with the maternal blood located in the intervillous space [71].

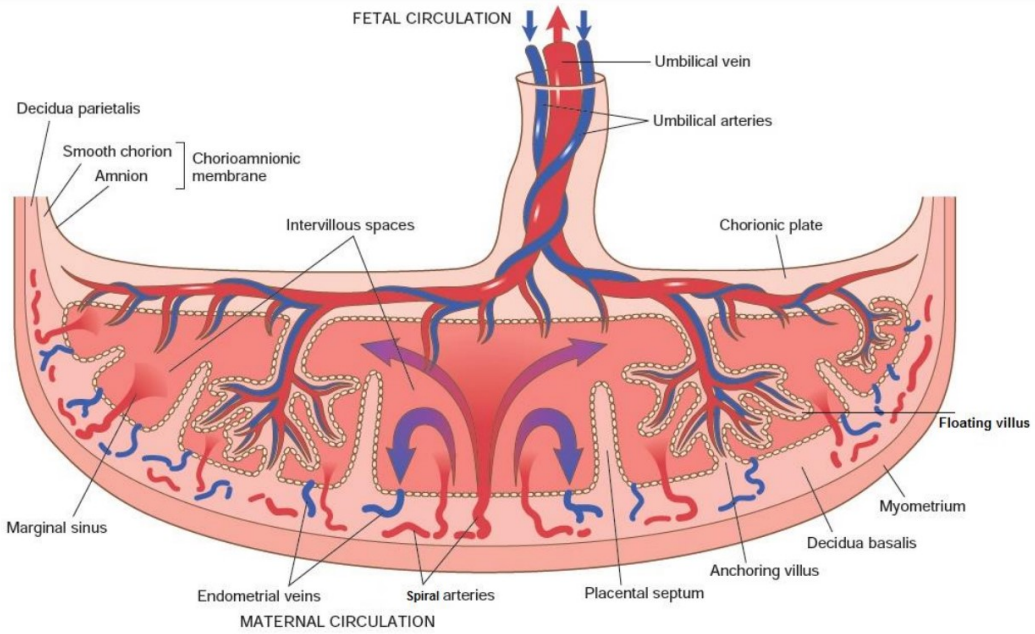

Figure 2.1: Anatomy of the placenta. The main components of the placenta are the chorionic villi from the fetal side, the decidua basalis from the maternal side and the intervillous spaces, which are filled with maternal blood coming from the spiral arteries, and contact with the chorionic villi so that the gas exchanges occur. Adapted from [147].

The exchanges between the mother and the fetus occur in the intervillous space, located between the maternal blood vessels and the fetal chorionic villi. The maternal oxygenated blood enters the intervillous space from the spiral arteries driven by the maternal blood pressure. Once there, the blood flows around the chorionic villi and the gas and substances are exchanged. The oxygen, nutrients, and hormones absorbed by the villi enter the fetal capillaries and the umbilical vein to reach the fetus. On the contrary, deoxygenated blood has the opposite trajectory reaching maternal circulation. An important aspect is that the maternal and fetal circulations are separate and they do not mix. The placental membrane divides fetal blood from maternal blood yet is thin enough to allow nutrients and waste to diffuse and transfer [51, 131, 71, 78].

Placental blood flow is completely pressure-dependent and not auto-regulated. Oxygen and carbon dioxide are usually absorbed by simple diffusion and occasionally facilitated diffusion since the placental tissues are highly permeable to these gases due to their lipophilicity. However, these exchanges are perfusion-limited. Consequently, insufficient oxygenation of the tissues might

lead to fetal growth restrictions (FGR), which can be triggered by an abnormality in any of the steps of the gas transference process [51, 131, 71, 78].

Oxygen transport to the fetal heart and brain is maximised due to the specific properties of fetal circulation, placental characteristics, and maternal adaptations. In the maternal part, uterine blood flow is essential for the placental transfer of oxygen and is estimated to increase from around 20–50 ml/min at the beginning of fetal development to 450–800 ml/min at term [102]. In the placenta, the chorionic villi are composed of five types of villi that proliferate, with a large portion of the exchange surface, in order to maximise contact with maternal blood. The placental membrane has only about 3.7 µm, which also improves the gases and substances transference between the mother and fetus [25]. As the fetus lives in a low-oxygen environment, oxygen exchange throughout the placenta is optimal. The umbilical blood flow and the umbilical venous blood oxygen content determine the rate of fetal oxygen extraction. When they are low, the oxygen extraction is increased [25].

2.2 Fetal Acidemia

The fetus relies on the mother for the exchange of oxygen and carbon dioxide, as well as the availability of glucose via the placenta to sustain aerobic metabolism and proper energy synthesis. In some situations, adequate maternal blood gas concentrations, uterine blood supply, placental transfer, and fetal gas transport are not guaranteed. In that case, the normal functioning of the above-mentioned processes can be disrupted, compromising the oxygen supply for the fetus and, consequently, leading to hypoxia and acidosis. Hypoxia is referent to a high hydrogen ion concentration in the fetal arterial blood caused by a deprivation of oxygen for a considerable amount of time, typically during birth [20]. This condition can lead to a decrease in the oxygen levels in the tissues, which increases the concentration of hydrogen ions. This process is called metabolic acidosis and the state of high hydrogen ion content, defined by a pH lower than 7.15 [59, 109] on the umbilical artery blood (UAB), is called acidemia [20]. Severe or acute (lasting hours), but mainly chronic acidemia (days or weeks), are related to long-term sequelae, especially at the neurological level, and considerable morbidity and death [20, 28].

2.2.1 Causes and risk factors associated

The causes of fetal hypoxia and acidemia are classified as maternal, placental, or fetal, according to where the oxygen flow is being disrupted. The main maternal causes of fetal acidemia are related to hypotension – abrupt drop in blood pressure – or hypovolemia – decrease in the extracellular fluid, diminishing the maternal blood supply and consequently the oxygen delivery to the uterus. In particular, the maternal causes for acute fetal hypoxia and acidosis include haemorrhage, i.e. blood loss; vasovagal attacks, characterized by sympathetic system overreaction to certain triggers leading to a hypotension state accompanied by a sudden loss of consciousness [110]; epidural anaesthesia since its major adverse effect is uteroplacental hypoperfusion, an incapacity to properly irrigate the intervillous space of the placenta where the maternal-fetal exchanges occur [3];

and increased uterine activity, which can interrupt the uterine blood flow by a pressure rise and if prolonged, as in hypertonus, may cause hypoxia and so acidosis [14]. For the maternal causes of chronic fetal acidosis, it is possible to highlight severe respiratory or cardiac diseases since they are associated with reduced blood oxygenation, and connective tissue diseases, e.g. systemic lupus erythematosus, which implies a reduced blood flow to the placenta [20, 107].

When the oxygen flow is affected in the placenta, it is likely to develop acute hypoxia in case of abruption, which refers to the detachment of the uterine spiral arteries from the placenta affecting the placental oxygen transfer rate. On the other side, impaired uteroplacental blood flow resulting from pregnancies with FGR or pre-eclampsia can be associated with chronic fetal hypoxia [20, 145]. Pre-eclampsia is a common disease associated with FGR and is triggered by a poor trophoblast invasion and, consequently, with inadequate spiral arteries remodelling and placental hypoperfusion in the intervillous spaces [21, 43]. To point out that this reduction of the uteroplacental blood flow must be of at least 55% for the fetus to develop hypoxia [25].

The oxygen flow can also be interrupted by a compression in the umbilical cord, which can happen especially during labour and delivery, but it is also possible to occur before labour due to reduced liquor or a knot in the cord. Similar to the uteroplacental blood flow reduction, umbilical blood flow has to be reduced by at least 50% to influence fetal oxygen uptake. Therefore, in the case of an occlusion of the umbilical cord for 3 to 4 min, the fetal oxygen extraction can be increased and accompany that reduction, not leading to hypoxia [25]. Moreover, several conditions of the fetus can cause chronic acidemia, such as anaemia from rhesus disease, which occurs when the maternal blood is RhD negative and thus develops antibodies against RhD antigen that cross the placenta and destroy the fetal erythrocytes, leading to anaemia [1]; parvovirus infection since it can lead to anaemia [58]; α-thalassaemia, which is characterized by the fetus not being able to produce normal fetal haemoglobin, provoking anaemia [42]; feto-maternal haemorrhage, referent to the loss of fetal blood to the maternal circulation, resulting in anaemia [166]. Fetal anaemia implies a decrease in the oxygen-carrying capacity of the fetal blood. Arterio-venous shunting in fetal tumours, serious cardiac structural abnormalities, or arrhythmias can also lead to acidemia due to the reduced fetoplacental blood flow [20].

In addition, researchers have associated several factors with an increased risk for fetal acidosis. Labour with breech delivery was associated with a lower mean cord arterial pH that might be explained by complications during labour and delivery that could be avoided in a cesarian, such as difficult delivery of the fetal head and cord prolapse or compression [69, 70]. Administration of oxytocin triggers uterine contractions, which in excess may lead to an abnormal blood supply of the placenta [70, 161]. Meperidine administration can also be connected with fetal acidemia due to maternal hypoventilation induced by the opioid [70]. The existence of pregestational diabetes can alter fetal metabolism, increasing umbilical glucose concentrations and reducing oxygen saturation and oxygen content in the umbilical vein [77, 152]. High-altitude environments are characterised by reduced oxygen availability and can be the cause of the inability of the fetus to obtain sufficient oxygen for its development, leading to fetal hypoxia and FGR [165]. In a study by Kapaya [77], women with urinary tract infections at any stage showed a significantly increased

occurrence of neonatal acidaemia compared to the control group (18.5% versus 6.6%).

2.2.2 Consequences

The consequences that accrue from both hypoxia and acidosis are categorised according to their severity and duration and the previous condition of the fetus and are, therefore, classified as acute or chronic, in case it lasts just a few hours or days, respectively [20]. When this decrease of oxygen happens in the neonatal phase for a short time, for example, during delivery, the human body is already capable of sustaining its functioning. Thus, there is just a slight rise in the mortality rate and the possibility of developing neurological sequelae [20, 41].

On the other hand, if the oxygen supply shortage is before birth, the probability of being related to long-term morbidity is increased. In [91], it was demonstrated that intrapartum fetal asphyxia with severe acidosis at delivery could implicate the development of complications in the nervous, cardiovascular or respiratory systems or in the kidneys. The most common outcome of severe hypoxia and acidosis is the presence of neonatal cerebral damage caused by the shortage in the brain oxygen supply, manifesting as early neonatal convulsions and implying a high risk of death or survival with cerebral palsy. The more severe, the higher the risk of long-term compromise [85]. One of the most commonly associated brain injuries is hypoxic-ischemic encephalopathy, caused by the lack of oxygen in the brain and considered a major cause of acute mortality and chronic neurologic disabilities such as cerebral palsy, mental retardation, and epilepsy [156].

2.2.3 Diagnosis and incidence

The diagnosis of hypoxia after birth is usually obtained by cardio-respiratory depression and muscle tone assessment. Its severity is quantified by resorting to the Apgar Score – a rating out of ten points with the following characteristics evaluated with 0, 1, or 2 points each: respiratory effort, reflex irritability, muscle tone, heart rate, and colour [4]. If a score lower than 7 is obtained five minutes after delivery is considered pathological and is confirmed by analysing the pH value of the UAB [16].

Before labour, a healthy fetus's arterial pH is approximately 7.35, whereas, before delivery, the pH of the UAB is around 7.25. The pH threshold values commonly used in fetal acidemia detection studies are 7.20 [56, 65], 7.15 [33], 7.10 [65], and 7.05 [171]. However, the consequences above these thresholds depend on the kind of acidosis and its severity. Respiratory acidosis, which usually occurs due to ventilation failure and carbon dioxide accumulation [111], is not directly linked to long-term neurological problems. Contrarily, metabolic acidosis is related to long-lasting hypoxia and even once hypoxia is reversed, it takes longer to repair its consequences. Thus, it is connected with irreversible organ damage [28].

It is established that the control of the FHR is impaired by brain oxygen deprivation and is, therefore, a good indicator of hypoxia. Based on this connection, electronic fetal monitoring (EFM) has been used to help detect fetal hypoxia and acidemia during and before birth [77, 138, 146, 149]. EFM is a frequent technique used to determine fetal well-being during labour

and delivery, which has essentially superseded fetal scalp pH measurements and intermittent auscultation and has helped prevent associated negative perinatal consequences. The methods used for the intrapartum monitoring of the fetus will be explored in Section 2.3.

Fetal acidemia has a very low incidence in developed countries, lower than 0.6%. Nevertheless, the cases not rapidly identified are usually related to irreversible neurological damage, morbidity, or death [105]. Thus, it is essential for obstetricians to be able to quickly identify and adjust fetal oxygen levels before permanent damages occur.

2.3 Fetal and maternal heart rate systems and monitors

Several studies [135, 141] have demonstrated the clinical benefit of monitoring FHR, emphasising the assessment of the fetal heart rate variability (HRV), which is connected to fetal heart autonomous nervous system regulation. The FHR is susceptible to being influenced by various factors and the lack of variability is a warning indication, as it can be related to fetal hypoxia and acidosis, among other pathological conditions.

The FHR baseline is between 110 and 160 beats per minute [160, 106], whereas, for the MHR, the baseline is established to be in the range of 60 to 100 bpm, and can be considered until 40 bpm for athletes. An alteration that goes out of these values for more than 10 minutes is considered tachycardia if above, and bradycardia if below. A lower resting heart rate is related to a more efficient heart function [11, 83].

2.3.1 FHR signal acquisition

FHR signals can be obtained by resorting to external or internal techniques. However, the use of a Doppler ultrasound device can be highlighted as the most used in clinical practice for being non-invasive and able to estimate the real heart rate intervals considered acceptable for analysis [26]. For intermittent measurements resourcing to this technique, the movement of cardiac structures is detected by applying the handheld Doppler probe to the maternal abdomen. This type of measurement only allows spot-check assessment of the fetal cardiac performance and is dependent on the operator. Thus, continuous measurements are required in specific situations, especially during birth. To continuously monitor the FHR resourcing to a Doppler probe, an ultrasound transducer is fixed on the maternal abdomen before and during labour. Nevertheless, external FHR monitoring methods are more susceptible to signal loss, inadvertent monitoring of the MHR and artefacts, especially in case of premature deliveries, high body-mass-index mothers, and during the final part of labour due to fetal and maternal movements. It may also fail to record fetal cardiac arrhythmias correctly [11, 68].

Consequently, in the above-mentioned situations, there is the need to resort to an invasive technique with a direct fetal scalp electrode and fetal ECG since this is the most accurate and trustworthy method for continuous FHR acquisition. However, this process can only be executed after the rupture of membranes and the start of cervical dilatation. Moreover, it is associated with a risk of infection and should be avoided in preterm fetuses [13, 64].

Additionally, there are several techniques currently being studied but not yet implemented in clinical practice. Transabdominal electrocardiography (ECG) has been showing promising results as a non-invasive technique to continuously obtain FHR more reliably than the Doppler ultrasound for the second stage of labour and in the presence of maternal movements, but it still faces difficulties in distinguishing the FHR from the MHR signal [148]. Fetal magnetocardiography (FMCG) measures faint magnetic fields from the current sources in the fetus heart, outside the maternal abdomen by super sensitive magnetometers (superconducting quantum interference device) in magnetically shielded rooms. Despite being a highly effective approach for detecting fetal arrhythmias and being employed in research settings, it is very expensive and, thus, unsuitable for clinical routine use [76, 130]. Fetal phonocardiography assesses heart-related sounds and has been proposed as a complementary tool to analyse FHR, for example, using a telemedicine system [84]. Lastly, fetal photoplethysmography (FPPG) has been proposed as a low-cost wearable FHR monitoring method with an acceptable accuracy compared to Doppler ultrasound [55, 68].

2.3.2 FHR monitoring to detect fetal acidemia

Intrapartum fetal monitoring is widely used in most developed countries as a method to help in the identification of fetal hypoxia/acidosis by detecting indicators of reduced fetal oxygenation. Particularly, the most common technique resorts to cardiotocography (CTG), which assesses simultaneous continuous monitoring of the FHR and uterine contractions, being the FHR usually obtained by a Doppler ultrasound [11, 82]. It is agreed that continuous CTG should be used in situations where there is a high risk of fetal hypoxia/acidosis and irregularities are identified during intermittent fetal auscultation. The use of continuous intrapartum CTG in low-risk women, on the other hand, is more controversial. In spite of the lack of evidence regarding its benefits, this procedure has become the standard of care in many countries and the routine use of CTG for low-risk women at the entrance to the labour ward has been associated with an increase in unnecessary obstetrical interventions, such as cesarean section and operative vaginal delivery, and no improvement in perinatal outcomes [11, 142]. Moreover, CTG has limitations regarding its validity, reproducibility, specificity, and inter and intra-observer agreement due to the complex nature of FHR traces [9, 11, 128].

Thus, research has been performed aiming to automate the detection of fetal hypoxia/acidosis by establishing a computerized system for analyzing CTGs. Linear and nonlinear methods to analyse the FHR have been proposed to improve its validity and consequently the prediction of acidemia. Promising results have been achieved in the discrimination between normal and acidemic fetuses over the minutes before delivery [65, 86, 87, 96, 97]. Moreover, nonlinear indices were studied as a mechanism to assess the loss of complexity in FHR due to fetal hypoxia, with the assumption that the loss of complexity can be an indicator of pathological situations [16, 132]. Despite the promising results that were achieved with nonlinear approaches, until this moment, only statistical tools have been implemented in clinical practice [28].

One of the main problems described in the literature [63, 121] concerning the FHR signal acquisition is the temporary capture of the MHR as that of the fetus, especially when external

monitoring is used – it has been reported in up to 90% of intrapartum recordings – or with internal monitoring in cases of fetal death. This contamination of the FHR can lead to miss diagnosis of fetal acidemia and fetal death.

2.3.3 MHR and FHR simultaneous signals

Simultaneous monitoring of the MHR and the FHR can be beneficial in certain maternal health circumstances and when differentiating between maternal and fetal heart rates is complicated [11]. It is established that maternal and fetal physiological parameters, such as blood gas exchange, are inextricably linked [40, 100]. There is also evidence that considerable MHR variations occur during the final minutes of labour in connection to the frequency of uterine contractions, which is directly associated with fetal acidemia. Thus, the analysis of both FHR and MHR can be able to provide useful information on the health state of the fetus.

Continuous simultaneous FHR and MHR monitoring is possible with some CTG monitors, allowing a comparison of both signals and easier detection of overlapping segments. The FHR signal is usually acquired by resorting to a Doppler ultrasound sensor placed in the maternal abdomen, whereas the MHR can be obtained either by ECG, where a sensor is connected to three electrodes on the maternal thorax [62], or with a pulse oximetry sensor and PPG [121]. Pulse oximetry is a technique to determine blood oxygen saturation using a clip-like device placed on a body extremity, such as a finger, that measures the light absorption of arterial blood [74].

In clinical practice, MHR recordings with ECG are often not feasible during labour because fetal monitors might not include this technique or the healthcare provider or the mother might believe it is unnecessary and disrupts the birthing experience. Alternatively, pulse oximetry can be used [62]. In some recent monitors, this technique has been incorporated in the tocodynamometer – a pressure transducer to measure uterine contractions – allowing continuous MHR monitoring without additional equipment [11]. However, the measurements collected with PPG are less accurate than those recorded with ECG, particularly when there is increased physical movement, namely during birth [92].

2.3.4 Literature review on MHR and FHR simultaneous monitoring

In a study by Pinto [121], 61 MHR and FHR simultaneously acquired records from the final hour of labour were analysed and MHR-FHR ambiguities were reduced by subtracting the MHR signal from the FHR when the absolute difference between them was less or equal to 5 beats per minute. This removal improved FHR tracing categorisation. However, broader studies are needed to corroborate these findings, and they may reduce unnecessary interventions associated with false positives for acidemia while maintaining sensitivity.

Furthermore, simultaneous analysis of maternal and fetal HRV was performed by Gonçalves [63] to assess their development throughout labour and their ability to detect newborn acidemia by measuring variables linked to autonomous nervous system function, sympatho-vagal balance and functioning of complex heart rate regulation systems. In 51 singleton-term pregnancies, MHR

and FHR were simultaneously recorded in the last two hours of labour and compared with newborn UAB pH. The results suggested that FHR changes were also present in MHR, with labour progression and fetal acidemia.

Moreover, the research by Pinto [120] aiming to assess the relationship between MHR and FHR during labour and its capacity to help in the prediction of newborn acidemia has associated non-acidemic fetuses with a decrease in the MHR–FHR correlations, whereas acidemic fetuses were associated with an increase in these correlations. The study assessed 59 simultaneous MHR and FHR recordings from the final minutes of labour that were analysed according to the FIGO guidelines [8]. The results suggested that in fetal acidemia situations, the fetus loses its autonomy and there is an increase in maternal–fetal attachment, which is usually related to stressful situations [5]. These findings indicate that it is possible to improve the capacity to predict fetal acidemia using combined MHR and FHR analysis. In the three studies [63, 120, 121] just described, MHR signals were obtained by ECG electrodes placed on the maternal chest and by pulse oximetry, whereas the FHR was obtained by a conventional ultrasound sensor placed on the maternal abdomen.

Other applications of these simultaneous signals have been pursued. Barrett [17] described a case report where an exact correlation between MHR and FHR as a response to different stimuli confirmed that the fetal scalp electrode was capturing the MHR and it was a case of fetal death. Khandoker [80] studied the alterations in MHR–FHR coupling in abnormal fetuses and found a weaker influence of FHR on MHR and a higher influence of MHR on FHR for these fetuses. In another study, the same researcher [79, 81] proved the capacity of MHR–FHR coupling strengths with fetal and maternal HRV parameters to estimate fetal development. Sancho-Rossignol [136] pointed out an association between mother exposure to domestic violence during childhood and a negative correlation between MHR and FHR in response to crying infant stimulus, while the MHR reactivity increased, the FHR reactivity reduced. Sarkar [137] developed a deep-learning approach to predict maternal and fetal stress from combined MHR and FHR ECG signals with very good accuracy and reproducibility.

Considering the applications of the simultaneous analysis of FHR and MHR presented, it is possible to verify its potential in revealing useful information relative to the health state of the fetus, being able to improve fetal monitoring performance. Thus, although MHR collection is not usual in clinical practice, it can be performed in a simple and non-invasive way, and if the benefit of MHR analysis in detecting fetal pathologies is confirmed, the collection of MHR can be recommended for clinical practice.

Chapter 3

Information theory-based indices

This chapter focuses on information theory-based methodologies and their applicability to HR studies. It starts by introducing the relevance of these pattern recognition techniques in clinics. Then, several entropy measures for univariate and bivariate systems are detailed and their current heart rate applications, emphasising FHR, are reviewed.

3.1 Entropy-based measures and clinical diagnosis

Pattern recognition techniques have been increasingly applied to biomedical data for clinical diagnostic and therapeutic support because they allow clinicians to make better-informed decisions in a timelier manner. However, in order to keep up with the evolving clinical measurement and monitoring systems, this is an area that requires continuous updates [6].

Uncertainty is an inseparable aspect of medical diagnosis problems and human life processes: a symptom is an uncertain indication of a disease as it may or may not occur with or as a result of the disease [72]. Furthermore, the dynamics of complex biological systems are commonly described as the outcome of interactions among diverse system components, each of which has some autonomy but also interacts with one another to create nontrivial collective behaviours [47]. Hence, human physiology can be modelled and characterised according to how they control the disorder caused by entropy, keeping the vital cycle equilibrium [66].

Entropy can be defined as the degree of complexity of the distribution of the samples of a signal, i.e., the rate of information production, and can be obtained by measuring how predictable a sampled signal is. A periodic variable will have a low entropy value, whereas a white noise will present a high entropy. Usually, in biomedical signals, entropy is not calculated directly over the samples of the series but over patterns of a certain length, measuring the complexity of the pattern distribution as a function of the pattern length [126, 172].

By estimating the entropy of a signal, it is possible to detect the existence of patterns. The lowest the entropy value, the fewer patterns the signal will have. Correlation between measures

quantifies their level of association. It may indicate redundancy between different entropy measurements, meaning they provide the same information about the signals if correlations are high, or indicate that there is no measure in common when correlations are close to zero.

The temporal evolution of simultaneous signals can be assessed in the context of information dynamics by decomposing its information into amounts and characterising it. The system activity can be mapped with a set of variables and then, the statistical dependence among the observed realisations of these variables can be collected in the form of multivariate time series to characterise the activity of the system [47]. The field of information dynamics is developing quickly due to the creation of useful measures for multivariate recordings and the availability of open-access tools for sharing them [124].

Information dynamics measures can also be used to analyse nonlinear correlations in the dynamical structure of a stochastic process in order to determine its degree of regularity. In bivariate systems, the predictive information can be broken down into two parts: the information that is stored within the target system and the information that is transferred to it from the other connected system. These methods can be used to analyse a single time series by comparing its present states with its past states or to study a bivariate system by comparing two different variables.

3.2 Traditional entropy methods

Entropy functions can be divided into the following categories: Base, for a single univariate time series; Cross, between two univariate synchronised time series; Multiscale, for a single univariate time series, calculated using a base entropy estimator for different time scales [53].

3.2.1 Univariate entropy methods

To evaluate univariate heart rate signals, the following base entropy methods will be analysed: Approximate Entropy, Sample Entropy, Fuzzy Entropy, Permutation Entropy, Conditional Entropy, Dispersion Entropy, Bubble Entropy and Attention Entropy. Multiscale Entropy will also be studied to compute the previously mentioned methods for different time scales.

3.2.1.1 Approximate Entropy

Pincus introduced Approximate Entropy (ApEn) [114] in 1991 as a method for determining the degree of regularity and unpredictability of oscillations in time-series data. It was motivated by the potential of nonlinear dynamic analysis to understand biological systems and was developed by adapting the Kolmogorov entropy, the rate of generation of new information, to be able to analyse relatively short and noisy clinical data. ApEn analyses the logarithmic probability of patterns close to each other to remain close in the subsequent comparison with a longer pattern. Lower values of ApEn mean more frequent patterns and a high degree of regularity. In clinical analysis, a relatively low ApEn value could be predictive of some pathology [39, 112, 132].

To compute ApEn, two input parameters must be defined: m, the length of the vectors to compare, and r, the distance threshold. Given N data points from a data signal $u(i)$, with $i = 1,...,N-m+1$, vector sequences are formed, from $x(1)$ through $x(N-m+1)$, defined by $x(i) = [u(i),...,u(i+m-1)]$. Based on the distance between the vectors $x(i)$ and $x(j)$, $d[x(i),x(j)]$, defined as the maximum difference between their scalar components, the following correlation measure is defined as

$$C_i^m(r) = \frac{\text{number of } j \leq N-m+1 \text{ such that } d[u(i),u(j)] \leq r}{N-m+1}. \tag{3.1}$$

The average of the natural logarithm of the $C_i^m(r)$ values can be obtained by

$$\Phi^m = \frac{1}{N-m+1} \sum_{i=1}^{N-m+1} ln(C_i^m(r)) \tag{3.2}$$

As N is a finite number in practice, the statistical estimation $ApEn(m,r)$ can be computed as

$$ApEn(m,r,N) = \Phi^m(r) - \Phi^{m+1}(r) \tag{3.3}$$

This method can distinguish a wide variety of systems, and for a small dimension value, being the most common $m = 2$, this estimation can be executed without the need for a vast amount of points. The threshold r is usually calculated with respect to the standard deviation σ, ranging between 0.1 to 0.25 times the standard deviations of $u(i)$ [112].

On the other hand, this algorithm counts each sequence as matching itself to avoid $ln(0)$, leading it to be a biased statistic. Consequently, ApEn is highly dependent on the record length and uniformly lower than expected for short datasets. It also lacks relative consistency since when comparing two signals by calculating their ApEn value, one is not always higher than the other independently of the conditions. Additionally, it relies on two essential parameters: the dimension m and the threshold r, and small modifications on these may lead to a drastic change in the entropy value [132].

3.2.1.2 Sample Entropy

In 2000, Richman and Moorman [132] presented Sample Entropy (SampEn), a similar method to ApEn but that tries to overcome its main disadvantages. This method eliminated self-matches in order to reduce the bias; it is simpler than the ApEn algorithm (improving by 50% the calculation time); it is independent of the record length; and presents relative consistency in cases where ApEn does not.

SampEn is defined as the negative natural logarithm of the conditional probability of two sequences that have been similar for m points to keep similar at the next point, excluding self-matches. It differs from ApEn in the fact that the probability value is obtained from the logarithm of conditional probability and not from the ratio of the logarithmic sums. A lower SampEn value also indicates the existence of more frequent patterns in a series.

For the computation of SampEn the establishment of values for m and r is also required. Considering $B_i^m(r)$ as the probability of two vectors to have m similar points, it can be defined as $(N-m-1)^{-1}$ times the number of vectors $x_m(j)$ similar to $x_m(i)$ within r, where $j = 1,...,N-m$ and $j \neq i$ to exclude self-matches. Similarly, considering $A_i^m(r)$ as the probability of two vectors to have $m+1$ similar points, it can be defined as $(N-m-1)^{-1}$ times the number of vectors $x_{m+1}(j)$ similar to $x_{m+1}(i)$ within r, where $j = 1,...,N-m$ and $j \neq i$. The averages of $B_i^m(r)$ and $A_i^m(r)$ are given by

$$B^m(r) = \frac{1}{N-m} \sum_{i=1}^{N-m} B_i^m(r) \tag{3.4}$$

$$A^m(r) = \frac{1}{N-m} \sum_{i=1}^{N-m} A_i^m(r) \tag{3.5}$$

Since the number of matches is always less than or equal to the number of possible vectors, the ratio $A^m(r)/B^m(r)$ is a conditional probability less than unity. Finally, being B the total number of template matches of length m and A the total number of template matches of length $m+1$, SampEn(m,r,N) can be calculated by

$$SampEn(m,r,N) = -\ln(A/B) \tag{3.6}$$

Similarly to ApEn, SampEn has the disadvantage of depending on the values chosen for m and r and slight modifications to these may lead to a drastic change in the entropy, as referred in [39, 61, 132].

3.2.1.3 Fuzzy Entropy

Both ApEn and SampEn use the Heaviside function to determine how similar two vectors are, which results in a typical two-state classifier that can be challenging to use in real-world situations where borders might be hazy. Thus, in 1965, Zadeh [169] defined fuzzy sets as a way to characterise such input-output interactions in an environment of imprecision. In fuzzy sets, each point is associated with a membership degree according to how much a pattern belongs to a class [30].

Fuzzy Entropy (FuzzEn), introduced by Chen [30] in 2007, measures the similarity of two vectors based on their shapes by using the fuzzy set concept and an exponential function as the fuzzy function to ensure that the similarity is continuous and the self-similarity is the maximum (convex) [30]. To compute FuzzEn, it is necessary to define the embedding dimension, m, and the distance threshold, r. For a time series X_i let $u_m(i)$ and $u_m(j)$ be vectors of length m. Considering d_{ij}^{mn} the infinity norm distance between vectors (where n is the exponential parameter) and an

exponential membership function, the average of the similarity degree among vectors X_i^m is

$$\Phi^m = \sum_{i=1}^{N-m} \left(\frac{1}{N-m-1} \sum_{j=1, j\neq i}^{N-m} exp(-d_{ij}^{mn}/r) \right) \tag{3.7}$$

Fuzzy Entropy is then given by [27]

$$FuzzEn(X,N,m,r,n) = ln[\Phi^m(n,r)] - ln[\Phi^{m+1}(n,r)] \tag{3.8}$$

FuzzEn overcomes the poor statistical stability of ApEn and SampEn by using fuzzy sets [88] and mitigates the arbitrariness of the threshold choice [27].

3.2.1.4 Permutation Entropy

Permutation Entropy (PermEn), developed in 2002 [15], computes the Shannon Entropy (ShEn) from a normalised histogram of ordinal patterns identified in subsequences selected from a time series when sorted in ascending order. The embedded dimension m determines the length of these subsequences.

ShEn was introduced in 1948 [139] and to compute its value for a N data time series, $X = \{x_i\}$, it measures the amount of information $H(X)$ by determining a function of its joint probability density function [22], as follows

$$H(X) = -\sum_{i}^{N} p(x_i) ln(p(x_i)) \tag{3.9}$$

PermEn generates subsequences from X starting on sample x_j with length m, $x_j^m = \{x_j, ..., x_{j+m-1}\}$, which are assigned a default growing set of indices given by $\pi^m = \{0, 1, ..., m-1\}$. The subsequence x_j^m is then sorted ascending, and modifications in sample order are reflected in the vector of indices. The resulting new indices vector is compared with all possible $m!$ ordinal patterns of length m and the counter c_i keeps track of the number of similarities found. A histogram is built with the results obtained and each bin is normalised by $N-(m-1)$ giving the probability of each ordinal pattern. This way the vector of probabilities can be written as [15, 38]

$$p_i = \frac{c_i}{N-(m-1)} \tag{3.10}$$

And the $PermEn(X,m,N)$ is obtained by

$$PermEn(X,m,N) = -\sum_{k=0}^{m!-1} p_k log(p_k) \tag{3.11}$$

This method stands out by its ability to extract relevant information about the dynamics of a system with minimum computational cost and robustness to noise. Besides, it can be applied to any type of time series [170]. On the other side, it only emphasises ordinal information rather than

amplitude, and there are potential negative effects of identical values in subsequent iterations due to motif ambiguity [38].

3.2.1.5 Corrected Conditional Entropy

Corrected Conditional Entropy (cCondEn), presented in 1998 by Porta [122], is based on Conditional Entropy (CondEn) and tries to overcome some of its disadvantages, mainly by improving its capacity to analyse short time series.

CondEn quantifies the amount of information conveyed by a sample of the series when the preceding L-1 samples are known. If a new sample has no new information on the series, meaning it is totally regular and its previous samples can accurately anticipate it, the conditional entropy is zero. If the future sample cannot be entirely deduced from the past, the series is complex, and the conditional entropy is high [67]. To obtain the Conditional Entropy, a time series $\{X_i\}$ of length N is normalised and a reconstructed L-dimensional phase space is obtained by considering $N-L+1$ vectors $x_L(i)$. Considering p_L as the joint probability of the pattern $x_L(i)$, CondEn can be derived from ShEn of $x_L(i)$, being this last one written as

$$ShEn(L) = E(L) = -\sum_{L} p_L \log p_L \tag{3.12}$$

Thus, CondEn can be written as a variation of the ShEn with respect to L [122]

$$CondEn(L) = E(L/L-1) = E(L) - E(L-1) \tag{3.13}$$

One of the issues with CondEn that have been noted is that regardless of the nature of underlying dynamics, CondEn drops to zero as a function of L (the number of samples used) when estimating from a short data series [67].

To overcome this problem, cCondEn was designed based on the search for the minimum of the function defined as

$$cCondEn(L) = \hat{E}(L/L-1) + \hat{E}_c(L) \tag{3.14}$$

In this function, $\hat{E}(L/L-1)$ is the estimate of the CondEn: $\hat{E}(L/L-1) = \hat{E}(L) - \hat{E}(L-1)$ and each of its components represent the estimate of the ShEn for L and *L-1* samples respectively, and can be obtained by approximating the joint probabilities p_L with the sample frequencies. The corrective term $\hat{E}_c(L)$ is given by the percentage of single points in the L-dimensional phase space times the estimated value of the ShEn for $L = 1$ [122].

Even for small data segments (about 300 hundred heartbeats), cCondEn can give a trustworthy measure of complexity. This complexity index is calculated without any a priori selection of the number of prior samples required to predict the future dynamics, in contrast to the approximate entropy calculation proposed by Pincus [114] where L is fixed to 2 [67, 122].

3.2.1.6 Dispersion Entropy

In 2016, Rostaghi [133] created Dispersion Entropy (DispEn) to address several drawbacks of existing approaches, such as Sample Entropy's lack of time efficiency for real-time applications or Permutation Entropy's failure to take into account variations in amplitude values. The combination of Shannon entropy and symbolic dynamics created DispEn, which can measure the degree of irregularity of studied signal segments quickly while keeping improved discriminating abilities.

The algorithm to compute DispEn of an univariate time-series x_j of length N can be categorised into four main steps:

1. The first step is mapping the time series to c classes labelled from 0 to 1, using a linear or non-linear mapping function.

2. A number of classes (c) is then mapped to the resulting signal by being dispersed over its amplitude range. Each sample is assigned to the closest class based on its amplitude. The outcome is a classified signal z_j. Since the signal contains m members, each of which can be one of the numbers from 1 to c, the number of different dispersion patterns that can be given to each time series $z_i^{m,c}$ is equal to c^m.

3. For each of c^m potential dispersion patterns, relative frequency is obtained by dividing the number of dispersion patterns by the total number of embedding signals:

$$p(\pi_{v_0 v_1 \ldots v_{m-1}}) = \frac{\text{Number}\left\{ i \mid i \leq N-(m-1)d, z_i^{m,c} \text{ has type } \pi_{v_0 v_1 \ldots v_{m-1}} \right\}}{N-(m-1)d} \tag{3.15}$$

4. Based on ShEn, the embedding dimension m, time delay d, and the number of classes c, DispEn is calculated as follows:

$$DispEn(x,m,c,d) = -\sum_{\pi=1}^{c^m} p\left(\pi_{v_0 v_1 \ldots v_{m-1}}\right) \ln\left(p\left(\pi_{v_0 v_1 \ldots v_{m-1}}\right)\right) \tag{3.16}$$

DispEn originated from SampEn and PermEn. Thus, it uses the tolerance r to be more robust to noise, and the dispersion patterns are based on the permutation patterns but include equal amplitude values in embedding vectors as well, considering not only the ordinal structure of a time series but also the differences between sequential samples [75, 133].

3.2.1.7 Bubble Entropy

In 2017, taking into account the fact that the selection of the parameters used to obtain a practical estimation is a critical element in any definition of entropy, Manis [94] proposed Bubble Entropy (BubbEn) aiming to not only eliminate the necessity of r but also minimise the importance of the second parameter m. BubbEn estimates the complexity of a time series by measuring the entropy of the series of swaps necessary to (bubble) sort its portions of length m when adding an extra

element. Thus, complexity is considered as being increased variability in the ordering of samples across scales rather than a lack of matching patterns [95].

The core algorithm of BubbEn is based on Permutation Entropy. BubbEn computes the relative frequency of the necessary swaps to obtain an ordered subsequence rather than the relative frequency of the ordinal patterns. The first step performed by the researchers was the development of the Conditional Rényi Permutation Entropy (CondRenPermEn), which combined Conditional Permutation Entropy (CondPermEn) and Rényi Permutation Entropy (RenPermEn), taking advantage of the PermEn and inspired by the sorting method of Rank–Entropy (RankEn) [38, 94].

First, using a bubble sort method, each subsequence x_m^j is sorted in ascending order and the counter vector c maintains all swaps required in each instance, with a limit provided by $[0, \frac{m(m-1)}{2}]$. Similarly to PermEn, each histogram bin is normalised by $N-m+1$. The following step is the calculation of the Rényi entropy of order 2 since RenPermEn was stated to achieve the best results when using a quadratic approach [94]. The RenPermEn is calculated from all of the resultant relative frequencies π, accounting for how probable a number of swaps are [38].

$$H_2^m(X) = -log \sum_{k=0}^{\frac{m(m-1)}{2}} p_k^2 \tag{3.17}$$

Following the CondPermEn algorithm, which determines the information contained in sorting the $m+1$ value among the previous m when their order is already known: $CondPermEn(m) = PermEn(m+1) - PermEn(m)$ [38, 94], and RenPermEn, CondRenPermEn is obtained by

$$CondPermRenEn = \frac{H_2^{m+1} - H_2^m}{\log(m+1)} \tag{3.18}$$

From the number of steps required to sort each vector, the CondPermRenEn of the distribution (H_{swaps}^m) is computed for $m+1$ and m, and $BubbEn(X,m,N)$ is obtained by normalising its difference.

$$BubbEn(X,m,N) = \frac{H_{swaps}^{m+1} - H_{swaps}^m}{\log(\frac{m+1}{m-1})} \tag{3.19}$$

BubbEn presents some advantages over other entropy measures: it does not require defining the parameter r; above a given value of m the distinguishing ability and stability of the method are not significantly dependent on m, allowing it to be an almost parameter-free method. However, the independence from the parameters comes with high computational costs, which makes this method impractical for large-scale data [94, 132].

3.2.1.8 Attention Entropy

Typically, entropy methods focus on the frequency distribution of all the occurrences in a time series, which demands at least a few thousand data points, restricting their practical applications.

Furthermore, these methods are also sensitive to parameter settings. Considering these shortcomings, in 2020, an entropy approach denominated Attention Entropy (AttnEn) [168] was proposed with the major innovation being that it assesses the frequency distribution of the intervals between the key observations in a time series instead of calculating the frequency of all observations. The most significant benefit is the capability to discriminate between two series with the same frequency distribution of the patterns but different distributions of the intervals of the key patterns.

Attention entropy is computed in three stages: define the key patterns; determine the intervals between two adjacent key patterns; and compute the Shannon entropy of the intervals.

Given a finite series X, to detect whether a point is a key pattern, a point x_i is defined as a peak point if it satisfies one of the following conditions:

- $x_{i-1} < x_i$ and $x_i > x_{i+1}$, where x_i is defined as local maxima;
- $x_i < x_{i-1}$ and $x_i < x_{i+1}$, where x_i is defined as local minima.

If each point represents one state of a system, the change in state may be viewed as the system's adaptation to the environment, which is predicted to be complicated for complex systems. The peak points show the local upper and lower boundaries of the state changes and, therefore, are possible key patterns.

Having the key patterns defined, the interval $i-j$ between two adjacent key patterns, where x_j is the key pattern that precedes x_i, can be calculated. There are four cases to consider:

- Intervals of local maxima to local maxima $(Max-Max)$;
- Intervals of local minima to local minima $(Min-Min)$;
- Intervals of local maxima to local minima $(Max-Min)$;
- Intervals of local minima to local maxima $(Min-Max)$.

Any of these cases can be chosen or the results of the four separate analyses can be merged by computing the average of the four individual entropy values. The second approach was highlighted as the recommended method since it can smooth possible data abnormalities and the existence of more data can make the method suitable to analyse shorter time series.

Then, the frequency of all intervals is calculated and the Shannon entropy is computed over the frequency distribution of the intervals.

AttnEn has the virtue of not requiring any parameter tuning, being robust to time-series length, and taking just linear time to calculate. However, there is a need to define the key patterns in advance. Using peak points as key patterns has the disadvantage of being sensitive to outliers and noise. Moreover, the specificity of the key patterns may difficult the validation of the result. Defining different key patterns and combining their results can overcome these limitations [168].

3.2.1.9 Multiscale Entropy

When studying pathologic processes including cardiac arrhythmias such as atrial fibrillation, which are related to erratic outputs, traditional entropy approaches indicate higher complexity values than healthy cardiac rhythms exhibiting long-range correlations. This paradox might be driven by the fact that these entropy metrics are based on single-scale analysis, not considering the complex temporal variations intrinsic to healthy physiologic dynamics [34].

Hence, in the early 2000s, Multiscale Entropy (MSE) [34, 35, 37] was introduced aiming to assess the complexity of time series by taking into account several time scales in physical systems. Given a one-dimensional discrete time series of length N $\{x_1,...,x_N\}$, consecutive coarse-grained time series $\{y^{(\tau)}\}$ are constructed by dividing the original dataset into non-overlapping windows of length τ and averaging the data points inside each of them, as depicted in Figure 3.1.

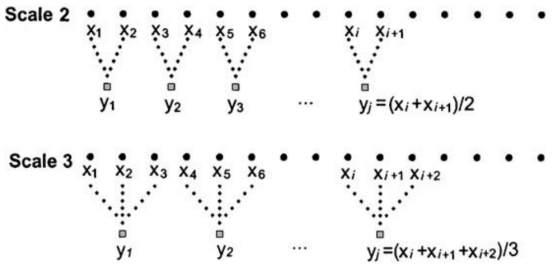

Figure 3.1: Example of the coarse-graining procedure performed by the Multiscale Entropy algorithm for scales 2 and 3. Adapted from [37].

Each element of the coarse-grained time series is calculated as a function of the scale factor τ, being y_j a data point in the newly constructed time series and x_i a data point in the original time series:

$$y_j^{(\tau)} = \frac{1}{\tau} \sum_{i=(j-1)\tau+1}^{j\tau} x_i, 1 \leq j \leq \frac{N}{\tau} \tag{3.20}$$

The first scale, $y^{(1)}$, corresponds to the original time series and the length of each coarse-grained time series is calculated by N/τ. Finally, a defined base entropy measure is calculated for each coarse-grained series and is plotted as a function of τ [34, 35, 37].

The inclusion of multiple entropy measurements allows the assessment of complexity at shorter and longer time scales and the measurement of the overall complexity of a system by calculating the sum of the entropy values for each time scale (complexity index). By examining different time scales, for example, of the heart rate dynamics, it is possible to properly assess how a disease impact the cardiac rhythm on its overall dynamic system [23].

However, it can happen that when analysing a short period of time, what appears to be a slight deviation of the baseline, is in fact a dynamical pattern that can only be identified in a more extended time interval. So, to properly describe a time series, a relatively long time series (a couple

of thousand data points) with stationary data might be needed [36]. Moreover, the understanding of how different scales of complexity in a physiological system relate to one another and how they are affected by regulatory processes is not always clear [57] and MSE has been considered biased by some studies [155] since the similarity criteria are kept constant over all scales, even though variance decreases with scale.

3.2.2 Bivariate entropy methods

To evaluate the synchrony between MHR and FHR, the cross-entropy methods Cross-Approximate Entropy, Cross-Sample Entropy, Cross-Fuzzy Entropy, Cross-Permutation Entropy, and Cross-Conditional Entropy will be detailed.

3.2.2.1 Cross-Approximate Entropy

In order to assess the degree of complexity between two univariate synchronised time series, Cross-Approximate Entropy (XApEn) [113, 116] was developed having as base the ApEn algorithm. Similarly to this last one, XApEn requires the input of the values for both m and r parameters. Despite the ApEn threshold value being calculated with respect to the standard deviation of the series, in XApEn the standard deviation is by definition set to one, due to the obligatory standard scoring [116].

Given the paired time series $u(i)$ and $v(i)$, this method measures the regularity of v patterns to be similar to u patterns with length m and a tolerance of r [115]. Standard scoring must be performed to allow the comparison between vectors from different sources and it implies centralisation and normalisation of the series given by $(x-\mu)/\sigma$, where x is the time series, μ is the mean and σ is the standard deviation. Lower values of XApEn indicate lower asynchrony, i.e., more matches of patterns between the series [144].

XApEn has some limitations. First, since the comparison is being held between two different time series data, self-matches cannot occur, which means that it is possible not to have matches and consequently to have a logarithm of zero in the algorithm, making the estimation impossible [144]. In order to solve this, if a template is unable to find at least one match for $m+1$ points, a probability must be assigned to it. Second, due to the logarithms inside the summation, the XApEn algorithm is direction-dependent: vectors from the time series u are considered the template to compare the vectors from v [132]. Moreover, the unreliable estimation of conditional probabilities is a source of inconsistency, the parameters required (m and r) are mutually dependent and there are high computational costs for long time series [144].

3.2.2.2 Cross-Sample Entropy

Richman and Moorman [132] developed the Cross-Sample Entropy (XSampEn), having as a base the SampEn algorithm, in an attempt to overcome the XApEn main disadvantages. The XSampEn algorithm determines how many vectors conformed by u and v occur for a statistically significant

range that could be understood as a similarity [129]. A lower XSampEn value also indicates a higher synchrony degree between the time series.

XSampEn only requires that one pair of vectors in the two series match for $m+1$ points. Moreover, this method is not direction-dependent. However, it still requires the definition of the parameters m, which usually takes 1 or 2 as a value, and r, for which the values recommended are between 0.1 and 0.25 [132].

3.2.2.3 Cross-Fuzzy Entropy

The same group of researchers that developed FuzzEn created Cross-Fuzzy Entropy (XFuzzEn) [167], which can be considered an adaptation of the first one to analyse bivariate systems. This measure quantifies the synchrony of patterns between two distinct but intertwined signals, like XApEn and XSampEn, differing from the previous ones by using fuzzy sets instead of the conventional two-state classifier. Similar to FuzzEn, this method evaluates the similarity of vectors based on their shapes – with an exponential function as the fuzzy function [167].

In order to compute the XFuzzEn of a bivariate system, it is necessary to define three parameters: m, the length of sequences; r, the width of the exponential function; n, the boundary of the exponential function [167].

3.2.2.4 Cross-Permutation Entropy

PermEn incorporates desirable characteristics, such as its capability to detect both linear and nonlinear dependence and its applicability on regular, chaotic, noisy, or real-world time series. Inspired by these, Shi [140] developed Cross-Permutation Entropy (XPermEn), a permutation-based approach to detect the correlation between two synchronous time series. A low value of XPermEn indicates a high coupling strength between two signals.

The algorithm to compute XPermEn differs from PermEn since the permutation pattern was replaced by the count of intersection points, and the probability distribution was redefined. However, it kept some of its advantages: it is simple, stable and efficient [140].

3.2.2.5 Cross-Conditional Entropy

Cross-Conditional Entropy (XCondEn) is an extension of the corrected Conditional Entropy to measure the degree of uncoupling between two time series. cCondEn quantifies the amount of information carried by the signal when its prior samples are known [122]. Thus, given that one signal has been observed and is fully understood, XCondEn may be viewed as a measure of the unpredictable nature of the other related signal. The uncoupling of signals is measured by the minimum value, which indicates how dependent the signals are on one another: a low XCondEn indicates a high dependency between the signals [2].

XCondEn, which produces accurate estimates even from small data segments, employs an estimator of the uncoupling function. This approach enables quick calculations and makes it

easier to use data collected in actual experimental circumstances where long-term recording is impractical [2].

3.3 Information Dynamics

For the information dynamics measures, Mutual Information, Information Storage and Information Transfer were explored. Self-Entropy and Transfer Entropy were resorted to as a way to compute Information Storage and Information Transfer, respectively. The concepts of Information Storage and Information Transfer form the basis of information dynamics, an evolving promising field to study the complex behaviour of dynamic systems.

3.3.1 Mutual Information

Introduced in the 90s by Collignon, Maes, Viola and Wells [93, 159, 163, 164] for the registration of multimodality medical images, mutual information (MI) quantifies how much information one random variable has about another. It is the reduction in uncertainty of one random variable as a result of knowing the other.

Being X and Y random variables and H the Shannon Entropy, the mutual information $I(X;Y)$ is given by

$$I(X;Y) = H(X) - H(X|Y) \tag{3.21}$$

The MI metric quantifies the degree of dependency between two random variables, i.e., the higher the MI value, the higher the dependency between the variables. MI is always non-negative and equals zero if and only if X and Y are independent. Moreover, it corresponds to the intersection of the information in X with the information in Y. Since X reveals as much about Y as Y about X, the reduction of uncertainty of X due to the knowledge of Y is equal to the reduction of uncertainty of Y due to the knowledge of X. Thus, MI is symmetric in both X and Y [153, 158].

3.3.2 Information Storage and Transfer

Information storage (IS) assesses nonlinear correlations quantifying the new information contained in the present of a variable but not in its past, the amount of information carried by the present that can be explained by the past and the amount of information in the past of a variable that is relevant to predicting its future [46].

Information Transfer (IT) can be explained as the information provided by a source about a destination's next state that was not contained in the past of the destination [29]. It is a directional signal or communication of dynamic information [90].

Considering a univariate system composed by Y, the information generated by Y (H_Y) is the sum of the information stored from its past (S_Y) and the new information (N_Y) as represented in Figure 3.2.

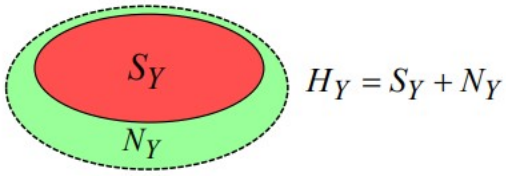

Figure 3.2: Graphical representation of a univariate system described by information dynamics, where the information of Y (H_Y) can be divided into the information stored from its past (S_Y) and the new information (N_Y). Adapted from [45].

On the other hand, if Y belongs to a bivariate system also composed of X, the information generated by Y (H_Y) includes the information stored in Y from its past (S_Y), the information transferred from X to Y ($T_{X\to Y}$) and the new information (N_Y) as depicted in Figure 3.3.

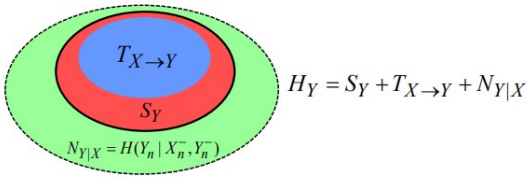

Figure 3.3: Graphical representation of a bivariate system described by information dynamics, where the information of Y (H_Y) can be divided into the information transferred from a related variable ($T_{X\to Y}$), the stored from its own past (S_Y) and the new information (N_Y). Adapted from [45].

3.3.2.1 Self-Entropy

Information Storage can be computed through Self-Entropy (SE), a measure of the amount of information about a variable that can be predicted by its past or by the past of another related variable. SE is traditionally used as a method to assess the regularity and predictability of a process or the information stored in it. Being $p(x,y)$ the joint probability mass function and $p(x)$ and $p(y)$ the marginal probability mass functions of the variables X and Y, the following equation defines SE for bivariate systems:

$$SE(X;Y) = I(X;Y) = H(X) - H(X|Y) = \sum_{x,y} p(x,y) \log \frac{p(x,y)}{p(x)p(y)} \tag{3.22}$$

If the process is entirely random, the past provides no knowledge about the present, resulting in zero IS; if, on the other hand, the series is highly predictable, the present can be fully predicted from the past, resulting in maximum IS.

SE is a measure that captures all the information from the past of a target that can be used to predict its current state, regardless of where that information came from. SE, $I(Y_n; Y_n^-) > 0$, arises

not only from internal processes within the target system ($Y_n^- \rightarrow Y_n$) but also from causal interactions from source to target; in the case of ($Y_n \leftarrow X_n^- \rightarrow Y_n^-$), X_n^- creates a statistical dependence between Y_n^- and Y_n. Thus, SE cannot be related to the presence of internal dynamics in the target process, except in the particular case of absent causal interaction from source to target [47].

3.3.2.2 Transfer Entropy

Transfer Entropy (TE) is a method widely used to compute information transfer for being a non-parametric measure able to determine the coupling of two variables by quantifying the information transferred between them. TE quantifies the information provided by a source about a destination's next state that was not contained in the past of the destination [47, 90].

Given two time series $X = \{x_1, x_2, ..., x_N\}$ and $Y = \{y_1, y_2, ..., y_N\}$ on X to Y direction, being i a given time point, t and τ the time lags of X and Y and k and l the length of the blocks of X and Y past values, respectively. $TE_{X\rightarrow Y}$ is calculated according to

$$TE_{X\rightarrow Y} = H(y_i|y_{i-t}^l) - H(y_i|y_{i-t}^l, x_{i-\tau}^k) = \sum_{y_i, y_{i-t}^l, x_{i-\tau}^k} p(y_i, y_{i-t}^l, x_{i-\tau}^k) \log\left(\frac{p(y_i|y_{i-t}^l, x_{i-\tau}^k)}{p(y_i|y_{i-t}^l)}\right) \quad (3.23)$$

Since TE is zero in the absence of causal interactions from driver to target, it can be withdrawn that its value is a reflection of the amount of information transferred in the target process. Hence, a strictly positive TE value shows that the driver is causing the target [7, 47, 99].

The TE can be calculated for any two time series, but only truly represents information transfer when measured on a causal link in the limit $k \rightarrow \infty$, which guarantees that no information from the destination's past is misinterpreted as transferred. Furthermore, the conditioning of the past makes this method to be directional [90].

3.4 Applicability on physiological signals

Several univariate and bivariate measures have been applied to physiological signals throughout the years. This review prioritised papers where the univariate entropy measures were applied to FHR or, if not yet implemented, applications to HRV. For the bivariate measures, studies on the relationship between the FHR and the MHR were preferred, and if not found, applications on cardiac signals were pursued.

Univariate measures

Approximate Entropy was developed to be suitable for analysing heart rate ECG taking into account its data length constraints. This method is robust to outliers and finite for stochastic, noisy deterministic and mixed processes, which makes it adequate to analyse biomedical signals [65, 112]. Researchers have been applying this entropy method on FHR and have reported a significant decrease of the ApEn value for fetal HRV in cases of fetal asphyxia, including hypoxia and both respiratory and metabolic acidosis [50, 86, 117].

Sample Entropy has also been widely employed in biomedical signals, especially in HRV. A study conducted by Gonçalves [65] assessed the capacity of linear and nonlinear FHR indices to discriminate between normal and acidemic fetuses over the minutes before delivery. The nonlinear indices ApEn and SampEn were computed from the heart rate records of 48 normal, 10 mildly acidemic and 10 moderate-to-severely acidemic fetuses and were found to be capable of distinguishing these groups. Moderate-to-severe fetal acidemia was linked to a considerable drop in nonlinear indices in the first and last minutes of the tracing. Furthermore, both Lim [87] and Gonçalves [65] identified a decrease in the nonlinear indices (ApEn and SampEn) of the fetal HRV with the progression of labour.

Fuzzy Entropy has been getting more attention in physiological signals, with new methods emerging from this one and already being implemented on FHR [108]. Azami [12] compared different FuzEn-based metrics on biomedical signals. Several synthetic and three clinical datasets (including ECG records of 20 young and 20 old healthy subjects) were used to assess the differences between the FuzzEn-based functions. The exponential fuzzy function was suggested for signals longer than 500 sample points and was expected to grow in biomedical signals analysis.

Permutation Entropy was considered by its developers as an appropriate complexity measure for chaotic time series for being extremely fast and robust to noise. Bandt and Pompe [15] tested PermEn on a speech signal to demonstrate its real-world analysis capacity, and it outperformed a well-known complexity indicator for short-time speech analysis. Due to its advantages, new versions of this measure have emerged and have been successfully applied in cardiorespiratory data [19].

Corrected Conditional Entropy has been mainly explored in the biomedical area by Porta [122], the developer of this measure. ApEn, SampEn and cCondEn were compared in an application to a graded head-up tilt test [125]. The study included ECG records of 17 healthy subjects during the test at different table inclinations. All entropy indices evidenced a progressive decrease of complexity as a function of the tilt table inclination, indicating that complexity is controlled by the autonomic nervous system. Thus, SampEn, ApEn, and cCondEn may be useful for monitoring the sympathovagal balance.

Dispersion Entropy was developed having PermEn as a base, and a comparison study between them has been conducted [133]. For both synthetic time series and real electroencephalogram (EEG) datasets, DispEn considerably outperformed PermEn: it was able to detect the noise bandwidth and simultaneous frequency and amplitude change, discriminated different groups, and had less computation time.

Bubble Entropy is considered an efficient entropy model for biomedical signal analysis due to not being significantly dependent on parameter definition and presenting a steady behaviour and increased discriminatory power [94]. The developer of this method, Manis, tested its application on assessing the relation between the FHR and the UAB pH [96]. From 503 normal births intrapartum CTG recordings of at least the last 90 minutes before birth, fetuses with normal pH values, which were considered between 7.25 and 7.35, were compared with fetuses with pH lower than 7.20. By analysing the FHR, the entropy methods assessed, including ApEn, SampEn and

BubbEn, successfully distinguished both groups.

The developer of Attention Entropy also tested its capacity to analyse a heart rate time series [168]. The dataset was composed of 72 healthy subjects (divided into two groups: less or equal to 55 years old and older than 55), 44 with congestive heart failure and 24 with atrial fibrillation. AttEn was compared to 14 state-of-the-art complexity analysis methods, namely ShEn, ApEn, SampEn, PermEn, BubbEn and MSE, and the results showed that it outperformed all of them on average in differentiating healthy and non-healthy subjects. Furthermore, in a time series with a length of 100, it was the only method able to distinguish all groups present with a statistically significant result. This demonstrates that assessing the frequencies of the intervals between patterns can be more effective than evaluating the frequencies of the patterns themselves, particularly for short time series.

To assess the potential of Multiscale Entropy, Costa [36] compared two time series with equal mean and standard deviation and identical power spectra, being the first relative to a healthy young subject and the second obtained by a computational algorithm that deteriorates the information of the original signal via phase randomisation. Conventional time and frequency domain measures were ineffective in determining the amount of information present in these signals, whereas MSE was capable of distinguishing them, confirming its potential in extracting information in different scales from heart rate time series.

Frassineti [54] evaluated the potential of MSE indexes to provide information for characterising neonatal seizures and to discriminate between newborns with seizure events and seizure-free ones. The study comprised 52 heart rate records of newborns obtained by ECG, of which 33 had seizure events. Entropy measures such as ApEn, SampEn, PermEn and Fuzzy Entropy were computed at different scales. Significant differences between the two groups were obtained with Multiscale Sample Entropy at scale 3 and Multiscale Fuzzy Entropy at scale 2. MSE could perform an identification that was not obtained with single-scale approaches.

Bivariate measures

Cross-Approximate Entropy, contrary to Approximate Entropy, is not widespread in the analysis of cardiac systems. In order to identify the reasons for this limited use, Skoric [143, 144] conducted a study comprising artificial, animal, and human (41 healthy males positioned in a hospital bed) systolic blood pressure and pulse interval. The first two were used for method development and testing and the last for validation in real short records. Regions where the parameter space does not guarantee reliable XApEn estimation were found. The proposed solution consisted of targeting the parameters within the stable region of the parameter space and performing the parameter choice jointly. Sun [151] resorted to XApEn to study the potential of electrocardiographic R–R intervals and pulse–pulse intervals acquired by PPG in assessing cardiac autonomic dysfunction and the compatibility of the measures. The results showed that PPG might not be adequate to study the heart rate function of overweight, elderly, or diabetic individuals. Chiu [32] investigated the potential of XApEn of mean arterial blood pressure and mean cerebral blood flow velocity

to assess diabetics with various degrees of autonomic neuropathy. The study achieved promising results as a noninvasive preliminary screening test for diabetics with or without neuropathy.

The pioneer of Cross-Sample Entropy [132] compared the performance of this entropy measure with XApEn in a heart rate dataset and XSampEn was able to show relative consistency where XApEn did not. This is an essential property since if one series pair is more synchronous than another, its cross-entropy value should be lower independently of the conditions examined. Liu [89] evaluated the synchronisation of cardiovascular systems, specifically between R–R intervals and pulse transit time, using XSampEn. Thirty normal subjects and thirty heart failure patients were enrolled in the study. In the first analysis, the results showed a lower XSampEn value for the heart failure group, implying a higher synchronisation. However, further research did not demonstrate a significant difference between the groups. Gonçalves [60] aimed to simultaneously assess maternal and fetal HRV during labour in relation to fetal gender. For that, simultaneous MHR and FHR recordings were obtained from 44 singleton term pregnancies during the last two hours of labour. Resorting to XSampEn, a significantly higher entropy value for mothers carrying female fetuses was found.

The developer of Cross-Fuzzy Entropy [167] tested its efficiency on biomedical signals by comparing it to Cross-Sample Entropy. On both simulated and real EEG datasets, XFuzzEn had better relative consistency and less dependence on record length. It was also applied to the simultaneous electromyography–mechanomyography signals to monitor local muscle fatigue, where records of 12 healthy subjects during the voluntary isometric contractions were used. The results showed an XFuzzyEn significant decrease in the development of muscle fatigue. Furthermore, its trend was similar to a commonly used muscle fatigue indicator.

Cross-Permutation Entropy was developed by Shi [140] to analyse coupling stock market indices. However, measures such as Cross-Bubble Transition Entropy have been developed, having XPermEn as a basis and aiming to improve physiological signals analysis. Chen [31] was able to obtain significant results for the application of the new measure on EEG records analysis.

Cross-Conditional Entropy, similar to cCondEn, was tested by Porta [127] in a graded head-up tilt test. This measure was applied to the coupling beat-to-beat series of heart period (RR interval) and ventricular repolarization duration (QT interval) in 17 healthy subjects at random table inclinations. A significant association was found with its strength progressively decreasing as a function of the tilt angles.

Information Dynamics

Research conducted by Warrick [163] examined the use of MI to address the synchronisation of uterine pressure and FHR. CTG records from 40 pathological, 103 metabolic acidotic and 105 normal fetuses of at least 3 hours of tracing just prior to delivery were assessed. MI discriminated acidotic and normal fetuses more often and earlier than conventional cross-correlation, which might reveal a higher efficiency in studying non-linear systems with non-Gaussian noise. Topalidou [154] resorted to entropy measures such as XApEn, XSampEn and Mutual Information to assess

the correlation of FHR with uterine contractions and fetal movements obtained by CTG. Twenty-three signals with lengths between 30 minutes and 4 hours were analysed. MI was used for single signal analyses, whereas the cross entropy methods were used for multiple signal analyses. MI and XApEn presented statistically significant sequence similarity for FHR–uterine contractions. Relevant results were also found in the influence of fetal movements.

Information Storage and Transfer have been widely used in cardiorespiratory research, namely in the assessment of the temporal evolution of respiration and heart rate as coupled systems, in the study of cardiovascular control mechanisms or in the prediction and characterisation of sleep apnea [47, 48, 118, 123, 157]. Faes [48] assessed the combined analysis of HRV and respiration variability (RV) resorting to SE (to measure the information stored in HRV), TE (to quantify the information transferred to HRV from RV), conditional SE and cross-entropy measures. Simulated cardiorespiratory dynamics data and real data from young healthy subjects (15 with head-up tilt and 16 with paced breathing) were evaluated. Both analyses evidenced conditional SE and cross-entropy as more appropriate to study cardiorespiratory interactions, which are mostly unidirectional from RV to HRV.

The same researcher, Faes [46], examined the ability of several approaches to assess nonlinearity in short-term HRV under various physiopathological conditions. HRV recordings from young and old healthy subjects, as well as myocardial infarction patients in the resting supine position and in the upright position with head-up tilt, were analysed using normalised complexity index, information storage and Gaussian linear contrast. In older and myocardial infarction participants, the first two approaches revealed more complicated dynamics. Only IS revealed a high percentage of nonlinear dynamics in the young group at rest, with a drop in the old and myocardial infarction at the upright position, whereas the other two methods found smaller percentages in all groups and situations.

Marzbanrad [98, 99] applied TE to assess the mechanism and patterns of the MHR–FHR coupling during gestation at various time delays and gestational ages. Maternal and fetal ECG showed significant coupling in 63 of the 65 records studied. The maximal TE from MHR to FHR rose considerably from early (16–25 weeks) to mid gestation (26–31 weeks), whereas the coupling delay reduced significantly from mid to late gestation (32–41 weeks). These changes occur in synchrony with the maturation of the fetal sensory and autonomic nervous systems as gestational age increases. Avci [7] analysed the same relationship with the difference of the FHR being obtained by FMCG. TE was computed in both directions in 74 recordings and fetal movement influence was also verified. The results showed that fetal movement has no significant effect on TE computation. No significant differences were found between the mid (28–32 weeks) and late gestational (32–38 weeks) age groups.

Synthesis

The literature research and presented findings indicate that ApEn and SampEn are widely used and commonly accepted definitions. They have been the basis of many heart rate research papers due to their descriptive and discriminatory capabilities. On the other hand, measures such as BubbEn and

AttnEn, which are relatively new methods, are not yet routinely used in entropy analyses but have shown promising results in cardiac analysis tests. MSE has the capability to reveal information present in the sequence of the values over time that is not able to be identified with single-scale entropy methods.

FHR entropy indexes can be suitable for fetal acidemia prediction based on the hypothesis that abnormally low entropy values, i.e., extremely regular FHR patterns, imply a greater likelihood of acidosis. Castiglioni [27] made a relevant comment when investigating what SampEn, FuzzEn and Distribution Entropy of HRV could tell on cardiovascular complexity: "We may conclude that Sample, Fuzzy, and Distribution Entropy methods are not alternatives one to the other, but they complement each other providing different information on HRV." Therefore, a group of different measures will likely be able to significantly improve signal complexity analysis.

The analysis of the MHR and FHR relationship as a coupled system using nonlinear entropy-based methods has been getting more attention during the last years with the development of new measures and the achievement of promising results. Although XApEn and XSampEn are not as widespread as ApEn and SampEn in heart rate studies, they have been able to provide new insights into this signal synchronisation.

Information Dynamics have been getting more attention in describing heart rate bivariate systems, with Transfer Entropy being the most recurrent method in recent articles.

To note that the short number of studies assessing FHR–MHR can also be explained by the fact that the simultaneous acquisition of these cardiac signals is a recent procedure in clinical practice, so there is a limited number of databases where these methods could be applied.

Chapter 4

Methodology

This chapter focuses on the methodology followed in the course of the work. The implementation of the entropy methods and the two toolkits that allow the computation of these indices are detailed. It also includes a preliminary study where some of the entropy methods implementations were assessed. Furthermore, the statistical analysis is outlined, in particular, to evaluate the discriminant capacity of the computed indices.

4.1 Implementation of the methods

In order to compute the entropy measures detailed in Chapter 3, there is the need to resort to two different toolkits: one for Base, Cross and Multiscale Entropy and another for Information Dynamics.

4.1.1 Base, Cross and Multiscale Entropy computation

The package that enables the entropy measures computation is EntropyHub: an open-source toolkit for entropic time series analysis that provides a comprehensive set of functions of many established entropy methods into one complete resort [53]. These tools make advanced entropic time series analysis straightforward and reproducible and are available to be computed through different programming languages: MATLAB, PYTHON or JULIA. In this dissertation, MATLAB was used since it was the one where both packages (for Entropy and Information Dynamics) were available.

4.1.1.1 Functions to compute Base Entropy

Approximate Entropy, which determines the degree of regularity and unpredictability of oscillations in time-series data, is based on the following arguments:

$$Ap, Phi = ApEn(Sig, m, tau, r, Logx) \tag{4.1}$$

In the call, *Sig* is the time series signal (a vector of length > 10), m is the dimension, *tau* represents the time delay, r is the distance threshold and *Logx* the logarithm base of the Shannon Entropy formula, allowing the entropy to be estimated in bits (base 2), nats (base e) or dits (base 10), for example [52].

The output vector given by *Ap* is the entropy estimation and has length $m+1$, the first value corresponds to the zeroth estimate, $\frac{\log(N)}{N} - \Phi_1$, and the last value to the estimate for the specified m. The value obtained by *Phi* is the number of matched state vectors for each embedding dimension from 0 to $m+1$ [52].

Sample Entropy, which was developed having ApEn as a base but diminishing the dependency on the signal length and the high implementation costs, can be computed by:

$$Samp, A, B = SampEn(Sig, m, tau, r, Logx) \tag{4.2}$$

Samp is a vector of length $m+1$ with the estimation of SampEn, where its first value is the zeroth estimate, $\frac{1}{N}\log(N(N-1)) - \log(A_1)$, and its last value is the estimate for the specified m. A corresponds to the number of matched state vectors for each embedding dimension from 0 to m and B to the number of matched state vectors for each embedding dimension from 1 to $m+1$ [52].

Fuzzy Entropy, which brought the inclusion of fuzzy sets to the entropy definition, is obtained by:

$$Fuzz, Ps1, Ps2 = FuzzEn(Sig, m, tau, Fx, r, Logx) \tag{4.3}$$

In addition to the elements that were already asked in ApEn and SampEn, to calculate FuzzEn, the type of fuzzy function for distance transformation (*Fx*) has to be specified. By default, it is equivalent to the exponential function given by $f(x) = \exp\left(-\frac{x^{r_2}}{r_1}\right)$. Regarding the outputs, *Fuzz* is the entropy estimate vector with a value for each embedding dimension from 1 to m, *Ps1* contains the average fuzzy distances for the embedding dimensions from 1 to m, and *Ps2* presents the average fuzzy distances for the embedding dimensions from 2 to $m+1$ [52].

Permutation Entropy computes the Shannon Entropy from a normalised histogram of ordinal patterns and can be obtained with:

$$Perm, Pnorm, cPE = PermEn(Sig, m, tau, Logx, Norm) \tag{4.4}$$

Norm is a boolean operator that determines the normalisation of the *Perm* value: false (default) normalises with respect to the number of permutation symbols (m); true normalises with respect to the number of all possible permutations ($m!$). With this function, it is possible to obtain *Perm*, the PermEn estimates for embedding dimensions 1 to m; *Pnorm*, the normalised PermEn estimates; and *cPE*, the Conditional Permutation Entropy [52].

Conditional Entropy quantifies the information in a sample when the previous ones are known.

It is computed by:

$$Cond, SEw, SEz = CondEn(Sig, m, tau, c, Logx, Norm) \tag{4.5}$$

The input parameter c represents the number of symbols in symbolic transformation and must be an integer bigger than one. The *Norm* is a boolean operator that allows one to choose if the *Cond* value is normalised. *Cond* is the corrected Conditional Entropy estimate, *SEw* is the ShEn estimate for m and *SEz* is the ShEn estimate for $m+1$ [52].

Dispersion Entropy quantifies the degree of complexity of a sample based on a SampEn and PermEn-inspired algorithm. The following function allows its calculation:

$$Dispx, RDE = DispEn(Sig, m, tau, c, Typex, Logx, Norm) \tag{4.6}$$

Similar to the previous method, c represents the number of symbols in transform and must be an integer bigger than one. *Typex* is the type of symbolic sequence transform. The Dispersion Entropy estimate is given by *Dispx*, and it is also possible to obtain the Reverse Dispersion Entropy estimate in *RDE* [52].

Bubble Entropy is an entropy model suitable for biomedical signal analysis that does not require defining the distance threshold r and is not significantly dependent on m. The following arguments can be used to compute its value for a time-series signal:

$$Bubb, H = BubbEn(Sig, m, tau, Logx) \tag{4.7}$$

The values obtained by *Bubb* correspond to the entropy estimation and H is the Conditional Rényi Entropy [52].

Attention Entropy is a new entropy model designed to be independent of input parameters and can be obtained by:

$$Attn, Hxx, Hnn, Hxn, Hnx = AttnEn(Sig, Logx) \tag{4.8}$$

Attn is the Attention Entropy estimation, whereas *Hxx* is the entropy of local maxima intervals, *Hnn* is the entropy of local minima intervals, *Hxn* is the entropy of intervals between local maxima and subsequent minima and *Hnx* is the entropy of intervals between local minima and subsequent maxima [52].

4.1.1.2 Functions to compute Cross Entropy

Cross-entropy models quantify the degree of asynchronism of two time series. Cross-Approximate Entropy is computed according to:

$$XAp, Phi = XApEn(Sig, m, tau, r, Logx) \tag{4.9}$$

For the Cross-entropy measures, the time series signal is a $N \times 2$ matrix where $N > 10$. Note that XApEn is direction-dependent. Therefore, the first column of the signal is used as a template, and the second is the matching sequence. The output *XAp* is a vector of length $m+1$ with the entropy estimation where the first value is referent to the zeroth estimate, $\frac{\log(N)}{N} - \Phi_1$, and the last value to the estimation for the specified m. *Phi* is the number of matched state vectors for each embedding dimension from 0 to $m+1$ [52].

The following arguments allow the calculation of Cross-Sample Entropy:

$$XSamp, Phi = XSampEn(Sig, m, tau, r, Logx) \tag{4.10}$$

XSampEn is the entropy estimation vector and has a length of $m+1$. Similarly to SampEn, its first value is the zeroth estimate, $\frac{1}{N}\log(N(N-1)) - \log(A_1)$, and the last is the estimate for the specified m. A is the number of matched state vectors for each embedding dimension from 0 to m, and B is the number of matched state vectors for each embedding dimension from 1 to $m+1$ [52].

Cross-Fuzzy Entropy is an extension of Fuzzy Entropy to analyse a bivariate system. Thus, the arguments to compute them are the same:

$$XFuzz, Ps1, Ps2 = XFuzzEn(Sig, m, tau, Fx, r, Logx) \tag{4.11}$$

XFuzz contains the Cross-Fuzzy Entropy estimates for each embedding dimension from 1 to m. *Ps1* has the average fuzzy distances for embedding dimensions from 1 to m and *Ps2* is similar but for embedding dimensions from 2 to $m+1$ [52].

Cross-Permutation Entropy can be calculated with the following function:

$$XPerm = XPermEn(Sig, m, tau, Logx) \tag{4.12}$$

XPerm contains the Cross-Permutation Entropy estimate. Note that XPermEn is undefined for an embedding dimension $m < 3$ [52].

Cross-Conditional Entropy can be calculated by resorting to the following function:

$$XCond, SEw, SEz = XCondEn(Sig, m, tau, c, Logx, Norm) \tag{4.13}$$

XCondEn requests the same parameters as cCondEn to be computed. *XCond* is the corrected Cross-Conditional Entropy estimate, *SEw* is the Cross-ShEn estimate for m and *SEz* is the Cross-ShEn estimate for *m+1*. An important note is that XCondEn is direction-dependent, meaning that the order of the data sequences in *Sig* matters: the first column is the sequence 'y' and the second column is the sequence 'u'. *XCond* is the amount of information carried by y(i) when the pattern u(i) is found [52].

4.1.1.3 Functions to compute Multiscale Entropy

Multiscale Entropy assesses the complexity of time series by taking into account several time scales in physical systems in the calculation of an entropy measure. To compute this entropy in EntropyHub, there is a need to start with the creation of the multiscale object ($Mobj$) according to the entropy method ($EnType$) defined: ApEn, SampEn, FuzzEn, PermEn, cCondEn, DispEn, BubbEn or AttnEn, in this case. The parameters required ($**kwargs$) by the measure chosen also have to be defined:

$$Mobj = MSobject(EnType, **kwargs) \tag{4.14}$$

Then, having the multiscale object defined along with the input of the time series signal and the number of grained time scales desired to assess, MSE can be computed by:

$$MSx, Ci = MSEn(Sig, Mobj, Scales) \tag{4.15}$$

MSx is an estimation of the entropy at each time scale (τ) and returns a vector with the same length as the number of scales defined. Ci is the complexity index, equivalent to the area under the multiscale entropy curve [52].

4.1.1.4 Parameter selection

The parameters required by the entropy functions detailed above were chosen based on the suggestions presented by Flood on the EntropyHub package guide [52] since no testing on the parameter influence on the entropy values was performed in the course of this work. However, when these measures were being created, their developers assessed the influence of each parameter on the entropy value. Thus, the values collected by Flood from the papers that describe the algorithm of each measure by its developer already take into account these performance evaluations.

The embedding dimension was set as $m = 2$, except for XPermEn, which is undefined for $m < 3$, so it was set as $m = 3$. The $m = 2$ choice was common in the literature [30, 54, 114, 132, 167] for physiological signals since a low embedding dimension is usually sufficient to capture the essential information while preserving the underlying dynamics of the signals.

The radius distance threshold was defined as $r = 0.2 \times std(Sig)$ [133], except for FuzzEn and XFuzzEn, which demand a two-element tuple with the default exponential fuzzy function, so it was set to $r = (0.2, 2)$. Pincus [115] suggested a fixed value of r of 0.1–0.25 of the standard deviation of the individual subject time series. This allows the comparison of the complexity of signals with different standard deviations. Moreover, the entropy becomes robust to the noise in the magnitude covered by r.

The time delay was set as $tau = 1$ for all measures. The logarithm base in the entropy formulas used was $Logx = exp(1)$, except for PermEn, XPermEn and AttnEn where $Logx = 2$. In the functions with the argument $Norm$, normalisation was set to $false$. Regarding the number of symbols in symbolic transformation, for CondEn and XCondEn were set as $c = 6$, whereas for

DispEn was set as $c = 3$. This last method also required defining the type of symbolic sequence transform (*Typex*) for mapping, which was set equal to *ncdf* – Normalised cumulative distribution function [133].

For the Multiscale Entropy, the number of scales was defined as 5 for all base entropy measures in the study. The base entropy functions correspond to the scale 1 value obtained with the MSE.

An important note is that due to XApEn and XCondEn being computed with direction-dependent functions, their value has to be computed twice: once with signal A as the template and signal B as the matching sequence, and another time with the opposite.

4.1.2 Information Dynamics computation

The package that enables the estimation of the information stored and transferred in a bivariate system is ITS Toolbox: a MATLAB toolbox for the practical computation of Information Dynamics [44]. It allows performing the estimation of several entropy methods based on information dynamics, using different approximation measures: Linear (Gaussian), Binning, Kernel, Nearest Neighbours [45].

4.1.2.1 Functions to compute Information Storage and Transfer

Self-Entropy enables the estimation of the amount of information stored, i.e., it is a measure of the amount of information about a variable that its past can predict. Transfer Entropy enables the estimation of the amount of information stored, i.e., it is a measure of the amount of information provided by a source about a destination's next state that was not contained in the past of the destination.

Using the linear estimator, information storage can be computed according to the expression:

$$out = its\_SElin(data, jj, V) \tag{4.16}$$

This function computes the SE of a time series given: the data, a $N \times M$ matrix of M time series, each having length N; jj, the index of the target variable – the one to compute the SE; V, a vector of candidates (to be pre-determined from uniform embedding – the ITS Toolbox has a developed function for its calculation [45]).

Regarding the information transferred, its computation is possible with the following arguments:

$$out = its\_BTElin(data, ii, jj, V) \tag{4.17}$$

This function computes the TE from the time series, given: the data, a $N \times M$ matrix of M time series, each having length N; ii, the index of driver variable (can be multivariate); jj, the index of the target variable; V, a vector of candidates (to be pre-determined from uniform embedding – the ITS Toolbox has a developed function for its calculation [45]).

Using the binning estimator, SE can be computed with the following:

$$out = its\_SEbin(data, V, jj, c, quantizza) \tag{4.18}$$

Similar to the expression using the linear estimator, the data is a $N \times M$ matrix, jj is the index of the target variable and V is the vector of candidates (to be pre-determined from uniform or non-uniform embedding – the ITS Toolbox has developed functions for their calculations [45]). Additionally, the input c, the number of quantization levels for binning, has to be defined, and *quantizza* allows to skip quantization if set as *n* (useful for when the data is already quantized).

To compute the TE with binning estimation, there is only the need to add *ii* as the index of the driver variable, according to:

$$out = its\_BTEbin(data, V, ii, jj, c, quantizza) \tag{4.19}$$

In order to use the kernel estimator to compute SE, the following arguments have to be defined:

$$out = its\_SEker(data, V, jj, r, norma) \tag{4.20}$$

Similar to the previous method, the vector of candidates can be determined from uniform or non-uniform embedding (both functions are available on [45]). This measure requires the definition of r as the threshold for distances (absolute value) and *norma* as the type of distance: 'Chebyshev' (default) or 'Euclidean'.

The same arguments with the addition of the index of the driver variable allow the computation of the TE with kernel estimation:

$$out = its\_BTEker(data, V, ii, jj, r, norma) \tag{4.21}$$

The following expression computes the SE with the k-nearest neighbour estimator:

$$out = its\_SEknn(data, V, jj, k, metric) \tag{4.22}$$

In the inputs, k is the number of the nearest neighbour to search for distance, and the *metric* can be 'maximum' (default) or 'euclidian'.

With the parameters already detailed, it is also possible to obtain TE with the k-nearest neighbour estimator:

$$out = its\_BTEknn(data, V, ii, jj, k, metric) \tag{4.23}$$

4.1.2.2 Parameter selection

The parameters required by the entropy functions detailed above were chosen based on the suggestions presented by the creator of the ITS Toolbox, Luca Faes, in the example for cardiovascular

variability series [44] since no testing on the parameter influence on the entropy values was performed in the course of this work.

The inputs *data*, the index of the driver variable *ii* and the index of the target variable *jj* were defined based on the system at study and the desired signals to assess. The vector of candidates is pre-determined by other functions of the toolbox according to the chosen estimator and additional parameters.

For the linear estimator, uniform embedding was used to obtain the embedding vector, and BIC (Bayesian information criterion, a metric to compare the fit of a model) was imposed to optimise the linear model. For the bin estimator, non-uniform embedding was performed with 6 quantization levels. *quantizza* was set to 'y' to perform the quantization. For the kernel estimator, non-uniform embedding was selected with the threshold for distances as 30% of the standard deviation of the target signal, and the default *norma* (Chebyshev) was used. For the k-nearest neighbour estimator, non-uniform embedding was set with the number of neighbours $k = 10$ and the default *metric*: maximum distance.

4.1.3 Preliminary study

A preliminary study was developed aiming to assess Base, Cross and Multiscale Entropy measures implementation in a real cardiac database. For that, the following measures were selected: ApEn, SampEn, BubbEn, AttnEn, XApEn, XSampEn and MSE. Since only the EntropyHub package [53] was needed, the programming language chosen to compute the entropy was PYTHON. (To note that this study is based on the work developed in the curricular unit *Projeto e Técnicas Laboratoriais*)

The implementation of the entropy methods was done by resorting to the MIMIC-III Waveform Database [103] from PhysioNet. This dataset is composed of 67,830 record sets for approximately 30,000 ICU patients containing multiple physiological signals and a time series of vital signals collected from bedside patient monitors. Among the signals available, the Heart Rate and Pulse only from neonatal intensive care units were selected. The numeric records contain a data file and a header with information such as the type of signals of the record or the signal length. This information was accessed by resorting to Waveform Database Software Package (WFDB) for PYTHON.

For training purposes, twenty records with the desired features have randomly been chosen from the dataset. The files were opened resorting to the OS library, their data extracted resorting to WFDB to read the data and header file simultaneously, and their entropy values were calculated.

Since in biomedical signals, entropy is usually calculated over patterns of a certain length, the records were analysed in 30 minute windows (1800 samples each) and a maximum of 50 windows per patient was imposed, equivalent to 25 hours of duration signals and 90 000 samples. Whenever the signal started without values for both Heart Rate and Pulse, the lines were deleted until at least one of the signals was detected.

In order to assess the correlation between Heart Rate and Pulse entropy, two scatter matrix plots and correlation matrices with heatmap were built to study the relationship between the Cross

entropy methods studied and each of the signals, using the first scale of the MSE values computed (equivalent to the Base entropy function) and the complexity index (*Ci*) (Figure 4.1).

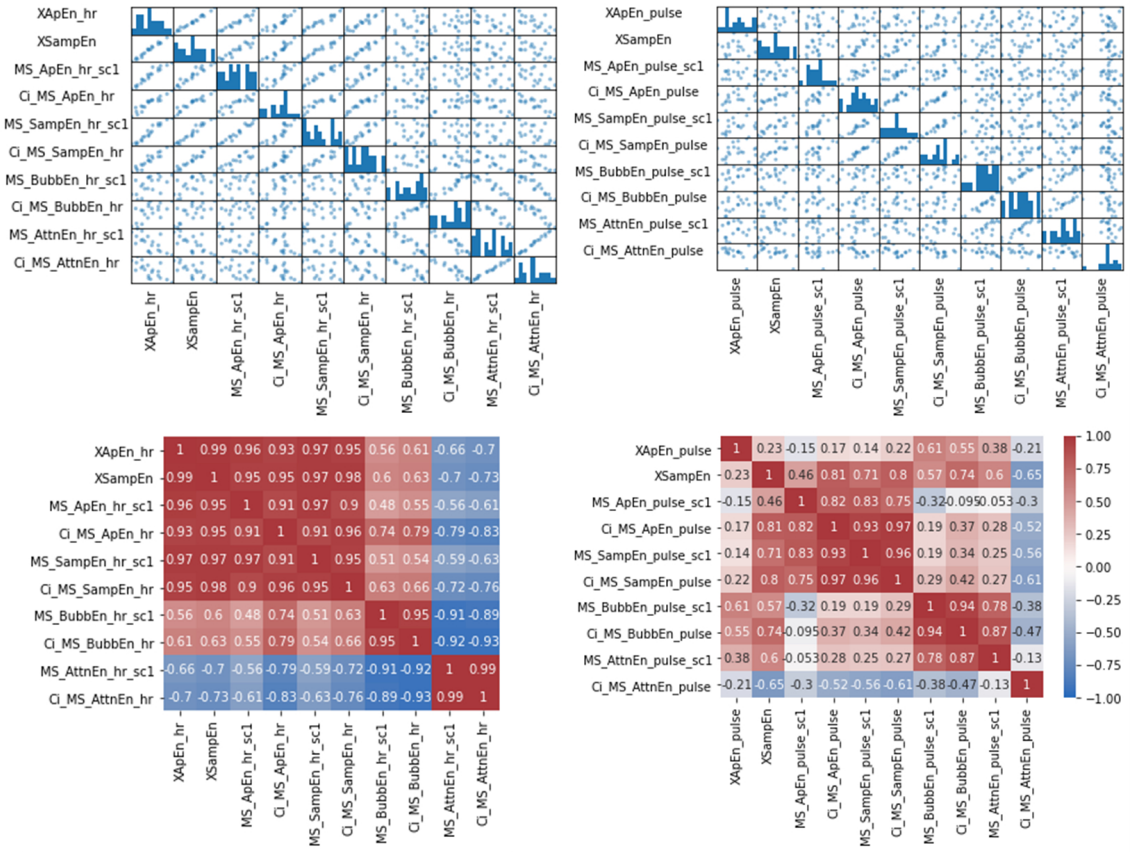

Figure 4.1: Scatter matrix plots and respective correlation matrices with heatmap to assess the association of the bivariate and univariate entropy methods between themselves when applied to heart rate (hr) and pulse signals (on the left and right respectively). To simplify the visualisation, only the scale 1 (sc1) and complexity index (Ci) of Multiscale Entropy (MS) are presented.

The studied Heart Rate MSE methods (left panels in Figure 4.1) present strong associations between them. There is a high positive correlation between XApEn, XSampEn, ApEn and SampEn, meaning that if one of them increases, the others will tend to increase too. Not as strong as these, but BubbEn also has a positive association with these Cross-entropy methods, and AttnEn has a weak negative association. These last two have a strong negative association between them. In the graphics that show the relationship between the Cross-entropy and Pulse MSE methods (right panels in Figure 4.1), we can immediately notice that, generally, the relationships are weaker. The XApEn has a weak relationship with every other entropy method studied. The same can be observed for the XSampEn, except in its relation with ApEn and SampEn where it shows a positive association. These two methods also have a positive correlation between them.

From the entropy methods assessed, it seems that both the XApEn and the XSampEn have a stronger relationship for the Heart Rate than for the Pulse. In order to further explore this hypothesis, more entropy methods would have to be studied, as well as a larger dataset.

4.2 Statistical analysis

In order to evaluate the discriminant capacity of the computed entropy-based indices, a statistical analysis was performed. To start, descriptive statistics were used to describe relevant features of the database records: absolute and relative frequencies of categorical variables; and minimum, maximum, median and interquartile range for continuous variables. Then, appropriate correlation coefficients were applied to study the relationships between the different indices computed. Finally, the discriminant capacity of the entropy measures for fetal acidemia was assessed with the Mann-Whitney test and Generalised Linear Mixed Models. Note that test results were considered significant for p-values < 0.05.

4.2.1 Correlation between entropy indices

The correlation between entropy methods quantifies the similarity of the aspects they capture from signal dynamics. A high correlation indicates that the measures provide the same information and, therefore, either one can be chosen to assess the signal. On the other hand, a low correlation reveals that the measures provide different information on the irregularity and complexity of the signal. Using both can be beneficial to improve signal analysis. Note that correlations might be positive, meaning both methods increase at the same time, or negative, meaning that when one increases, the other decreases proportionally. Taking this into account, a correlation study between the entropy methods allows an appropriate selection of the measures.

The calculation of the correlations was done by resorting to Pandas library in PYTHON with the function $dataframe.corr(method)$. The method corresponds to the correlation coefficient to be used: 'kendall', 'pearson' or 'spearman'. Since not all measures followed a normal distribution, Spearman's correlation coefficient was selected. This method does not rely on any specific distribution assumption and is more robust to outliers than Pearson [104].

4.2.2 Mann-Whitney test

The Mann-Whitney U test, also referred to as the Wilcoxon rank sum test, examines differences between two groups based on a single, ordinal or quantitative variable without implying a specific distribution [101]. The median, interquartile interval and the Mann-Whitney p-value were also used to assess the differences between groups.

The entropy indices were obtained from a database with 54 normal fetuses and only 7 acidemic, which is a significant difference between the number of observations of each group. Furthermore, as referred to previously, some measures did not follow a normal distribution. Therefore, Mann-Whitney U Test was used to assess the capacity of the indices computed in distinguishing non-acidemic from acidemic fetuses. The test computation was done by resorting to the function $p = ranksum(x, y)$ in MATLAB, which returns the p-value of a two-sided Wilcoxon rank sum test for the null hypothesis that the data in x and y are samples from continuous distributions with equal medians.

Not only the p-value but also the statistical power of the test was calculated. The power of the tests conducted was calculated to verify the capacity of the model to find a statistically significant difference between the groups when the difference does exist. The power is given by $1-\beta$, where β represents the likelihood of incorrectly determining there is no substantial difference when there is. The statistical power also depends on the effect size (the raw difference between group means) and sample size: a high effect size allows the detection of the difference in a small number of samples [150]. Cohen categorised the effects into small ($d = 0.2$), medium ($d = 0.5$) and large ($d \geq 0.8$) and suggested an adequate β error of 0.2 [24], which is widely accepted. The calculation of the statistical power was done by resorting to G*Power 3.1 [49], where a medium effect size was considered.

4.2.3 Generalised Linear Mixed Models

In order to understand if the time influenced the entropy indices, these were represented graphically. For each measure, two boxplots (one for normal and one for acidemic) were constructed for each time interval to allow a visual evaluation of the influence of time on the evolution of the indices of each group.

A Generalised Linear Mixed Model (GLMM) describe the relationship between a response variable and independent variables using coefficients that can vary with respect to one or more grouping variables. A GLMM is composed of fixed effects – the variables of interest – and random effects – variations within groups. Some relevant aspects are the fact that it allows different data distribution and is robust to unequal-sized groups. These characteristics make the model suitable for analysing repeated measures and complex time series [73].

GLMM was implemented by resorting to the function $glme = fitglme(tbl, formula)$ in MATLAB. For the first input parameter (*tbl*), a table was created with the following columns: 'Subject', 'Method', 'Time' and 'Group'. The method is the entropy value computed for a specific method and time interval, the time corresponds to the 10 min interval used to compute that entropy (encoded from 1 to 12), and the group can be 0 for non-acidemic and 1 for acidemic. Relative to the second input parameter, two different formulas were tested: $'Group \sim Method + Time + (1|Subject)'$ and $'Group \sim Method + (1|Time) + (1|Subject)'$. In the first one, the group is given by the entropy method and the time (as fixed effects) and accounts for subject variability (as a random effect), whereas in the second one, time is considered as a random effect, similar to a repeated measure.

To evaluate the overall fit of the GLMM developed, several output parameters should be taken into account: the model fit statistics, such as AIC (Akaike information criterion, the most suitable for complex small-sized data); the fixed effects coefficients, such as the estimate and the p-value to understand the magnitude and statistical significance of the variable; the random effect covariance parameters, where the estimate quantifies the subject variability.

Chapter 5

Application of entropy indices on FHR and MHR analysis

In this chapter, the main results obtained in this dissertation are presented. It starts with the exploration of the main features of the database used for the work and a description of the pre-processing. Then, the theory-based indices assessment is described: the correlation between measures, the discriminant capacity for fetal acidemia and the influence of time on these. The discriminant capacity was evaluated first using the Mann-Whitney test and then with Generalised Linear Mixed Models to include the effect of time and variability between subjects. Finally, an interpretation of the significance of the results is presented.

5.1 Data exploration and pre-processing

The dataset used for the following work of this dissertation is composed of sixty-one recordings of MHR and FHR that were acquired during the last two hours of labour in singleton term pregnancies. The UAB pH threshold for fetal acidemia was defined as 7.15 [59, 63, 109] and the study sample (collected for a previous study [63]) was divided and analysed in two groups: normal (non-acidemic) fetuses and acidemic fetuses. The study was approved by the local Ethics Committee and all participants gave informed consent to participate [63].

The MHR signal was acquired by ECG with two unipolar chest electrodes placed in the standard positions for the procedure (2nd right and left intercostal spaces and 5th left intercostal space in the medioclavicular line), whereas the FHR was acquired with a conventional external ultrasound sensor placed on the maternal abdomen. Both signals were conveyed to a STAN® 31 fetal monitor (Neoventa, Gothemburg, Sweden). This monitor amplified, digitalised at a sample rate of 1600 Hz with a precision of 12 bits, and filtered the signals [134].

The MHR was determined by measuring the interval between R waves in the ECG and rounding to the nearest quarter beat, expressed in beats per minute, and the same autocorrelation function

was applied to the fetal signal to calculate the heart periods [26]. This monitor was connected to the Omniview-SisPorto® 3.5 system through an RS232 port, which received the signals at a sampling rate of 4Hz (Speculum, Lisbon, Portugal) [10, 119] and converted the data into Excel® files for subsequent analysis (for more details regarding signal acquisition refer to [63]).

Tables 5.1 and 5.2 summarise the main features of the subjects that constitute this database, including characteristics of the mother and fetus, the type of labour and CTG duration.

Table 5.1: Records characteristics, described by the number of cases and the respective percentage, considering the umbilical arterial blood pH threshold for acidemia as 7.15.

Data	**Normal fetuses** (n=54)	**Acidemic fetuses** (n=7)
Mother		
Associated pathologies	10 (18.5%)	2 (28.6%)
Medication	33 (61.1%)	6 (85.7%)
Labour		
With epidural	52 (96.3%)	7 (100.0%)
Delivery mode		
Normal vaginal	29 (53.7%)	3 (42.9%)
Operative vaginal	20 (37.0%)	3 (42.9%)
Cesarean section	5 (9.3%)	1 (14.3%)
Newborn sex		
Male	33 (61.1%)	1 (14.3%)
Female	21 (38.9%)	6 (85.7%)

Table 5.2: Records characteristics, described by the minimum, maximum, median, 1st and 3rd quartiles, considering the umbilical arterial blood pH threshold for acidemia as 7.15.

Data	**Normal fetuses** (n=54)			**Acidemic fetuses** (n=7)		
	Min	Max	Med [Q1;Q3]	Min	Max	Med [Q1;Q3]
Mother						
Age (years)	16	38	28 [24;32]	18	35	25 [21;30]
Height (cm)	150	173	162 [159;165]	152	169	157 [154;161]
Weight (kg)	54	89	71 [65;79]	53	84	68 [64;74]
Parity	0	2	0 [0;0.8]	0	1	0 [0;0.5]
Gestational age (weeks)	38	48	41.3 [40.2;43.3]	37	41	40 [38.9;40.5]
CTG						
Duration (min)	88	908	267 [154.3;399.5]	112	363	260 [174;320]
Newborn						
Birth weight (g)	2685	4045	3193 [3029;3418]	2400	3445	3105 [3050;3238]
1 min Apgar score	7	10	9 [9;10]	9	10	9 [9;9]
5 min Apgar score	9	10	10 [10;10]	9	10	10 [10;10]
Arterial pH	7.16	7.37	7.27 [7.21;7.30]	7.05	7.13	7.11 [7.08;7.12]

The criteria for inclusion were: more or equal to 37 weeks of gestational age; unifetal gestation; fetus in cephalic position; 4 to 6 cm of cervix dilatation; spontaneous labour; record of at least 5 min in the case of eutocic delivery and 30 min for a cesarean section; CTG of at least 120

min duration with signal loss less than 10% and signal quality of more than 90%. On the other hand, the exclusion criteria were based on the presence of malfunctions or induced labour.

As an example of the database signals, Figure 5.1 depicts the two hours of the simultaneous MHR and FHR for a normal fetus and an acidemic fetus.

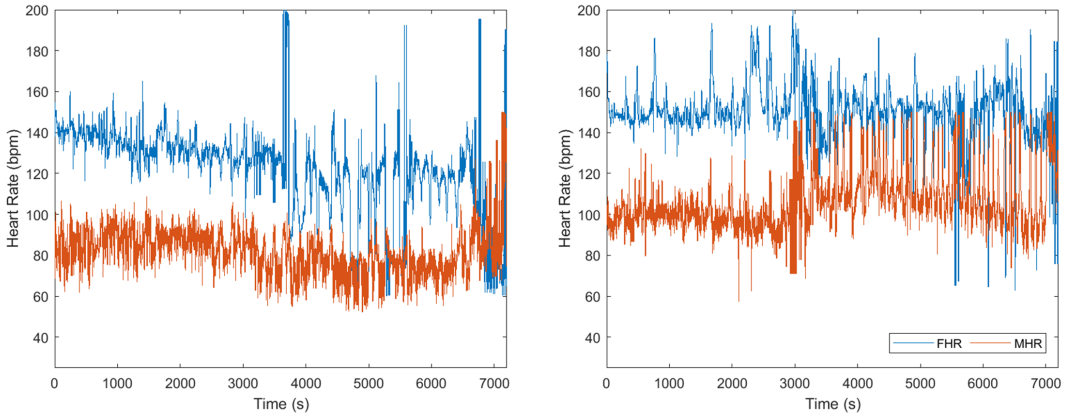

Figure 5.1: Examples of the simultaneously acquired fetal and maternal heart rate signals for a normal (left) and an acidemic (right) fetus, already pre-processed.

The increase of fetal and maternal movements in the moments before birth leads to more frequent disruption of MHR and FHR signals by signal loss and artefacts. In order to minimise this contamination in the computation of nonlinear indices, a pre-processing algorithm has been implemented previously [65]. This algorithm was developed for FHR and identifies fetal heartbeats lower than 60 bpm and beat-to-beat differences higher than 25 bpm. If they do not exceed 2 seconds in duration, they are replaced using spline interpolation. On the other side, longer periods are replaced by a previous segment of the same length but without signal loss. This way, the temporal basis is preserved [65]. In the case of the MHR, the value of 50 bpm was added to each data point of the MHR that differed from zero and the same pre-processing algorithm was applied (for more details on the pre-processing of the signals, refer to [65]).

5.2 Entropy functions execution time

For the entropy indices computation, the functions and respective parameters set in Section 4.1 were used. In biomedical signals, the entropy is not usually calculated directly for the complete time series but over segments of a determined time length. For this dissertation, a 10-minute interval was selected to compute the indices, capturing short-term signal variations. This focuses on fast pattern modifications, which are more likely to be significant for clinical analysis, and keeps the computational time low. Note that since the functions used to compute cross entropy did not incorporate normalisation of the signals, this was previously computed with $X_{normalised} = \frac{X-\mu}{\sigma}$.

A uniformly distributed random signal was generated to estimate the execution time of the different entropy methods. To mimic the FHR signals, the amplitude of the signal at each point in time was randomly chosen from the range 110–200 [106, 160].

The four estimators that the ITS package allows to choose as approximation measures – Linear (Gaussian), Binning, Kernel, Nearest Neighbours – had their execution time tested. For that, the number of samples of the random signals generated was increased from 200 to 3000, in increments of 200, and for each length, the procedure was repeated 30 times.

A boxplot with the execution time according to the number of samples and the estimator for the ITS functions is presented in Figure 5.2. Both kernel and nearest neighbour estimators presented a dependency on the lower number of samples to be able to match the fast execution time observed for the linear and binning estimators. For this dissertation, a 10-minute window (equivalent to 2400 samples) was chosen to compute the entropy indices. Taking this into account, a choice was made to only use the linear and binning estimators for the following work due to time efficiency.

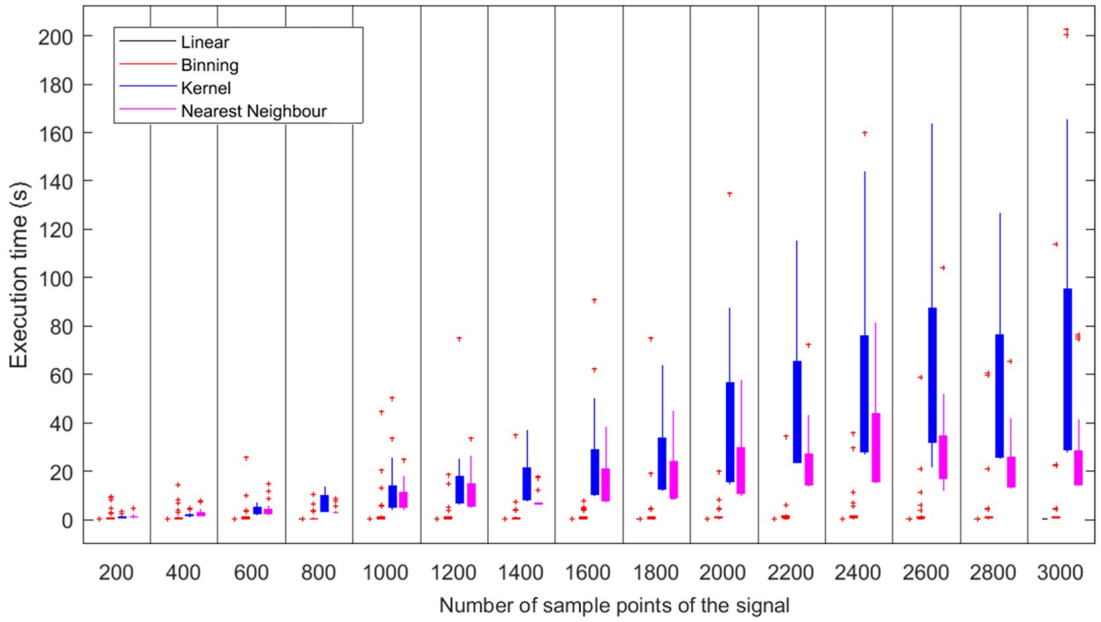

Figure 5.2: Information dynamics estimators execution time (seconds) for uniformly distributed random signals with different lengths (from 200 to 3000, where each point was randomly chosen from the range 110–200). To note that the y-axis was restricted to 0–120s to improve visualisation, the values of outliers from the last group reached 200s with the nearest neighbour estimator.

Similarly, considering the 10min window to compute the entropy values, the execution time of all methods was assessed for 30 uniformly distributed random signals with 2400 samples (each sample is in the range 110–200). Figure 5.3 portrays a boxplot with the execution time of the methods, which were all considered to be time-efficient.

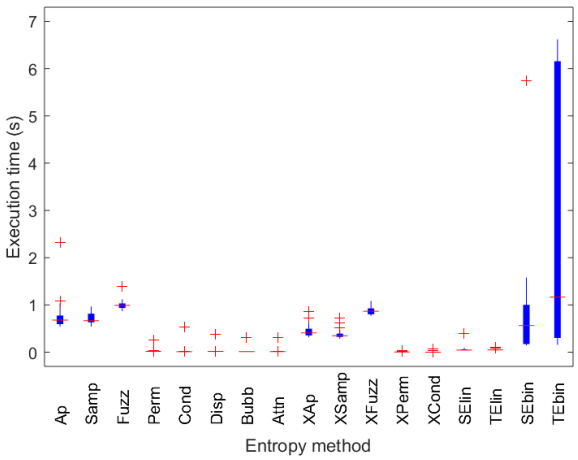

Figure 5.3: Entropy methods execution time (seconds) for uniformly distributed random signals with 2400 samples (equivalent to 10min of the heart rate signals). Legend: Ap – Approximate, Samp – Sample, Fuzz – Fuzzy, Perm – Permutation, Cond – Conditional, Disp – Dispersion, Bubb – Bubble, Attn – Attention, X – Cross, SE – Self, TE – Transfer Entropy, lin – linear, bin – binning.

5.3 Correlation between entropy indices

Correlation matrices with heatmaps were developed in order to explore the associations between the univariate and bivariate measures. To simplify the visualisation, although 5 time scales were computed for each method, only scale 2 and the complexity index will be displayed for the MSE.

To evaluate the association between the univariate measures, three correlation matrices with heatmap were constructed: to assess the association of the entropy values of each signal among themselves (Fig. 5.4) and between the two (Fig. 5.5).

In Figure 5.4, it is noticeable that the correlations (both positive and negative) are stronger when applied to the MHR than when applied to the FHR. In both, the strongest association is between ApEn and SampEn. Entropy measures FuzzEn, CondEn and DispEn also have a significant positive association between themselves. PermEn and BubbEn have a positive association between themselves and a negative one with AttnEn. ApEn and SampEn also reveal a negative correlation with the standard deviation.

Analysing only the MHR entropy values association, ApEn, SampEn, FuzzEn, PermEn, CondEn, DispEn and BubbEn have positive correlations among them, being stronger the ones that were referred to above as common to both signals. Another group constituted by AttnEn and SE also displayed positive associations between themselves and with the mean and standard deviation. Between the first (ApEn, SampEn, FuzzEn, PermEn, CondEn, DispEn and BubbEn) and second groups (AttnEn and SE), the association is negative.

In Figure 5.5, it is noticeable that the correlations of the entropy values computed for the FHR have weak associations with the entropy values of the MHR. This means they are capturing different aspects of the physiological event.

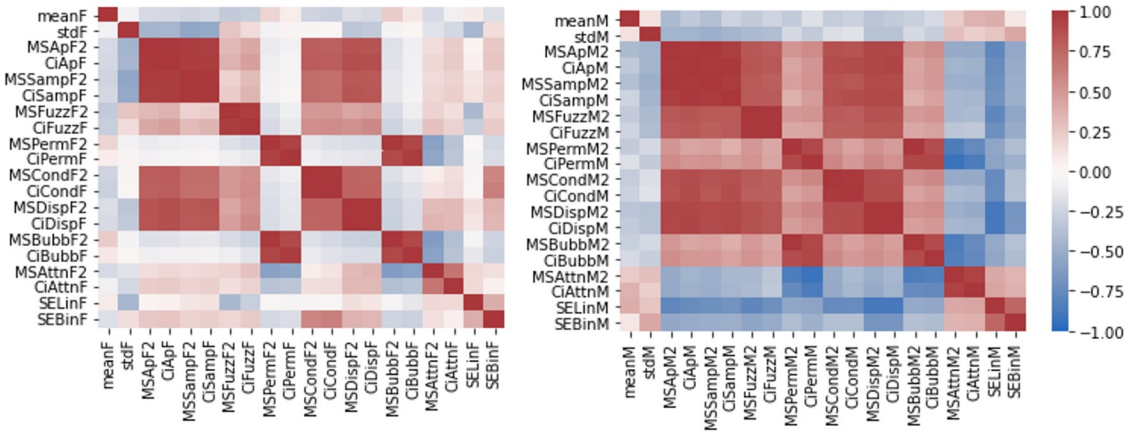

Figure 5.4: Correlation matrices (Spearman coefficient) with heatmap to assess the association of the univariate entropy methods between themselves when applied to fetal heart rate (left) and when applied to maternal heart rate (right). Legend: F – fetal heart rate, M – Maternal Heart Rate, MS – Multiscale, 2 – temporal scale 2, Ci – Complexity index, std – standard deviation, Ap – Approximate, Samp – Sample, Fuzz – Fuzzy, Perm – Permutation, Cond – Conditional, Disp – Dispersion, Bubb – Bubble, Attn – Attention, SE – Self, lin – linear, bin – binning.

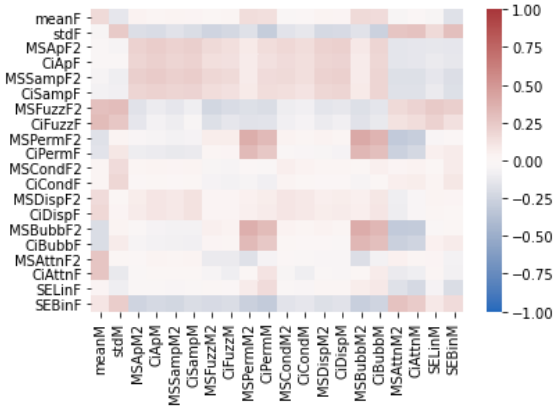

Figure 5.5: Correlation matrices (Spearman coefficient) with heatmap to assess the association between the univariate entropy methods by comparing them when applied to fetal heart rate to when applied to maternal heart rate. The methods also include the mean and standard deviation of each signal. Legend: F – fetal heart rate, M – Maternal Heart Rate, MS – Multiscale, 2 – temporal scale 2, Ci – Complexity index, std – standard deviation, Ap – Approximate, Samp – Sample, Fuzz – Fuzzy, Perm – Permutation, Cond – Conditional, Disp – Dispersion, Bubb – Bubble, Attn – Attention, SE – Self, lin – linear, bin – binning.

The association between the bivariate measures themselves and a comparison of bivariate with univariate measures was also assessed (Figure 5.6 and 5.7). First, regarding the association between the bivariate measures themselves, a significant correlation is the positive one between XApEn when the MHR is used as the template, XSampEn and XFuzzEn. Between XCondEn for MHR and XAp for FHR there is also a positive association.

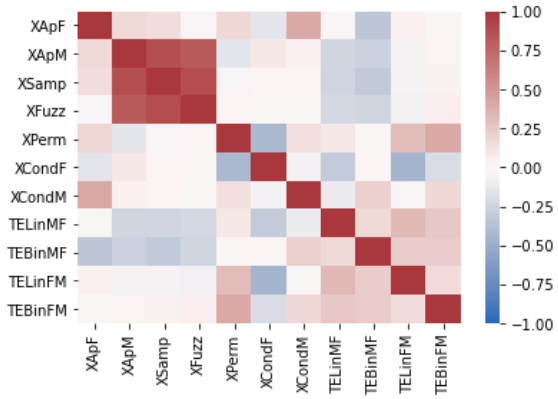

Figure 5.6: Correlation matrices (Spearman coefficient) with heatmap to assess the association of the bivariate entropy methods between themselves when applied to the coupled fetal–maternal heart rate signals. Legend: F – fetal heart rate, M – Maternal Heart Rate, X – Cross, Ap – Approximate, Samp – Sample, Fuzz – Fuzzy, Perm – Permutation, Cond – Conditional, TE – Transfer Entropy, lin – linear, bin – binning, MF – information from MHR to FHR, FM – information from FHR to MHR.

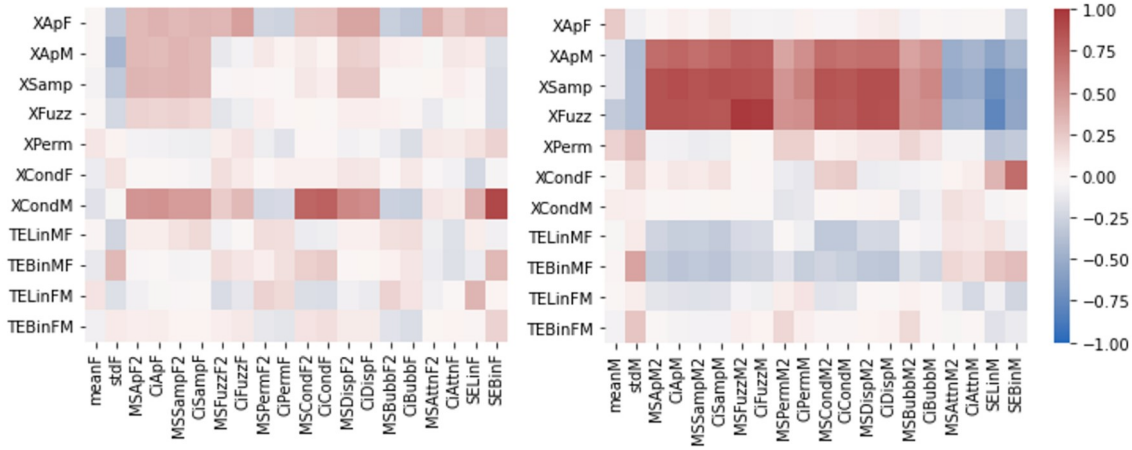

Figure 5.7: Correlation matrices (Spearman coefficient) with heatmap to assess the association between the bivariate entropy methods and the univariate measures (fetal heart rate on the left and maternal heart rate on the right). Legend: F – fetal heart rate, M – Maternal Heart Rate, MS – Multiscale, 2 – temporal scale 2, Ci – Complexity index, X – Cross, std – standard deviation, Ap – Approximate, Samp – Sample, Fuzz – Fuzzy, Perm – Permutation, Cond – Conditional, Disp – Dispersion, Bubb – Bubble, Attn – Attention, SE – Self-Entropy, TE – Transfer Entropy, lin – linear, bin – binning, MF – information from MHR to FHR, FM – information from FHR to MHR.

For the evaluation of the association between the bivariate measures and the univariate measures, similarly to the univariate analysis, the correlations are stronger when the bivariate measures are compared to the MHR entropy values than when compared to the FHR values. In the FHR univariate measures compared with the bivariate values, XCondEn for MHR presents the most significant association with the MSE of FHR, followed by XApEn for FHR. In the comparison with

MHR univariate measures, XApEn for MHR, XSampEn, and XFuzzEn present strong positive correlations with ApEn, SampEn, FuzzEn, CondEn and DispEn; significant positive associations with PermEn and BubbEn; strong negative correlations with Attn, SE and the standard deviation. The TE computed from MHR to FHR with binning estimation presents the opposite relationship that was just described. Another correlation to highlight is the positive one between XCondEn for FHR and SE of MHR.

5.4 Discriminant capacity for fetal acidemia

The Mann-Whitney test was used to assess the discriminant capacity of the entropy methods for fetal acidemia. For that, different time intervals were chosen to assess the discriminatory capacity. Table 5.3 summarises the results of the statistical test for time intervals that correspond to a mean of entropy indices, while Table 5.4 describes the indices computed for 10 min intervals. Additionally, they describe the measures with their median and interquartile interval. Note that although a p-value < 0.05 was considered significant, it does not mean that all the others are to discard. Thus, in both tables, all p-values < 0.1 were presented with the p-values < 0.05 highlighted. (For the extended version of the Mann-Whitney test results: Section A.1.)

Table 5.3: Entropy indices assessment with median, interquartile interval and p-value of the Mann-Whitney test for distinguishing between non-acidemic and acidemic fetuses (considering time intervals longer than 10 min). This table includes all p-values < 0.1, highlighting p-values < 0.05. Legend: FHR – fetal heart rate, MHR – maternal heart rate, sc – scale of the Multiscale Entropy, Ci – Complexity index, Med – medial, Q1 – first quartile, Q3 – third quartile.

Time Interval	**Measure**	**Normal Fetuses Med [Q1;Q3]**	**Acidemic Fetuses Med [Q1;Q3]**	**p-value**
2 hours	Mean FHR	142 [132;148]	134 [124;138]	**0.027**
1st hour	AttnEn MHR sc4	2.378 [2.168;2.576]	2.038 [2.005;2.375]	0.065
	AttnEn MHR sc5	2.25 [2.09;2.46]	2.08 [1.93;2.16]	0.088
	AttnEn Ci	14.0 [13.2;14.9]	13.0 [12.5;14.2]	0.096
2nd hour	Mean FHR	140 [132;145]	131 [123;134]	**0.011**
	XCond FHR	1.31 [1.21;1.39]	1.43 [1.32;1.49]	0.053
	SE bin MHR	1.37 [1.05;1.60]	1.56 [1.11;1.75]	0.059
Last 20 min	SampEn FHR sc1	0.12 [0.10;0.16]	0.15 [0.14;0.16]	0.072
	SampEn FHR sc2	0.21 [0.18;0.29]	0.27 [0.25;0.30]	0.065
	SampEn FHR sc3	0.30 [0.26;0.41]	0.37 [0.35;0.42]	0.072
	SampEn FHR sc4	0.37 [0.32;0.49]	0.48 [0.42;0.54]	0.059
	SampEn FHR sc5	0.44 [0.34;0.58]	0.53 [0.44;0.63]	0.096
	SampEn FHR Ci	1.43 [1.21;1.92]	1.81 [1.62;2.04]	0.065
	TE lin FHR–MHR	15.3 [6.4;28.1] E-04	4.0 [1.6;7.4] E-04	**0.029**

Since the entropy indices were calculated over 10 min segments and the time intervals studied in Table 5.3 are longer than 10 min, these correspond to the mean of the segments included in the desired time interval. For example, the entropy of the last 20 min is equivalent to the mean of the indices calculated for the penultimate 10 min and the last 10 min.

Some relevant results are the ones obtained for the FHR mean, Sample Entropy of FHR and Transfer Entropy from FHR to MHR with the linear estimator. The FHR mean was proved to be significantly different throughout the whole signal, mainly during the second hour. The same can be stated for Transfer Entropy when computed for the last 20 minutes before birth. Regarding Sample Entropy, although not able to significantly differ the groups according to the established threshold (p-value < 0.05), presented promising results for the last 20 minutes before birth.

Table 5.4: Entropy indices assessment with median, interquartile interval and p-value of the Mann-Whitney test for distinguishing between non-acidemic and acidemic fetuses (considering time intervals of 10 min). This table includes all p-values < 0.1, highlighting p-values < 0.05. Legend: FHR – fetal heart rate, MHR – maternal heart rate, sc – scale of the Multiscale Entropy, Ci – Complexity index, Med – medial, Q1 – first quartile, Q3 – third quartile.

Time Interval	**Measure**	**Normal Fetuses Med [Q1;Q3]**	**Acidemic Fetuses Med [Q1;Q3]**	**p-value**
Penult 10 min	ApEn FHR sc3	0.45 [0.37;0.53]	0.54 [0.46;0.60]	0.053
	ApEn FHR sc4	0.53 [0.42;0.61]	0.61 [0.55;0.70]	0.056
	SampEn FHR sc1	0.11 [0.08;0.14]	0.15 [0.14;0.16]	0.053
	SampEn FHR sc2	0.20 [0.15;0.25]	0.27 [0.22;0.30]	**0.045**
	SampEn FHR sc3	0.29 [0.20;0.34]	0.34 [0.35;0.42]	**0.017**
	SampEn FHR sc4	0.35 [0.25;0.40]	0.48 [0.41;0.53]	**0.020**
	SampEn FHR sc5	0.41 [0.27;0.47]	0.54 [0.45;0.60]	**0.031**
	SampEn FHR Ci	1.37 [0.98;1.60]	1.82 [1.58;1.99]	**0.026**
	TE lin FHR–MHR	14.5 [5.2;34.5] E-04	2.1 [1.1;9.6] E-04	**0.034**
Last 10 min	XCondEn MHR	1.40 [1.22;1.47]	1.31 [1.17;1.36]	0.096
	cCondEn MHR sc1	0.36 [0.32;0.43]	0.46 [0.40;0.51]	0.056
	cCondEn MHR sc2	0.57 [0.50;0.67]	0.70 [0.63;0.76]	0.076
	cCondEn MHR sc3	0.71 [0.61;0.79]	0.82 [0.73;0.89]	0.076
	cCondEn MHR sc4	0.78 [0.69;0.86]	0.91 [0.85;0.93]	0.076
	cCondEn MHR Ci	3.30 [2.78;3.66]	3.86 [3.51;4.08]	0.065
	TE lin MHR–FHR	3.4 [0.7;12.1] E-04	11.0 [3.7;32.7] E-04	0.076
	TE bin MHR–FHR	0 [0.000;0.013]	0.023 [0;0.038]	**0.041**

Similar to the previous analysis, the entropy measures that achieved the best discriminatory capacity were Sample Entropy and Transfer Entropy. Focusing on the penultimate 10 minutes before birth, SampEn of FHR and TE from FHR to MHR with the linear estimator were able to significantly distinguish acidemic fetuses. ApEn of FHR for some MSE scales showed promising

results by achieving threshold values. In the last 10 minutes before birth, only Transfer Entropy from MHR to FHR with the binning estimator was able to discriminate fetal acidemia with a p-value < 0.05. cCondEn and XCondEn of MHR showed their potentiality with p-values < 0.1.

The power of the tests conducted was also calculated to verify the capacity of the model to find a statistically significant difference between the groups when the difference does exist [150]. For the calculation, G*Power 3.1 [49] was used. Table 5.5 presents the inputs defined in order to simulate the correspondent statistical power of the test. To emphasise that a medium effect size was considered and a power of 0.223 was obtained.

Table 5.5: Parameters defined to calculate the Mann-Whitney test power and respective result.

Statistical Test	**Effect Size**	**alpha**	**Group 1 Sample Size**	**Group 2 Sample Size**	**Power**
Mann-Whitney (two groups)	Medium ($d = 0.5$)	0.05	54	7	0.223

5.5 Effect of time on the indices

Aiming to evaluate if the entropy indices were being influenced by the time before birth, box-plots were constructed to compare the evolution of non-acidemic and acidemic indices throughout time. The first measure and the easiest to identify the differences in the evolution of the indices throughout time between the groups is the mean of the FHR (Figure 5.8).

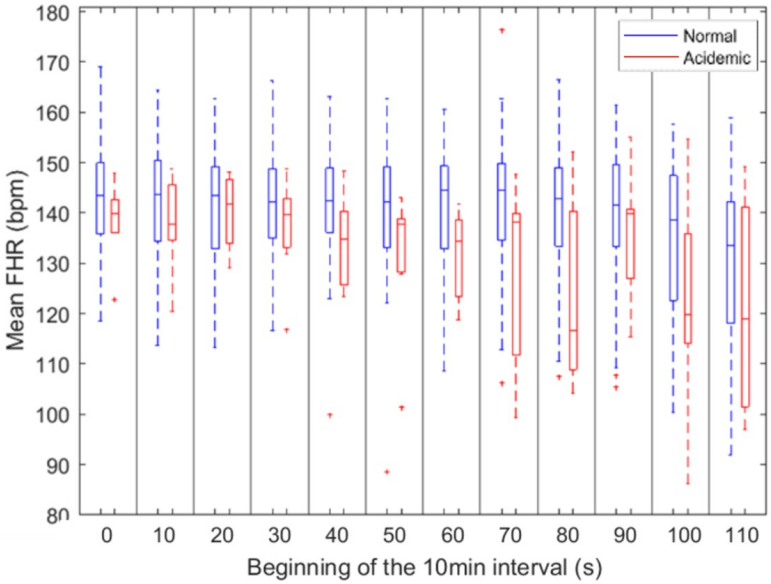

Figure 5.8: Fetal heart rate means evolution throughout time for non-acidemic vs acidemic fetuses. The mean was calculated for each 2-hour record over 10 min segments, being the beginning of the segment indicated on the x-axis.

Regarding the entropy measures, boxplots were also constructed to assess the different evolution of the groups throughout time. However, these differences are not so evident for most indices computed. Figure 5.9 has an example of a boxplot for one univariate entropy applied to FHR and another applied to MHR, one cross-entropy and one information dynamics.

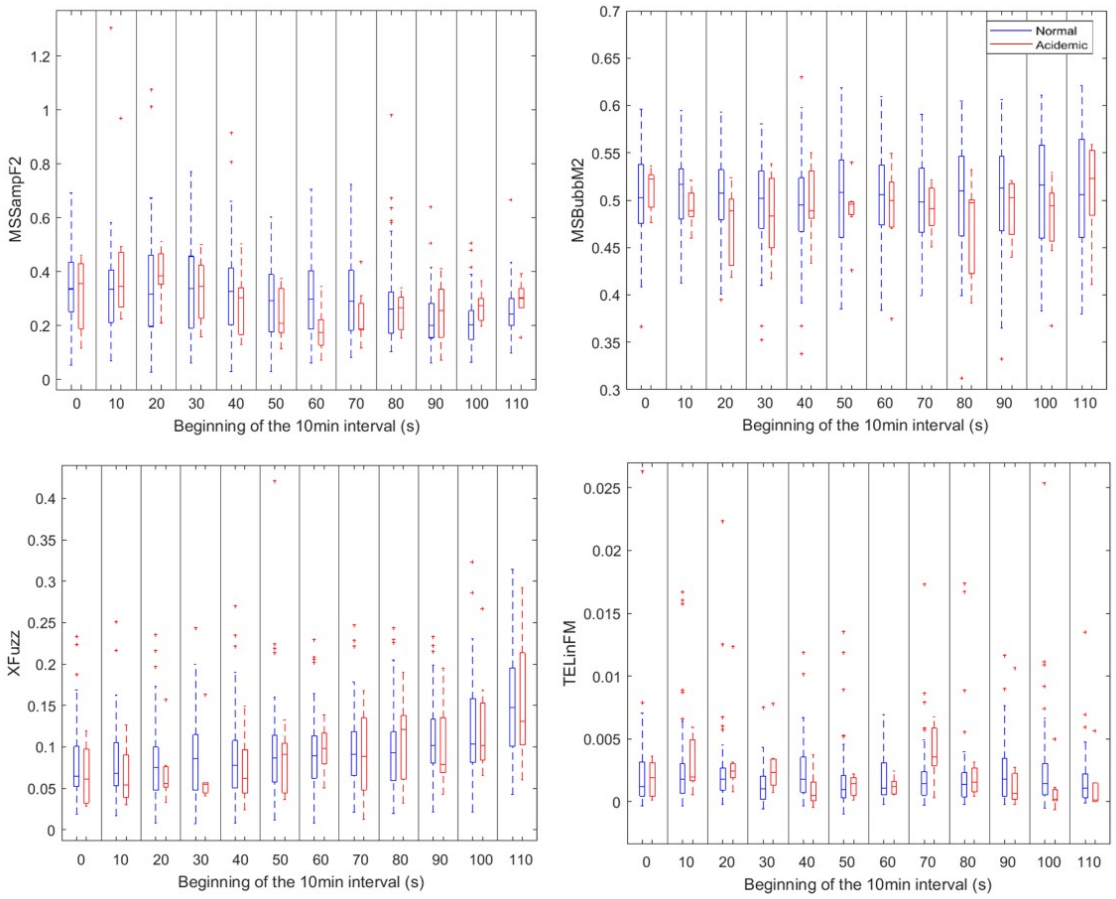

Figure 5.9: Entropy indices evolution throughout time for non-acidemic vs acidemic fetuses. As an example, four measures are depicted: Multiscale Sample Entropy of fetal heart rate (FHR) scale 2 (MSSampF2), Multiscale Bubble Entropy of maternal heart rate (MHR) scale 2 (MSBubbM2), Cross-Fuzzy Entropy (XFuzz) and Transfer Entropy of FHR to MHR with the linear estimator (TELinFM). Each measure was calculated for each 2-hour record over 10 min segments, being the beginning of the segment indicated on the x-axis.

5.6 Discriminant capacity for fetal acidemia considering the influence of time

In order to quantify the influence of time on the evolution of the indices of each group (non-acidemic and acidemic), Generalised Linear Mixed Models were computed and fitted into the data. As detailed in Section 4.2.3, two different models were tested, varying the time as a fixed

and a random effect. Tables 5.6 and 5.7 are examples of the results obtained for each model for 5 of the measures tested, including the FHR mean, an example of a univariate entropy applied to FHR and another applied to MHR, one cross-entropy and one information dynamics. These tables reveal high AIC values for the fitting of the models. No significant results (p-values > 0.05) were found regarding the influence of the predictor variables (fixed effects) on the outcome of the models (acidemic or non-acidemic). (For the extended version of the GLMM results: Section A.2.)

Table 5.6: Output parameters of the Generalised Linear Mixed Models computed considering entropy method and time fixed effects, and subject variability a random effect. As an example, four measures are presented: scale 2 of Multiscale Sample Entropy of fetal heart rate (FHR), scale 2 of Multiscale Bubble Entropy of maternal heart rate (MHR), Cross-Fuzzy Entropy and Transfer Entropy of FHR to MHR with the linear estimator.

Measure	**Model fit**	**Fixed effects coefficients (95% CIs)**				**Random effects**
	AIC	**'Method' Estimate**	**'Method' p-value**	**'Time' Estimate**	**'Time' p-value**	**'Subject' Estimate**
mean FHR	5021	-0.014	0.536	-0.0037	0.972	3.535
XFuzzEn	5009	-2.208	0.812	0.0191	0.872	3.545
SampEn FHR sc2	5007	-0.169	0.950	0.0038	0.972	3.546
BubbEn FHR sc2	5009	-1.400	0.912	0.0073	0.953	3.543
TE lin FHR-MHR	5007	-13.001	0.923	0.0047	0.964	3.546

Table 5.7: Output parameters of the Generalised Linear Mixed Model computed considering entropy method a fixed effect, and time and subject variability as random effects. As an example, four measures are represented: scale 2 of Multiscale Sample Entropy of fetal heart rate (FHR), scale 2 of Multiscale Bubble Entropy of maternal heart rate (MHR), Cross-Fuzzy Entropy and Transfer Entropy of FHR to MHR with the linear estimator.

Measure	**Model fit**	**Fixed effects coefficients (95% CIs)**		**Random effects**	
	AIC	**'Method' Estimate**	**'Method' p-value**	**'Time' Estimate**	**'Subject' Estimate**
mean FHR	5021	-0.014	0.537	3.30E-05	3.534
XFuzzEn	5008	-1.493	0.854	3.19E-05	3.545
SampEn FHR sc2	5007	-0.194	0.940	2.85E-05	3.546
BubbEn FHR sc2	5008	-1.360	0.914	1.70E-05	3.544
TE lin FHR-MHR	5007	-13.522	0.919	1.98E-05	3.546

5.7 Discussion

The main results achieved in the course of this work are related to the correlation between the indices and their discriminant capacity for fetal acidemia, which was assessed with two different approaches.

Starting with the execution time of the entropy indices, this test was motivated by the observation that the information dynamics-based entropy methods were taking a considerably long amount of time to compute. Since this could represent a barrier to their application throughout the work, this study was meant to find the cause of this problem and minimise it. A randomly generated signal allowed to identify kernel and k-nearest neighbours estimators as the ones with significantly higher computation time. Thus, a decision was made to leave out these estimators to ensure the feasibility of the subsequent analysis. This ensured the practicability of the analysis for real-world applications since it has to be made in a timelier manner.

Note that since all entropy measures were kept, the study did not suffer a significant impact from the removal of the estimators. However, these estimators will likely bring additional interesting aspects that the used ones do not reveal. Therefore, future optimisation of their computational time might be beneficial.

A correlation assessment can reveal interesting aspects of the relationships not only between different measures but also between the signals from which these were computed. Significant positive associations were found between ApEn, SampEn, FuzzEn, cCondEn and DispEn when applied to FHR and also when applied to MHR. Considering the algorithms of these measures and the methods that are the basis of their development, these correlations could be anticipated. The same can be stated for the positive association between PermEn and BubbEn. These last two measures also presented a negative association with AttnEn, which is an interesting finding that might be the focus of future study: a comparison of the behaviour of these indices.

When comparing univariate measures applied to FHR with the same measures but applied to MHR, almost no significant correlation is immediately identified. This lack of associations might be explained by the fact that FHR and MHR are distinct physiological signals with different variability. Additionally, it is necessary to consider that these signals were obtained with different methodologies: FHR from ultrasound and MHR from ECG. Therefore, they might have been influenced by noise or the differences between the acquisition procedures.

Similar to the univariate measures, XApEn, XSampEn and XFuzzEn present a high positive correlation, which, again, can be explained by the similarity of their theoretical formulations. The Cross-Entropy methods, in general, have a higher association with the univariate measures that are applied to the MHR than with the same ones but applied to the FHR, suggesting a closer relationship with the overall behaviour of the MHR. Another interesting finding was the significant association of the XCond of the MHR with both the cCondEn and the SE (which computes the CondEn in its algorithm) of the FHR. This finding highlights the possibility of the FHR and MHR being related and influencing each other, hypothesizing that the predictability of FHR patterns may be affected by MHR dynamics. A similar situation was verified between XCondEn of FHR

and SE of MHR.

This type of study supports the correct implementation of the measures on the database since the values obtained behave as would be expected from their theoretical formulation analysis. Regarding the not yet so studied measures, the novel findings on their relationships with known measures might help understand their behaviours. It is important to state that further studies with wider databases are needed to state the validity and reliability of these conclusions since factors such as stress, hormonal fluctuations, or fetal movements can influence the indices obtained. Furthermore, this highlighted the advantage of using multiple measures since they can reveal different aspects of both FHR and MHR and possibly improve the comprehension of their underlying mechanisms.

The entropy values between the acidemic and non-acidemic groups were compared using the Mann-Whitney test since the data do not adhere to the assumptions of normality required by other tests. Regarding the longer time intervals tested (1 or 2 hours duration), most measures were unable to distinguish the groups. However, when focusing 10min length time intervals, this number increased. For all cases, the entropy was computed over 10min length segments. To obtain the entropy value of a longer time interval, the mean of the segments included in that time window was calculated. This can have a negative effect on the discriminant capacity when longer time intervals are considered since some of the information is lost on the way. Additionally, this can also mean that fetal acidemia might be related to faster subtle FHR pattern modifications, which can only be identified when focusing on a shorter time interval.

To emphasise the significant results (p-value < 0.05) found for Multiscale Sample Entropy of FHR and Transfer Entropy from FHR to MHR, both when computed in the penultimate 10 min before birth. This data implies that in distinguishing acidemic from non-acidemic individuals, the entropy measure during this particular period of time span is particularly significant. Regarding the last 10 min before birth, some almost borderline values were encountered, but that might be affected by the increase of movements and contractions frequency closer to birth that consequently increases the noise of the signals.

Besides the p-value, another important metric is the power of the test, which was equal to 22.3%. Considering that it is widely accepted that a test is reliable if its power is of at least 80%, the low power obtained might justify the lack of discriminating indices. The low power of the test also suggests a low probability of the measures being able to identify differences between groups when they do exist (false negatives), which can be due to the insufficient sample size in the study.

Taking into account both the low power of the test and the capability of some measures to still identify differences between the groups in the penultimate 10 min before birth, there is an indication of the entropy indices being promising measures for distinguishing between the acidemic and non-acidemic groups. This evidenced the potential of measures such as Sample Entropy and Transfer Entropy to improve fetal acidemia diagnosis. Further studies, including larger sample sizes, would be needed to generalise the current findings.

Another important aspect to note is relative to the binning estimator. When TE is computed with this estimator, several values are equal to zero. In Table 5.4, for the last 10 minutes, the values computed for Transfer Entropy from MHR to FHR have a median of zero, indicating that

most subjects had that value assigned to them. Therefore, although the test found a statistically significant difference between the groups, this might only be to the abnormally high number of normal fetuses that obtained a zero value for this measure, and the real capacity of the method to discriminate the groups might not be being evaluated correctly. A parameter adjustment might be needed to improve the veracity of the results, such as the increase in quantisation levels. However, a study would have to be pursued to optimise the rest of the parameters in function of this increase.

The research on the influence of time on entropy indices was made by resorting to Generalised Linear Mixed Models. For that, two different models were designed: one considering time as a fixed effect and another as a random effect. However, in both cases, neither the entropy value nor the time were found to be statistically different (p-value < 0.05) between groups.

Regarding the fixed effects coefficients, their estimate gives information on how the outcome would change as a function of the predictor variable. In this case, for the measures presented, the estimation of the group is expected to decrease with the increase of the entropy value, and for most measures, it is expected to increase slightly with the increase of time. Although the lack of statistically significant results and the small coefficients estimated for the time as a predictor variable of the group could imply that time does not significantly affect entropy indices, it is essential to take into account the characteristics of the study that might influence this outcome, such as the small sample size.

In the random effects, the estimate of time quantifies the variation in the result variable that is due to the time variability within each subject. The fact that this value is substantially lower than the estimate of time as a fixed effect suggests that the overall effect of time has a higher influence on the group than the individual time variations.

While the AIC value is a comparative measure to assess which of two or more models fit the data better, a value around 5000 is indicative that the present model might not be the most adequate for the data in the study. Further research could include alternative models or the inclusion of additional variables.

Chapter 6

Conclusion

In this chapter, the objectives of the study, the main results obtained and their scientific relevance are recapitulated. The achievement of the objectives proposed is also tackled. Then, the main conclusions drawn from the work developed are analysed in light of their limitations. Finally, considering the findings of this dissertation and the literature review, relevant future work is suggested.

6.1 Main contributions

The main objectives of this dissertation are the estimation of information theory-based indices of FHR–MHR dynamics and the assessment of their discriminant capacity for the diagnosis of fetal acidemia. In order to achieve this, several entropy measures chosen based on their current application in physiological signals were computed from a database with simultaneous FHR and MHR real signals of the two hours prior to birth. Signal segments of 10 minutes were selected to compute the indices, which is appropriate for clinical practice analysis: rapid subtle pattern modifications might be related to emerging health issues, and the analysis is performed in a timelier manner.

A correlation analysis between the different indices computed supported the appropriate implementation of the measures on the database since the expected relationships between measures with similar theoretical formulations were verified. For example, positive associations were found between Approximate, Sample and Fuzzy Entropy. Additionally, associations between not yet so studied measures with different approaching algorithms were found, but further studies are needed to verify the generalisation of these relationships since several maternal and fetal aspects can influence them. Furthermore, this analysis highlighted the advantage of using multiple measures since they can reveal different aspects of both FHR and MHR and possibly improve the comprehension of their underlying mechanisms.

The discriminant capacity of the indices computed was assessed with the Mann-Whitney test. To highlight the statistically significant results (p-value < 0.05) of Multiscale Sample Entropy of FHR and Transfer Entropy from FHR to MHR, both were computed in the penultimate 10 min

before birth. More methods were able to discriminate fetal acidemia in the intervals closer to birth, suggesting that this pathology might be related to faster subtle FHR pattern modifications that are more likely to occur with the progression of labour. It is important to note that these results were obtained with low statistical power (22.3%) due to the small sample size of the data, meaning that a wider database is likely to have even more measures able to distinguish fetal acidemia.

In order to evaluate the influence of time on the capacity of the indices to distinguish acidemic fetuses, Generalised Linear Mixed Models were designed: one considering time as a fixed effect and another as a random effect. In both, the entropy value was set as a fixed effect, and the within group subject variability was accounted for in random effects. However, in both models, neither the entropy value nor the time were found to be statistically different (p-value < 0.05) between groups. Although the lack of statistically significant results and the small coefficients estimated for the time as a predictor variable of the group could imply that time does not significantly affect entropy indices, it is essential to take into account the characteristics of the study that might influence this outcome, such as the small sample size. Furthermore, AIC values around 5000 were obtained, suggesting that the model might not be adequately fitting the data.

Taking all this into account, it is possible to state that the main objective of the dissertation was achieved: information theory-based indices of FHR–MHR dynamics were estimated and proven to be able to discriminate fetal acidemia when tested in a database with the simultaneous FHR and MHR signals. Therefore, the results supported the recommendation of the collection of the MHR in clinical practice, which is done in a simple and non-invasive way and could improve fetal acidemia detection. This work also provided a comprehensive analysis of the capacity of different entropy-based algorithms to extract information from these signals, which can aid clinicians in interpreting these signals. This dissertation also provided guidelines for the application of the measures in similar studies.

6.2 Limitations

Despite having achieved significant and satisfactory results, such as the evidence of the capacity of information theory-based indices to improve fetal acidemia detection, the conclusions drawn must be analysed in light of their limitations.

The major limitation of this study was the small sample size of the database used: 61 subjects, of which only 7 were acidemic. This limited number of records restricts the possibility of generalising the conclusions made. On the other hand, the differences observed between the subjects in the study, e.g. in the type of labour and gestational age, included within subject variability and allowed the results to be more representative of the overall population.

The information theory-based indices chosen and on which the work was based, although supported by the literature review conducted, are not yet widely considered significant for clinical analysis. Besides, the interpretation of the outcome of some of these measures on physiological signals applications is also still being investigated. Thus, further studies are needed to establish the clinical relevance of these indices as well as their interpretation in biomedical signals.

Moreover, this work resorted to a time interval of 10 minutes to compute the indices. Although it is in accordance with related biomedical signal studies, the exploration of different time windows could improve the analysis of the signals.

Despite the aforementioned limitations, the present work lays the ground for further investigations on using entropy measures applied to FHR and MHR simultaneous signals to improve fetal monitoring and clinical diagnosis.

6.3 Future work

Several aspects detailed throughout this dissertation can be explored to enhance the knowledge of the relationship between entropy and FHR–MHR dynamics. To start, the estimators offered by ITS to compute Self-Entropy and Transfer Entropy could be explored. Regarding the binning estimator, it was found that when used to calculate Transfer Entropy, most results were equal to zero. An increase in the quantisation levels is suggested but requires an adjustment of the rest of the parameters that would have to be investigated. For kernel and k-nearest neighbour, an improvement in their computation times would make them more suitable for clinical practice and allow them to be easily used on FHR–MHR simultaneous signals analysis.

The most obvious suggestion for further research is to expand the study to a bigger sample size database with variability in subject features. This would allow a more representative study to be conducted, leading to a more robust statistical analysis and the possibility to generalise the findings. Additionally, the study might be extended with the inclusion of relevant signals, such as uterine contractions, or additional entropy measures, such as Multiscale Cross Entropy.

Different time windows for the computation of the entropy indices could also be considered. For example, in the study of the influence of time on the discriminant capacity of the indices for fetal acidemia, calculating the entropy using sliding windows might improve the Generalised Linear Mixed Models analysis.

Finally, an essential study to validate the results and their applicability to clinical practice is the association between entropy measures and clinical subject features, such as the type of labour or gestational age. This relationship can give insightful information on the possible clinical use of entropy measurements as tools for prediction or diagnosis. These studies quantify the clinical relevance of entropy measures and their applicability in fetal monitoring and fetal acidemia diagnosis.

Appendix A

Extended results

A.1 Mann-Whitney test results

Table A.1: Median, interquartile interval and p-value of the Mann-Whitney test for the 2 hour signal.

Measure	**Normal Fetuses Med [Q1;Q3]**	**Acidemic Fetuses Med [Q1;Q3]**	**p-value**
mean FHR	141.6 [132.2 ; 148.3]	134.1 [124.0 ; 137.8]	0.027
std FHR	14.0 [11.6 ; 16.4]	15.5 [12.4 ; 19.6]	0.336
mean MHR	88.0 [81.6 ; 96.0]	82.1 [79.3 ; 89.2]	0.186
std MHR	7.58 [6.60 ; 8.92]	9.05 [7.21 ; 11.01]	0.164
XApEn FHR	0.13 [0.01 ; 0.19]	0.10 [0.02 ; 0.18]	0.743
XApEn MHR	0.32 [0.22 ; 0.40]	0.28 [0.16 ; 0.37]	0.396
XSampEn	0.37 [0.30 ; 0.42]	0.32 [0.27 ; 0.46]	0.830
XFuzzEn	0.092 [0.070 ; 0.113]	0.082 [0.056 ; 0.125]	0.659
XPermEn	0.015 [0.006 ; 0.031]	0.010 [0.005 ; 0.018]	0.293
XCondEn FHR	1.29 [1.22 ; 1.38]	1.29 [1.26 ; 1.43]	0.282
XCondEn MHR	1.10 [1.02 ; 1.18]	1.13 [1.09 ; 1.23]	0.396
ApEn FHR sc1	0.27 [0.23 ; 0.31]	0.26 [0.24 ; 0.29]	0.760
ApEn FHR sc2	0.42 [0.38 ; 0.49]	0.43 [0.38 ; 0.45]	0.847
ApEn FHR sc3	0.51 [0.47 ; 0.59]	0.53 [0.48 ; 0.57]	0.991
ApEn FHR sc4	0.58 [0.54 ; 0.67]	0.59 [0.55 ; 0.66]	0.919
ApEn FHR sc5	0.64 [0.59 ; 0.72]	0.65 [0.60 ; 0.72]	0.865

Continued on next page

Table A.1: Median, interquartile interval and p-value of the Mann-Whitney test for the 2 hour signal. (Continued)

ApEn FHR Ci	2.42 [2.21 ; 2.78]	2.52 [2.23 ; 2.65]	1.000
SampEn FHR sc1	0.18 [0.15 ; 0.22]	0.17 [0.16 ; 0.21]	0.579
SampEn FHR sc2	0.29 [0.25 ; 0.34]	0.31 [0.24 ; 0.33]	0.830
SampEn FHR sc3	0.38 [0.33 ; 0.46]	0.42 [0.33 ; 0.43]	0.973
SampEn FHR sc4	0.46 [0.39 ; 0.55]	0.51 [0.39 ; 0.53]	0.955
SampEn FHR sc5	0.53 [0.44 ; 0.64]	0.58 [0.45 ; 0.62]	0.919
SampEn FHR Ci	1.86 [1.58 ; 2.22]	2.03 [1.56 ; 2.08]	0.937
FuzzEn FHR sc1	0.041 [0.032 ; 0.044]	0.034 [0.030 ; 0.046]	0.955
FuzzEn FHR sc2	0.075 [0.061 ; 0.084]	0.062 [0.059 ; 0.088]	1.000
FuzzEn FHR sc3	0.12 [0.10 ; 0.13]	0.10 [0.09 ; 0.14]	0.919
FuzzEn FHR sc4	0.15 [0.12 ; 0.17]	0.13 [0.12 ; 0.18]	0.973
FuzzEn FHR sc5	0.18 [0.15 ; 0.20]	0.16 [0.14 ; 0.21]	0.973
FuzzEn FHR Ci	0.57 [0.47 ; 0.63]	0.48 [0.44 ; 0.66]	0.955
PermEn FHR sc1	1.19 [1.08 ; 1.23]	1.20 [1.13 ; 1.26]	0.579
PermEn FHR sc2	1.91 [1.83 ; 1.96]	1.88 [1.87 ; 1.91]	0.422
PermEn FHR sc3	2.07 [2.04 ; 2.11]	2.06 [2.05 ; 2.07]	0.709
PermEn FHR sc4	2.19 [2.15 ; 2.22]	2.17 [2.16 ; 2.20]	0.901
PermEn FHR sc5	2.27 [2.24 ; 2.30]	2.27 [2.26 ; 2.29]	0.919
PermEn FHR Ci	9.62 [9.40 ; 9.79]	9.60 [9.53 ; 9.70]	0.692
cCondEn FHR sc1	0.19 [0.18 ; 0.22]	0.20 [0.18 ; 0.22]	0.937
cCondEn FHR sc2	0.32 [0.30 ; 0.36]	0.33 [0.30 ; 0.36]	0.812
cCondEn FHR sc3	0.41 [0.38 ; 0.46]	0.42 [0.39 ; 0.47]	0.659
cCondEn FHR sc4	0.48 [0.44 ; 0.53]	0.51 [0.46 ; 0.54]	0.490
cCondEn FHR sc5	0.54 [0.50 ; 0.60]	0.57 [0.52 ; 0.62]	0.359
cCondEn FHR Ci	1.94 [1.79 ; 2.17]	2.02 [1.86 ; 2.21]	0.579
DispEn FHR sc1	1.21 [1.15 ; 1.24]	1.22 [1.17 ; 1.22]	0.955
DispEn FHR sc2	1.31 [1.25 ; 1.35]	1.32 [1.26 ; 1.33]	0.937
DispEn FHR sc3	1.38 [1.32 ; 1.44]	1.38 [1.33 ; 1.40]	0.865
DispEn FHR sc4	1.44 [1.37 ; 1.51]	1.43 [1.40 ; 1.47]	0.847

Continued on next page

Table A.1: Median, interquartile interval and p-value of the Mann-Whitney test for the 2 hour signal. (Continued)

DispEn FHR sc5	1.50 [1.42 ; 1.57]	1.48 [1.45 ; 1.52]	0.901
DispEn FHR Ci	6.86 [6.55 ; 7.09]	6.83 [6.59 ; 6.93]	0.865
BubbEn FHR sc1	0.22 [0.20 ; 0.23]	0.22 [0.21 ; 0.24]	0.830
BubbEn FHR sc2	0.36 [0.34 ; 0.38]	0.35 [0.34 ; 0.36]	0.519
BubbEn FHR sc3	0.44 [0.42 ; 0.46]	0.43 [0.42 ; 0.43]	0.709
BubbEn FHR sc4	0.50 [0.48 ; 0.51]	0.49 [0.48 ; 0.50]	0.795
BubbEn FHR sc5	0.54 [0.52 ; 0.56]	0.54 [0.53 ; 0.55]	0.883
BubbEn FHR Ci	2.06 [1.97 ; 2.13]	2.04 [2.02 ; 2.06]	0.675
AttnEn FHR sc1	3.37 [3.20 ; 3.53]	3.28 [3.06 ; 3.50]	0.462
AttnEn FHR sc2	3.75 [3.68 ; 3.84]	3.82 [3.74 ; 3.84]	0.209
AttnEn FHR sc3	3.36 [3.32 ; 3.45]	3.40 [3.33 ; 3.42]	0.743
AttnEn FHR sc4	3.07 [2.99 ; 3.15]	3.07 [3.04 ; 3.10]	0.865
AttnEn FHR sc5	2.83 [2.77 ; 2.93]	2.85 [2.81 ; 2.88]	0.726
AttnEn FHR Ci	16.4 [16.3 ; 16.6]	16.3 [16.2 ; 16.6]	0.709
ApEn MHR sc1	0.63 [0.52 ; 0.75]	0.57 [0.50 ; 0.72]	0.709
ApEn MHR sc2	0.90 [0.74 ; 1.00]	0.83 [0.74 ; 1.03]	0.991
ApEn MHR sc3	1.00 [0.84 ; 1.11]	0.93 [0.87 ; 1.13]	0.919
ApEn MHR sc4	1.08 [0.93 ; 1.17]	1.00 [0.93 ; 1.20]	0.795
ApEn MHR sc5	1.07 [0.96 ; 1.17]	1.02 [0.96 ; 1.20]	0.919
ApEn MHR Ci	4.68 [3.96 ; 5.22]	4.35 [4.00 ; 5.26]	1.000
SampEn MHR sc1	0.51 [0.43 ; 0.62]	0.46 [0.42 ; 0.56]	0.611
SampEn MHR sc2	0.81 [0.65 ; 0.92]	0.74 [0.69 ; 0.90]	0.991
SampEn MHR sc3	0.97 [0.78 ; 1.11]	0.88 [0.84 ; 1.10]	0.955
SampEn MHR sc4	1.10 [0.89 ; 1.26]	1.02 [0.92 ; 1.29]	0.795
SampEn MHR sc5	1.15 [0.96 ; 1.32]	1.10 [0.96 ; 1.38]	0.937
SampEn MHR Ci	4.60 [3.71 ; 5.22]	4.17 [3.84 ; 5.24]	1.000
FuzzEn MHR sc1	0.14 [0.10 ; 0.18]	0.12 [0.08 ; 0.20]	0.760
FuzzEn MHR sc2	0.21 [0.15 ; 0.27]	0.18 [0.12 ; 0.32]	0.777
FuzzEn MHR sc3	0.29 [0.20 ; 0.34]	0.24 [0.17 ; 0.42]	0.865

Continued on next page

Table A.1: Median, interquartile interval and p-value of the Mann-Whitney test for the 2 hour signal. (Continued)

FuzzEn MHR sc4	0.33 [0.25 ; 0.42]	0.29 [0.20 ; 0.49]	0.847
FuzzEn MHR sc5	0.36 [0.28 ; 0.46]	0.34 [0.22 ; 0.53]	0.847
FuzzEn MHR Ci	1.37 [0.98 ; 1.63]	1.16 [0.80 ; 1.97]	0.865
PermEn MHR sc1	1.25 [1.19 ; 1.31]	1.21 [1.18 ; 1.25]	0.171
PermEn MHR sc2	2.20 [2.14 ; 2.25]	2.19 [2.14 ; 2.20]	0.359
PermEn MHR sc3	2.36 [2.30 ; 2.40]	2.33 [2.32 ; 2.37]	0.549
PermEn MHR sc4	2.43 [2.37 ; 2.48]	2.43 [2.42 ; 2.47]	0.743
PermEn MHR sc5	2.46 [2.41 ; 2.51]	2.48 [2.44 ; 2.52]	0.462
PermEn MHR Ci	10.7 [10.5 ; 11.0]	10.7 [10.5 ; 10.8]	0.611
cCondEn MHR sc1	0.39 [0.34 ; 0.46]	0.44 [0.36 ; 0.48]	0.435
cCondEn MHR sc2	0.62 [0.55 ; 0.71]	0.69 [0.57 ; 0.73]	0.396
cCondEn MHR sc3	0.74 [0.67 ; 0.83]	0.83 [0.67 ; 0.88]	0.409
cCondEn MHR sc4	0.82 [0.74 ; 0.92]	0.91 [0.76 ; 0.97]	0.462
cCondEn MHR sc5	0.88 [0.81 ; 0.97]	0.97 [0.80 ; 1.03]	0.549
cCondEn MHR Ci	3.45 [3.12 ; 3.86]	3.83 [3.17 ; 4.10]	0.435
DispEn MHR sc1	1.39 [1.35 ; 1.44]	1.38 [1.33 ; 1.45]	0.812
DispEn MHR sc2	1.57 [1.51 ; 1.63]	1.55 [1.48 ; 1.67]	0.901
DispEn MHR sc3	1.65 [1.58 ; 1.72]	1.63 [1.55 ; 1.78]	0.955
DispEn MHR sc4	1.72 [1.64 ; 1.78]	1.69 [1.60 ; 1.84]	0.955
DispEn MHR sc5	1.76 [1.67 ; 1.82]	1.72 [1.63 ; 1.88]	1.000
DispEn MHR Ci	8.08 [7.77 ; 8.39]	7.96 [7.59 ; 8.62]	0.901
BubbEn MHR sc1	0.24 [0.23 ; 0.24]	0.23 [0.22 ; 0.24]	0.178
BubbEn MHR sc2	0.50 [0.47 ; 0.53]	0.50 [0.47 ; 0.50]	0.384
BubbEn MHR sc3	0.58 [0.55 ; 0.60]	0.57 [0.56 ; 0.59]	0.611
BubbEn MHR sc4	0.60 [0.59 ; 0.62]	0.60 [0.59 ; 0.62]	0.490
BubbEn MHR sc5	0.60 [0.59 ; 0.61]	0.60 [0.59 ; 0.61]	0.726
BubbEn MHR Ci	2.52 [2.46 ; 2.59]	2.52 [2.44 ; 2.56]	0.692
AttnEn MHR sc1	3.62 [3.46 ; 3.86]	3.58 [3.41 ; 3.78]	0.627
AttnEn MHR sc2	3.09 [2.90 ; 3.24]	2.98 [2.96 ; 3.11]	0.564

Continued on next page

Table A.1: Median, interquartile interval and p-value of the Mann-Whitney test for the 2 hour signal. (Continued)

AttnEn MHR sc3	2.70 [2.43 ; 2.85]	2.56 [2.44 ; 2.67]	0.336
AttnEn MHR sc4	2.42 [2.23 ; 2.67]	2.30 [2.13 ; 2.42]	0.164
AttnEn MHR sc5	2.33 [2.12 ; 2.53]	2.11 [2.04 ; 2.38]	0.157
AttnEn MHR Ci	14.2 [13.3 ; 15.1]	13.6 [13.3 ; 14.0]	0.186
SE lin FHR	1.69 [1.51 ; 1.81]	1.80 [1.56 ; 1.89]	0.384
SE bin FHR	0.98 [0.92 ; 1.05]	1.07 [0.92 ; 1.20]	0.178
SE lin MHR	1.35 [1.13 ; 1.54]	1.25 [1.13 ; 1.72]	0.726
SE bin MHR	1.00 [0.91 ; 1.07]	1.08 [0.92 ; 1.15]	0.217
TE lin MHR–FHR	1.89 [1.52 ; 2.70] E-03	1.78 [1.32 ; 2.48] E-03	0.448
TE bin MHR–FHR	4.60 [3.26 ; 7.38] E-03	6.16[3.72 ; 9.72] E-03	0.336
TE lin FHR–MHR	2.14 [1.34 ; 3.02] E-03	1.95 [1.62 ; 2.31] E-03	0.830
TE bin FHR–MHR	5.00 [2.94 ; 8.12] E-03	5.62 [4.92 ; 7.20] E-03	0.777

Table A.2: Median, interquartile interval and p-value of the Mann-Whitney test for the first hour before birth.

Measure	**Normal Fetuses Med [Q1;Q3]**	**Acidemic Fetuses Med [Q1;Q3]**	**p-value**
mean FHR	142.1 [135.4 ; 149.6]	137.4 [134.4 ; 141.3]	0.209
std FHR	9.5 [7.2 ; 12.5]	12.0 [6.5 ; 16.5]	0.627
mean MHR	84.5 [79.4 ; 93.0]	82.0 [75.4 ; 86.1]	0.164
std MHR	6.26 [5.66 ; 7.71]	6.83 [5.99 ; 8.29]	0.519
XApEn FHR	0.12 [0.01 ; 0.22]	0.16 [-0.11 ; 0.22]	0.883
XApEn MHR	0.36 [0.27 ; 0.47]	0.27 [0.16 ; 0.45]	0.314
XSampEn	0.39 [0.33 ; 0.47]	0.33 [0.32 ; 0.48]	0.760
XFuzzEn	0.080 [0.054 ; 0.103]	0.067 [0.043 ; 0.081]	0.359
XPermEn	0.007 [0.001 ; 0.021]	0.006 [0.000 ; 0.008]	0.533
XCondEn FHR	1.29 [1.19 ; 1.38]	1.26 [1.23 ; 1.37]	0.973
XCondEn MHR	1.07 [0.97 ; 1.16]	1.09 [0.92 ; 1.21]	0.743
ApEn FHR sc1	0.29 [0.23 ; 0.36]	0.25 [0.22 ; 0.36]	0.830

Continued on next page

Table A.2: Median, interquartile interval and p-value of the Mann-Whitney test for the first hour before birth. (Continued)

ApEn FHR sc2	0.45 [0.37 ; 0.53]	0.45 [0.37 ; 0.56]	0.883
ApEn FHR sc3	0.55 [0.46 ; 0.65]	0.58 [0.47 ; 0.67]	0.709
ApEn FHR sc4	0.62 [0.53 ; 0.71]	0.68 [0.54 ; 0.75]	0.692
ApEn FHR sc5	0.66 [0.58 ; 0.78]	0.75 [0.60 ; 0.82]	0.692
ApEn FHR Ci	2.60 [2.17 ; 3.03]	2.73 [2.20 ; 3.21]	0.795
SampEn FHR sc1	0.21 [0.16 ; 0.27]	0.18 [0.15 ; 0.26]	0.777
SampEn FHR sc2	0.35 [0.26 ; 0.40]	0.33 [0.24 ; 0.41]	0.937
SampEn FHR sc3	0.42 [0.34 ; 0.52]	0.45 [0.33 ; 0.55]	0.847
SampEn FHR sc4	0.52 [0.41 ; 0.63]	0.56 [0.40 ; 0.65]	0.760
SampEn FHR sc5	0.58 [0.48 ; 0.72]	0.65 [0.46 ; 0.76]	0.709
SampEn FHR Ci	2.07 [1.63 ; 2.52]	2.18 [1.58 ; 2.62]	0.883
FuzzEn FHR sc1	0.024 [0.018 ; 0.032]	0.018 [0.011 ; 0.026]	0.178
FuzzEn FHR sc2	0.043 [0.034 ; 0.059]	0.033 [0.021 ; 0.047]	0.193
FuzzEn FHR sc3	0.070 [0.052 ; 0.091]	0.055 [0.036 ; 0.074]	0.235
FuzzEn FHR sc4	0.10 [0.07 ; 0.12]	0.08 [0.05 ; 0.10]	0.193
FuzzEn FHR sc5	0.12 [0.08 ; 0.14]	0.09 [0.07 ; 0.12]	0.193
FuzzEn FHR Ci	0.35 [0.26 ; 0.44]	0.28 [0.18 ; 0.36]	0.209
PermEn FHR sc1	1.20 [1.10 ; 1.24]	1.23 [1.11 ; 1.24]	0.659
PermEn FHR sc2	1.92 [1.85 ; 1.97]	1.88 [1.83 ; 1.94]	0.336
PermEn FHR sc3	2.08 [2.02 ; 2.13]	2.04 [2.02 ; 2.10]	0.476
PermEn FHR sc4	2.18 [2.14 ; 2.21]	2.15 [2.13 ; 2.19]	0.490
PermEn FHR sc5	2.26 [2.23 ; 2.29]	2.26 [2.24 ; 2.29]	0.726
PermEn FHR Ci	9.64 [9.39 ; 9.82]	9.60 [9.38 ; 9.71]	0.490
cCondEn FHR sc1	0.20 [0.17 ; 0.23]	0.20 [0.18 ; 0.23]	0.847
cCondEn FHR sc2	0.31 [0.28 ; 0.35]	0.35 [0.28 ; 0.37]	0.611
cCondEn FHR sc3	0.40 [0.35 ; 0.46]	0.45 [0.37 ; 0.48]	0.396
cCondEn FHR sc4	0.47 [0.42 ; 0.54]	0.54 [0.44 ; 0.57]	0.226
cCondEn FHR sc5	0.52 [0.46 ; 0.59]	0.62 [0.51 ; 0.64]	0.151
cCondEn FHR Ci	1.91 [1.69 ; 2.19]	2.17 [1.77 ; 2.29]	0.314

Continued on next page

Table A.2: Median, interquartile interval and p-value of the Mann-Whitney test for the first hour before birth. (Continued)

DispEn FHR sc1	1.21 [1.14 ; 1.25]	1.20 [1.19 ; 1.25]	0.777
DispEn FHR sc2	1.33 [1.24 ; 1.37]	1.34 [1.28 ; 1.38]	0.726
DispEn FHR sc3	1.39 [1.31 ; 1.46]	1.41 [1.35 ; 1.47]	0.534
DispEn FHR sc4	1.46 [1.36 ; 1.53]	1.48 [1.40 ; 1.53]	0.504
DispEn FHR sc5	1.50 [1.41 ; 1.58]	1.53 [1.45 ; 1.60]	0.476
DispEn FHR Ci	6.89 [6.44 ; 7.17]	6.99 [6.65 ; 7.22]	0.595
BubbEn FHR sc1	0.23 [0.21 ; 0.24]	0.23 [0.21 ; 0.24]	0.659
BubbEn FHR sc2	0.36 [0.33 ; 0.39]	0.34 [0.33 ; 0.37]	0.303
BubbEn FHR sc3	0.44 [0.41 ; 0.46]	0.42 [0.41 ; 0.45]	0.448
BubbEn FHR sc4	0.49 [0.47 ; 0.51]	0.48 [0.47 ; 0.50]	0.422
BubbEn FHR sc5	0.54 [0.52 ; 0.55]	0.54 [0.52 ; 0.55]	0.847
BubbEn FHR Ci	2.06 [1.96 ; 2.13]	2.00 [1.96 ; 2.09]	0.519
AttnEn FHR sc1	3.32 [3.08 ; 3.58]	3.17 [3.04 ; 3.25]	0.178
AttnEn FHR sc2	3.80 [3.68 ; 3.89]	3.89 [3.73 ; 3.92]	0.253
AttnEn FHR sc3	3.39 [3.33 ; 3.50]	3.46 [3.35 ; 3.48]	0.534
AttnEn FHR sc4	3.09 [3.02 ; 3.17]	3.12 [3.03 ; 3.19]	0.692
AttnEn FHR sc5	2.86 [2.80 ; 2.96]	2.91 [2.80 ; 2.98]	0.549
AttnEn FHR Ci	16.48 [16.21 ; 16.72]	16.35 [16.24 ; 16.68]	0.901
ApEn MHR sc1	0.67 [0.58 ; 0.77]	0.72 [0.59 ; 0.74]	0.865
ApEn MHR sc2	0.96 [0.79 ; 1.06]	1.00 [0.85 ; 1.07]	0.919
ApEn MHR sc3	1.05 [0.91 ; 1.19]	1.13 [0.97 ; 1.15]	0.919
ApEn MHR sc4	1.13 [0.98 ; 1.23]	1.19 [1.04 ; 1.23]	0.709
ApEn MHR sc5	1.14 [1.02 ; 1.20]	1.16 [1.05 ; 1.22]	0.795
ApEn MHR Ci	4.96 [4.33 ; 5.48]	5.26 [4.50 ; 5.35]	0.830
SampEn MHR sc1	0.54 [0.45 ; 0.65]	0.54 [0.50 ; 0.59]	0.777
SampEn MHR sc2	0.87 [0.70 ; 1.01]	0.89 [0.79 ; 0.96]	0.955
SampEn MHR sc3	1.04 [0.84 ; 1.22]	1.11 [0.96 ; 1.12]	0.991
SampEn MHR sc4	1.17 [0.96 ; 1.33]	1.28 [1.08 ; 1.32]	0.709
SampEn MHR sc5	1.25 [1.03 ; 1.38]	1.32 [1.11 ; 1.43]	0.743

Continued on next page

Table A.2: Median, interquartile interval and p-value of the Mann-Whitney test for the first hour before birth. (Continued)

SampEn MHR Ci	4.91 [4.01 ; 5.66]	5.24 [4.47 ; 5.36]	0.883
FuzzEn MHR sc1	0.12 [0.08 ; 0.17]	0.10 [0.07 ; 0.14]	0.409
FuzzEn MHR sc2	0.20 [0.12 ; 0.25]	0.15 [0.11 ; 0.22]	0.348
FuzzEn MHR sc3	0.25 [0.17 ; 0.33]	0.20 [0.16 ; 0.31]	0.448
FuzzEn MHR sc4	0.29 [0.21 ; 0.40]	0.24 [0.19 ; 0.37]	0.396
FuzzEn MHR sc5	0.31 [0.24 ; 0.44]	0.26 [0.20 ; 0.40]	0.303
FuzzEn MHR Ci	1.16 [0.84 ; 1.53]	0.95 [0.73 ; 1.45]	0.371
PermEn MHR sc1	1.24 [1.16 ; 1.29]	1.18 [1.16 ; 1.24]	0.244
PermEn MHR sc2	2.21 [2.15 ; 2.25]	2.19 [2.14 ; 2.21]	0.409
PermEn MHR sc3	2.36 [2.31 ; 2.41]	2.37 [2.33 ; 2.39]	0.865
PermEn MHR sc4	2.45 [2.39 ; 2.50]	2.48 [2.43 ; 2.50]	0.504
PermEn MHR sc5	2.48 [2.44 ; 2.53]	2.53 [2.47 ; 2.55]	0.217
PermEn MHR Ci	10.73 [10.49 ; 10.93]	10.74 [10.48 ; 10.89]	0.901
cCondEn MHR sc1	0.39 [0.35 ; 0.48]	0.42 [0.36 ; 0.47]	0.709
cCondEn MHR sc2	0.62 [0.55 ; 0.74]	0.65 [0.57 ; 0.74]	0.595
cCondEn MHR sc3	0.73 [0.68 ; 0.85]	0.76 [0.67 ; 0.88]	0.643
cCondEn MHR sc4	0.82 [0.75 ; 0.93]	0.84 [0.74 ; 0.99]	0.675
cCondEn MHR sc5	0.88 [0.81 ; 0.97]	0.89 [0.77 ; 1.04]	0.883
cCondEn MHR Ci	3.44 [3.14 ; 3.93]	3.56 [3.12 ; 4.15]	0.675
DispEn MHR sc1	1.40 [1.36 ; 1.46]	1.43 [1.37 ; 1.48]	0.675
DispEn MHR sc2	1.59 [1.52 ; 1.66]	1.63 [1.53 ; 1.71]	0.611
DispEn MHR sc3	1.67 [1.60 ; 1.76]	1.73 [1.62 ; 1.80]	0.549
DispEn MHR sc4	1.73 [1.65 ; 1.82]	1.81 [1.67 ; 1.87]	0.490
DispEn MHR sc5	1.78 [1.69 ; 1.85]	1.86 [1.69 ; 1.91]	0.519
DispEn MHR Ci	8.16 [7.81 ; 8.60]	8.47 [7.88 ; 8.78]	0.549
BubbEn MHR sc1	0.24 [0.22 ; 0.24]	0.23 [0.22 ; 0.24]	0.226
BubbEn MHR sc2	0.51 [0.47 ; 0.53]	0.49 [0.47 ; 0.51]	0.371
BubbEn MHR sc3	0.59 [0.56 ; 0.61]	0.59 [0.57 ; 0.60]	0.973
BubbEn MHR sc4	0.61 [0.59 ; 0.62]	0.62 [0.61 ; 0.63]	0.106

Continued on next page

Table A.2: Median, interquartile interval and p-value of the Mann-Whitney test for the first hour before birth. (Continued)

BubbEn MHR sc5	0.61 [0.59 ; 0.62]	0.61 [0.60 ; 0.61]	0.991
BubbEn MHR Ci	2.53 [2.47 ; 2.59]	2.54 [2.47 ; 2.58]	0.847
AttnEn MHR sc1	3.74 [3.54 ; 3.89]	3.60 [3.24 ; 3.92]	0.564
AttnEn MHR sc2	3.07 [2.89 ; 3.22]	2.93 [2.81 ; 3.16]	0.422
AttnEn MHR sc3	2.60 [2.43 ; 2.81]	2.34 [2.29 ; 2.69]	0.138
AttnEn MHR sc4	2.38 [2.17 ; 2.58]	2.04 [2.00 ; 2.38]	0.065
AttnEn MHR sc5	2.25 [2.09 ; 2.46]	2.08 [1.93 ; 2.16]	0.088
AttnEn MHR Ci	13.96 [13.19 ; 14.86]	12.97 [12.52 ; 14.21]	0.096
SE lin FHR	1.71 [1.58 ; 1.87]	1.90 [1.66 ; 2.01]	0.325
SE bin FHR	0.94 [0.88 ; 1.00]	0.96 [0.88 ; 1.08]	0.519
SE lin MHR	1.27 [1.10 ; 1.53]	1.18 [1.00 ; 1.70]	0.991
SE bin MHR	0.98 [0.88 ; 1.05]	0.97 [0.88 ; 1.09]	1.000
TE lin MHR–FHR	2.17 [1.37 ; 3.03] E-03	2.04 [1.66 ; 2.88] E-03	0.726
TE bin MHR–FHR	3.46 [1.79 ; 5.33] E-03	2.75 [2.15 ; 5.08] E-03	0.919
TE lin FHR–MHR	2.03 [1.23 ; 3.05] E-03	1.98 [1.67 ; 2.18] E-03	1.000
TE bin FHR–MHR	4.66 [0.00 ; 8.08] E-03	5.66 [3.21 ; 7.15] E-03	0.882

Table A.3: Median, interquartile interval and p-value of the Mann-Whitney test for the second hour before birth.

Measure	**Normal Fetuses Med [Q1;Q3]**	**Acidemic Fetuses Med [Q1;Q3]**	**p-value**
mean FHR	139.9 [132.1 ; 145.3]	130.7 [122.6 ; 134.5]	0.011
std FHR	17.5 [13.9 ; 20.3]	19.2 [16.6 ; 27.2]	0.253
mean MHR	91.5 [83.7 ; 99.8]	89.5 [81.9 ; 93.3]	0.435
std MHR	8.70 [6.90 ; 11.38]	10.71 [8.25 ; 13.38]	0.178
XApEn FHR	0.15 [0.02 ; 0.22]	0.11 [0.05 ; 0.14]	0.476
XApEn MHR	0.29 [0.18 ; 0.36]	0.19 [0.16 ; 0.29]	0.348
XSampEn	0.33 [0.27 ; 0.40]	0.30 [0.24 ; 0.41]	0.611
XFuzzEn	0.11 [0.08 ; 0.13]	0.10 [0.07 ; 0.16]	0.991

Continued on next page

Table A.3: Median, interquartile interval and p-value of the Mann-Whitney test for the second hour before birth. (Continued)

XPermEn	0.022 [0.011 ; 0.040]	0.017 [0.007 ; 0.031]	0.293
XCondEn FHR	1.31 [1.21 ; 1.38]	1.42 [1.32 ; 1.49]	0.053
XCondEn MHR	1.14 [1.04 ; 1.27]	1.27 [1.11 ; 1.30]	0.314
ApEn FHR sc1	0.25 [0.21 ; 0.28]	0.23 [0.19 ; 0.28]	0.627
ApEn FHR sc2	0.40 [0.35 ; 0.44]	0.38 [0.34 ; 0.45]	0.760
ApEn FHR sc3	0.50 [0.44 ; 0.56]	0.49 [0.43 ; 0.57]	0.973
ApEn FHR sc4	0.57 [0.51 ; 0.63]	0.58 [0.51 ; 0.65]	0.955
ApEn FHR sc5	0.62 [0.56 ; 0.69]	0.63 [0.55 ; 0.70]	0.955
ApEn FHR Ci	2.34 [2.04 ; 2.61]	2.29 [2.03 ; 2.65]	0.937
SampEn FHR sc1	0.16 [0.13 ; 0.19]	0.14 [0.11 ; 0.18]	0.348
SampEn FHR sc2	0.26 [0.22 ; 0.30]	0.23 [0.21 ; 0.29]	0.579
SampEn FHR sc3	0.35 [0.28 ; 0.40]	0.31 [0.29 ; 0.41]	0.955
SampEn FHR sc4	0.43 [0.35 ; 0.48]	0.39 [0.37 ; 0.50]	0.847
SampEn FHR sc5	0.49 [0.40 ; 0.56]	0.45 [0.42 ; 0.58]	0.883
SampEn FHR Ci	1.69 [1.38 ; 1.92]	1.48 [1.42 ; 1.95]	0.919
FuzzEn FHR sc1	0.055 [0.040 ; 0.059]	0.049 [0.046 ; 0.058]	0.973
FuzzEn FHR sc2	0.10 [0.08 ; 0.11]	0.10 [0.09 ; 0.11]	0.955
FuzzEn FHR sc3	0.16 [0.12 ; 0.17]	0.14 [0.13 ; 0.17]	0.919
FuzzEn FHR sc4	0.21 [0.15 ; 0.22]	0.19 [0.17 ; 0.22]	0.955
FuzzEn FHR sc5	0.24 [0.19 ; 0.27]	0.22 [0.21 ; 0.26]	0.883
FuzzEn FHR Ci	0.76 [0.57 ; 0.83]	0.70 [0.65 ; 0.81]	1.000
PermEn FHR sc1	1.17 [1.09 ; 1.24]	1.17 [1.13 ; 1.25]	0.643
PermEn FHR sc2	1.91 [1.84 ; 1.96]	1.88 [1.86 ; 1.94]	0.847
PermEn FHR sc3	2.07 [2.03 ; 2.11]	2.07 [2.03 ; 2.10]	0.973
PermEn FHR sc4	2.20 [2.16 ; 2.22]	2.20 [2.20 ; 2.24]	0.462
PermEn FHR sc5	2.28 [2.25 ; 2.31]	2.31 [2.25 ; 2.32]	0.371
PermEn FHR Ci	9.66 [9.39 ; 9.80]	9.66 [9.44 ; 9.87]	0.611
cCondEn FHR sc1	0.20 [0.17 ; 0.22]	0.21 [0.17 ; 0.22]	0.865
cCondEn FHR sc2	0.34 [0.30 ; 0.37]	0.34 [0.30 ; 0.37]	0.919

Continued on next page

Table A.3: Median, interquartile interval and p-value of the Mann-Whitney test for the second hour before birth. (Continued)

cCondEn FHR sc3	0.43 [0.37 ; 0.47]	0.44 [0.39 ; 0.48]	0.659
cCondEn FHR sc4	0.51 [0.45 ; 0.56]	0.51 [0.46 ; 0.58]	0.760
cCondEn FHR sc5	0.57 [0.50 ; 0.62]	0.57 [0.51 ; 0.66]	0.760
cCondEn FHR Ci	2.04 [1.79 ; 2.23]	2.06 [1.84 ; 2.31]	0.812
DispEn FHR sc1	1.20 [1.14 ; 1.23]	1.20 [1.15 ; 1.21]	0.627
DispEn FHR sc2	1.30 [1.25 ; 1.33]	1.30 [1.24 ; 1.32]	0.534
DispEn FHR sc3	1.38 [1.32 ; 1.42]	1.37 [1.30 ; 1.40]	0.435
DispEn FHR sc4	1.43 [1.37 ; 1.49]	1.43 [1.35 ; 1.46]	0.314
DispEn FHR sc5	1.48 [1.41 ; 1.55]	1.47 [1.41 ; 1.52]	0.396
DispEn FHR Ci	6.80 [6.51 ; 7.00]	6.78 [6.46 ; 6.91]	0.462
BubbEn FHR sc1	0.22 [0.21 ; 0.23]	0.22 [0.21 ; 0.23]	0.919
BubbEn FHR sc2	0.36 [0.33 ; 0.38]	0.35 [0.34 ; 0.37]	0.865
BubbEn FHR sc3	0.44 [0.41 ; 0.45]	0.43 [0.41 ; 0.45]	1.000
BubbEn FHR sc4	0.50 [0.48 ; 0.51]	0.50 [0.50 ; 0.52]	0.490
BubbEn FHR sc5	0.55 [0.53 ; 0.56]	0.56 [0.53 ; 0.57]	0.303
BubbEn FHR Ci	2.07 [1.96 ; 2.14]	2.08 [2.00 ; 2.12]	0.812
AttnEn FHR sc1	3.38 [3.11 ; 3.60]	3.44 [3.03 ; 3.54]	1.000
AttnEn FHR sc2	3.72 [3.65 ; 3.83]	3.80 [3.72 ; 3.83]	0.371
AttnEn FHR sc3	3.35 [3.30 ; 3.45]	3.37 [3.27 ; 3.43]	0.865
AttnEn FHR sc4	3.05 [2.97 ; 3.16]	3.03 [2.95 ; 3.13]	0.675
AttnEn FHR sc5	2.82 [2.75 ; 2.94]	2.79 [2.72 ; 2.96]	0.675
AttnEn FHR Ci	16.39 [16.12 ; 16.58]	16.45 [16.04 ; 16.64]	0.812
ApEn MHR sc1	0.61 [0.48 ; 0.73]	0.57 [0.43 ; 0.70]	0.726
ApEn MHR sc2	0.87 [0.71 ; 0.98]	0.83 [0.64 ; 1.01]	0.937
ApEn MHR sc3	0.97 [0.82 ; 1.10]	0.96 [0.76 ; 1.12]	0.955
ApEn MHR sc4	1.03 [0.89 ; 1.14]	1.00 [0.84 ; 1.18]	0.847
ApEn MHR sc5	1.05 [0.94 ; 1.14]	1.02 [0.89 ; 1.18]	0.937
ApEn MHR Ci	4.59 [3.90 ; 5.14]	4.39 [3.56 ; 5.18]	0.973
SampEn MHR sc1	0.51 [0.39 ; 0.62]	0.47 [0.34 ; 0.54]	0.692

Continued on next page

Table A.3: Median, interquartile interval and p-value of the Mann-Whitney test for the second hour before birth. (Continued)

SampEn MHR sc2	0.76 [0.57 ; 0.90]	0.77 [0.54 ; 0.90]	0.991
SampEn MHR sc3	0.91 [0.71 ; 1.08]	0.93 [0.68 ; 1.09]	0.865
SampEn MHR sc4	1.02 [0.85 ; 1.19]	1.00 [0.80 ; 1.26]	0.812
SampEn MHR sc5	1.10 [0.93 ; 1.27]	1.06 [0.87 ; 1.33]	0.830
SampEn MHR Ci	4.30 [3.40 ; 5.13]	4.23 [3.23 ; 5.13]	1.000
FuzzEn MHR sc1	0.15 [0.10 ; 0.20]	0.13 [0.08 ; 0.25]	0.937
FuzzEn MHR sc2	0.24 [0.16 ; 0.30]	0.20 [0.13 ; 0.38]	0.991
FuzzEn MHR sc3	0.33 [0.22 ; 0.38]	0.28 [0.18 ; 0.51]	0.955
FuzzEn MHR sc4	0.38 [0.27 ; 0.45]	0.35 [0.22 ; 0.59]	0.865
FuzzEn MHR sc5	0.42 [0.30 ; 0.52]	0.41 [0.25 ; 0.64]	0.795
FuzzEn MHR Ci	1.59 [1.09 ; 1.82]	1.38 [0.87 ; 2.38]	0.901
PermEn MHR sc1	1.28 [1.22 ; 1.34]	1.23 [1.19 ; 1.28]	0.209
PermEn MHR sc2	2.20 [2.15 ; 2.28]	2.20 [2.14 ; 2.21]	0.359
PermEn MHR sc3	2.35 [2.27 ; 2.42]	2.34 [2.29 ; 2.37]	0.549
PermEn MHR sc4	2.41 [2.33 ; 2.48]	2.45 [2.37 ; 2.46]	0.991
PermEn MHR sc5	2.44 [2.38 ; 2.51]	2.47 [2.41 ; 2.50]	0.973
PermEn MHR Ci	10.73 [10.40 ; 10.98]	10.72 [10.44 ; 10.78]	0.504
cCondEn MHR sc1	0.40 [0.33 ; 0.44]	0.41 [0.36 ; 0.50]	0.504
cCondEn MHR sc2	0.62 [0.53 ; 0.68]	0.65 [0.57 ; 0.77]	0.490
cCondEn MHR sc3	0.75 [0.62 ; 0.82]	0.76 [0.68 ; 0.91]	0.409
cCondEn MHR sc4	0.83 [0.71 ; 0.90]	0.85 [0.75 ; 1.01]	0.348
cCondEn MHR sc5	0.89 [0.80 ; 0.95]	0.90 [0.80 ; 1.08]	0.396
cCondEn MHR Ci	3.49 [2.96 ; 3.77]	3.57 [3.16 ; 4.27]	0.476
DispEn MHR sc1	1.39 [1.34 ; 1.45]	1.35 [1.29 ; 1.44]	0.675
DispEn MHR sc2	1.55 [1.47 ; 1.64]	1.50 [1.42 ; 1.65]	0.709
DispEn MHR sc3	1.63 [1.53 ; 1.72]	1.59 [1.49 ; 1.76]	0.777
DispEn MHR sc4	1.70 [1.59 ; 1.77]	1.64 [1.53 ; 1.82]	0.865
DispEn MHR sc5	1.75 [1.63 ; 1.80]	1.67 [1.56 ; 1.87]	0.955
DispEn MHR Ci	8.02 [7.54 ; 8.37]	7.74 [7.29 ; 8.55]	0.777

Continued on next page

Table A.3: Median, interquartile interval and p-value of the Mann-Whitney test for the second hour before birth. (Continued)

BubbEn MHR sc1	0.24 [0.23 ; 0.25]	0.23 [0.22 ; 0.24]	0.151
BubbEn MHR sc2	0.51 [0.47 ; 0.55]	0.51 [0.47 ; 0.51]	0.359
BubbEn MHR sc3	0.58 [0.54 ; 0.61]	0.58 [0.55 ; 0.59]	0.564
BubbEn MHR sc4	0.60 [0.57 ; 0.62]	0.61 [0.57 ; 0.62]	0.865
BubbEn MHR sc5	0.60 [0.59 ; 0.62]	0.60 [0.57 ; 0.61]	0.549
BubbEn MHR Ci	2.52 [2.43 ; 2.61]	2.54 [2.39 ; 2.56]	0.462
AttnEn MHR sc1	3.61 [3.36 ; 3.88]	3.70 [3.54 ; 3.86]	0.812
AttnEn MHR sc2	3.15 [2.88 ; 3.36]	3.04 [3.01 ; 3.18]	0.709
AttnEn MHR sc3	2.74 [2.46 ; 2.96]	2.56 [2.55 ; 2.81]	0.534
AttnEn MHR sc4	2.52 [2.24 ; 2.73]	2.29 [2.25 ; 2.58]	0.462
AttnEn MHR sc5	2.41 [2.12 ; 2.59]	2.20 [2.12 ; 2.50]	0.396
AttnEn MHR Ci	14.48 [13.36 ; 15.32]	13.85 [13.79 ; 14.64]	0.504
SE lin FHR	1.53 [1.39 ; 1.74]	1.67 [1.47 ; 1.75]	0.384
SE bin FHR	1.05 [0.95 ; 1.15]	1.18 [0.97 ; 1.20]	0.201
SE lin MHR	1.37 [1.05 ; 1.60]	1.56 [1.11 ; 1.75]	0.435
SE bin MHR	1.01 [0.92 ; 1.13]	1.19 [1.03 ; 1.23]	0.059
TE lin MHR–FHR	1.57 [1.02 ; 2.66] E-03	1.46 [1.02 ; 2.13] E-03	0.490
TE bin MHR–FHR	0.57 [0.29 ; 1.01] E-02	1.02 [0.48 ; 1.25] E-02	0.292
TE lin FHR–MHR	1.91 [1.21 ; 2.97] E-03	1.67 [1.50 ; 2.34] E-03	0.795
TE bin FHR–MHR	5.31 [0.00 ; 9.35] E-03	7.10 [3.13 ; 9.28] E-03	0.715

Table A.4: Median, interquartile interval and p-value of the Mann-Whitney test for the last 20 minutes before birth.

Measure	**Normal Fetuses Med [Q1;Q3]**	**Acidemic Fetuses Med [Q1;Q3]**	**p-value**
mean FHR	134.8 [119.8 ; 142.5]	118.0 [112.5 ; 130.8]	0.106
std FHR	23.8 [20.5 ; 28.5]	25.3 [15.2 ; 27.7]	0.830
mean MHR	98.7 [86.6 ; 104.5]	97.9 [88.1 ; 100.8]	0.595
std MHR	11.1 [7.8 ; 15.1]	13.9 [8.4 ; 21.0]	0.348

Continued on next page

Table A.4: Median, interquartile interval and p-value of the Mann-Whitney test for the last 20 minutes before birth. (Continued)

XApEn FHR	0.13 [0.05 ; 0.20]	0.11 [0.08 ; 0.19]	0.760
XApEn MHR	0.20 [0.08 ; 0.28]	0.11 [0.08 ; 0.29]	0.760
XSampEn	0.27 [0.21 ; 0.36]	0.25 [0.23 ; 0.38]	0.549
XFuzzEn	0.12 [0.09 ; 0.17]	0.12 [0.10 ; 0.16]	0.973
XPermEn	0.038 [0.022 ; 0.072]	0.038 [0.010 ; 0.065]	0.556
XCondEn FHR	1.34 [1.20 ; 1.45]	1.42 [1.32 ; 1.51]	0.138
XCondEn MHR	1.26 [1.15 ; 1.39]	1.18 [1.09 ; 1.36]	0.534
ApEn FHR sc1	0.24 [0.20 ; 0.27]	0.24 [0.23 ; 0.28]	0.519
ApEn FHR sc2	0.40 [0.35 ; 0.47]	0.41 [0.39 ; 0.48]	0.396
ApEn FHR sc3	0.50 [0.46 ; 0.57]	0.53 [0.50 ; 0.59]	0.314
ApEn FHR sc4	0.58 [0.50 ; 0.67]	0.62 [0.56 ; 0.69]	0.303
ApEn FHR sc5	0.62 [0.54 ; 0.71]	0.65 [0.56 ; 0.73]	0.435
ApEn FHR Ci	2.30 [2.04 ; 2.66]	2.44 [2.25 ; 2.76]	0.396
SampEn FHR sc1	0.12 [0.10 ; 0.16]	0.15 [0.14 ; 0.16]	0.072
SampEn FHR sc2	0.22 [0.18 ; 0.29]	0.27 [0.25 ; 0.30]	0.065
SampEn FHR sc3	0.30 [0.26 ; 0.41]	0.37 [0.35 ; 0.42]	0.072
SampEn FHR sc4	0.37 [0.32 ; 0.49]	0.48 [0.42 ; 0.54]	0.059
SampEn FHR sc5	0.44 [0.34 ; 0.58]	0.53 [0.44 ; 0.63]	0.096
SampEn FHR Ci	1.43 [1.21 ; 1.92]	1.81 [1.62 ; 2.04]	0.065
FuzzEn FHR sc1	0.08 [0.06 ; 0.10]	0.07 [0.04 ; 0.11]	0.991
FuzzEn FHR sc2	0.15 [0.11 ; 0.19]	0.13 [0.08 ; 0.21]	0.901
FuzzEn FHR sc3	0.22 [0.17 ; 0.28]	0.20 [0.12 ; 0.31]	0.991
FuzzEn FHR sc4	0.29 [0.22 ; 0.35]	0.26 [0.16 ; 0.42]	0.955
FuzzEn FHR sc5	0.33 [0.26 ; 0.41]	0.31 [0.20 ; 0.47]	0.955
FuzzEn FHR Ci	1.06 [0.81 ; 1.32]	0.96 [0.61 ; 1.52]	0.973
PermEn FHR sc1	1.17 [1.09 ; 1.24]	1.14 [1.11 ; 1.23]	0.919
PermEn FHR sc2	1.88 [1.81 ; 1.94]	1.89 [1.79 ; 1.92]	0.611
PermEn FHR sc3	2.08 [2.01 ; 2.13]	2.03 [2.00 ; 2.07]	0.409
PermEn FHR sc4	2.22 [2.17 ; 2.26]	2.19 [2.17 ; 2.26]	0.883

Continued on next page

Table A.4: Median, interquartile interval and p-value of the Mann-Whitney test for the last 20 minutes before birth. (Continued)

PermEn FHR sc5	2.31 [2.27 ; 2.34]	2.31 [2.29 ; 2.35]	0.579
PermEn FHR Ci	9.73 [9.30 ; 9.86]	9.51 [9.44 ; 9.82]	0.937
cCondEn FHR sc1	0.22 [0.20 ; 0.25]	0.21 [0.19 ; 0.26]	0.812
cCondEn FHR sc2	0.37 [0.34 ; 0.42]	0.39 [0.32 ; 0.47]	0.709
cCondEn FHR sc3	0.49 [0.45 ; 0.54]	0.50 [0.40 ; 0.59]	0.847
cCondEn FHR sc4	0.58 [0.52 ; 0.64]	0.58 [0.47 ; 0.73]	0.795
cCondEn FHR sc5	0.64 [0.58 ; 0.71]	0.64 [0.56 ; 0.79]	0.830
cCondEn FHR Ci	2.31 [2.11 ; 2.52]	2.32 [1.94 ; 2.84]	0.812
DispEn FHR sc1	1.21 [1.17 ; 1.23]	1.18 [1.13 ; 1.25]	0.709
DispEn FHR sc2	1.31 [1.28 ; 1.36]	1.30 [1.23 ; 1.38]	0.726
DispEn FHR sc3	1.40 [1.34 ; 1.44]	1.36 [1.29 ; 1.47]	0.643
DispEn FHR sc4	1.46 [1.41 ; 1.52]	1.43 [1.34 ; 1.54]	0.643
DispEn FHR sc5	1.52 [1.46 ; 1.58]	1.48 [1.39 ; 1.61]	0.627
DispEn FHR Ci	6.89 [6.69 ; 7.15]	6.78 [6.42 ; 7.24]	0.659
BubbEn FHR sc1	0.22 [0.20 ; 0.23]	0.21 [0.20 ; 0.23]	0.659
BubbEn FHR sc2	0.35 [0.32 ; 0.38]	0.36 [0.32 ; 0.36]	0.692
BubbEn FHR sc3	0.44 [0.40 ; 0.46]	0.42 [0.40 ; 0.43]	0.371
BubbEn FHR sc4	0.51 [0.48 ; 0.53]	0.50 [0.49 ; 0.53]	0.865
BubbEn FHR sc5	0.56 [0.54 ; 0.57]	0.56 [0.55 ; 0.58]	0.564
BubbEn FHR Ci	2.11 [1.94 ; 2.17]	2.03 [1.98 ; 2.13]	0.830
AttnEn FHR sc1	3.61 [3.08 ; 3.96]	3.00 [2.93 ; 3.97]	0.579
AttnEn FHR sc2	3.71 [3.60 ; 3.82]	3.77 [3.66 ; 3.82]	0.611
AttnEn FHR sc3	3.32 [3.20 ; 3.43]	3.38 [3.26 ; 3.43]	0.627
AttnEn FHR sc4	3.00 [2.88 ; 3.09]	3.01 [2.95 ; 3.08]	0.883
AttnEn FHR sc5	2.76 [2.69 ; 2.91]	2.75 [2.68 ; 2.81]	0.448
AttnEn FHR Ci	16.38 [15.92 ; 16.79]	15.97 [15.86 ; 16.82]	0.579
ApEn MHR sc1	0.58 [0.40 ; 0.68]	0.62 [0.41 ; 0.69]	0.830
ApEn MHR sc2	0.79 [0.60 ; 0.95]	0.83 [0.59 ; 1.00]	0.675
ApEn MHR sc3	0.88 [0.69 ; 1.02]	0.90 [0.71 ; 1.15]	0.564

Continued on next page

Table A.4: Median, interquartile interval and p-value of the Mann-Whitney test for the last 20 minutes before birth. (Continued)

ApEn MHR sc4	0.95 [0.75 ; 1.08]	0.94 [0.78 ; 1.13]	0.627
ApEn MHR sc5	0.98 [0.81 ; 1.08]	0.93 [0.83 ; 1.12]	0.675
ApEn MHR Ci	4.24 [3.15 ; 4.78]	4.22 [3.32 ; 5.08]	0.659
SampEn MHR sc1	0.46 [0.31 ; 0.55]	0.49 [0.31 ; 0.57]	0.812
SampEn MHR sc2	0.66 [0.49 ; 0.82]	0.71 [0.48 ; 0.98]	0.611
SampEn MHR sc3	0.82 [0.61 ; 0.97]	0.89 [0.59 ; 1.18]	0.549
SampEn MHR sc4	0.90 [0.71 ; 1.10]	1.06 [0.70 ; 1.19]	0.462
SampEn MHR sc5	0.98 [0.80 ; 1.17]	1.16 [0.78 ; 1.19]	0.534
SampEn MHR Ci	3.84 [2.85 ; 4.63]	4.32 [2.87 ; 5.10]	0.519
FuzzEn MHR sc1	0.17 [0.11 ; 0.24]	0.16 [0.10 ; 0.26]	0.901
FuzzEn MHR sc2	0.26 [0.18 ; 0.33]	0.24 [0.17 ; 0.38]	0.919
FuzzEn MHR sc3	0.34 [0.25 ; 0.43]	0.34 [0.22 ; 0.51]	0.830
FuzzEn MHR sc4	0.41 [0.30 ; 0.51]	0.42 [0.26 ; 0.59]	0.777
FuzzEn MHR sc5	0.46 [0.33 ; 0.56]	0.48 [0.31 ; 0.64]	0.643
FuzzEn MHR Ci	1.61 [1.18 ; 2.07]	1.64 [1.03 ; 2.37]	0.812
PermEn MHR sc1	1.34 [1.23 ; 1.41]	1.30 [1.22 ; 1.36]	0.371
PermEn MHR sc2	2.21 [2.12 ; 2.30]	2.23 [2.14 ; 2.24]	0.709
PermEn MHR sc3	2.33 [2.24 ; 2.44]	2.33 [2.21 ; 2.37]	0.659
PermEn MHR sc4	2.40 [2.30 ; 2.47]	2.41 [2.27 ; 2.44]	0.865
PermEn MHR sc5	2.42 [2.34 ; 2.49]	2.43 [2.31 ; 2.48]	0.847
PermEn MHR Ci	10.6 [10.3 ; 11.0]	10.7 [10.4 ; 10.8]	0.675
cCondEn MHR sc1	0.37 [0.30 ; 0.44]	0.45 [0.38 ; 0.48]	0.132
cCondEn MHR sc2	0.57 [0.48 ; 0.68]	0.70 [0.60 ; 0.72]	0.157
cCondEn MHR sc3	0.71 [0.59 ; 0.81]	0.80 [0.70 ; 0.84]	0.138
cCondEn MHR sc4	0.79 [0.66 ; 0.88]	0.89 [0.80 ; 0.95]	0.121
cCondEn MHR sc5	0.86 [0.72 ; 0.91]	0.94 [0.86 ; 1.00]	0.127
cCondEn MHR Ci	3.31 [2.79 ; 3.68]	3.77 [3.35 ; 3.98]	0.132
DispEn MHR sc1	1.37 [1.31 ; 1.45]	1.34 [1.28 ; 1.41]	0.659
DispEn MHR sc2	1.52 [1.43 ; 1.62]	1.50 [1.40 ; 1.60]	0.937

Continued on next page

Table A.4: Median, interquartile interval and p-value of the Mann-Whitney test for the last 20 minutes before birth. (Continued)

DispEn MHR sc3	1.59 [1.49 ; 1.71]	1.60 [1.47 ; 1.70]	0.865
DispEn MHR sc4	1.65 [1.55 ; 1.75]	1.68 [1.51 ; 1.75]	0.919
DispEn MHR sc5	1.69 [1.58 ; 1.81]	1.71 [1.55 ; 1.78]	0.883
DispEn MHR Ci	7.80 [7.35 ; 8.33]	7.85 [7.21 ; 8.24]	0.991
BubbEn MHR sc1	0.25 [0.23 ; 0.26]	0.24 [0.23 ; 0.25]	0.226
BubbEn MHR sc2	0.51 [0.46 ; 0.56]	0.52 [0.47 ; 0.52]	0.643
BubbEn MHR sc3	0.57 [0.53 ; 0.61]	0.57 [0.51 ; 0.59]	0.777
BubbEn MHR sc4	0.60 [0.56 ; 0.61]	0.60 [0.55 ; 0.60]	0.490
BubbEn MHR sc5	0.61 [0.58 ; 0.62]	0.57 [0.55 ; 0.61]	0.263
BubbEn MHR Ci	2.50 [2.38 ; 2.64]	2.52 [2.35 ; 2.57]	0.504
AttnEn MHR sc1	3.55 [3.34 ; 3.82]	3.84 [3.36 ; 3.91]	0.325
AttnEn MHR sc2	3.20 [2.89 ; 3.32]	3.07 [3.02 ; 3.40]	0.991
AttnEn MHR sc3	2.80 [2.51 ; 3.04]	2.69 [2.64 ; 3.06]	0.919
AttnEn MHR sc4	2.62 [2.34 ; 2.83]	2.46 [2.40 ; 2.81]	0.865
AttnEn MHR sc5	2.46 [2.24 ; 2.70]	2.29 [2.21 ; 2.79]	0.812
AttnEn MHR Ci	14.5 [13.6 ; 15.4]	14.4 [14.2 ; 15.1]	0.955
SE lin FHR	1.37 [1.26 ; 1.61]	1.57 [1.19 ; 2.04]	0.435
SE bin FHR	1.17 [1.03 ; 1.27]	1.17 [1.02 ; 1.24]	0.883
SE lin MHR	1.48 [1.03 ; 1.66]	1.47 [1.25 ; 1.68]	0.659
SE bin MHR	1.05 [0.92 ; 1.22]	1.15 [1.02 ; 1.29]	0.244
TE lin MHR–FHR	1.28 [0.46 ; 1.99] E-03	1.48 [1.01 ; 2.01] E-03	0.448
TE bin MHR–FHR	0.77 [0.00 ; 1.21] E-02	1.76 [0.17 ; 2.84] E-02	0.136
TE lin FHR–MHR	1.53 [0.64 ; 2.81] E-03	3.99 [1.62 ; 7.40] E-04	0.029
TE bin FHR–MHR	0.00 [0.00 ; 1.08] E-02	0.00 [0.00 ; 5.73] E-03	0.546

Table A.5: Median, interquartile interval and p-value of the Mann-Whitney test for the penultimate 10 minutes before birth.

Measure	**Normal Fetuses Med [Q1;Q3]**	**Acidemic Fetuses Med [Q1;Q3]**	**p-value**

Continued on next page

Table A.5: Median, interquartile interval and p-value of the Mann-Whitney test for the penultimate 10 minutes before birth. (Continued)

mean FHR	138.7 [122.2 ; 147.6]	119.8 [114.1 ; 135.9]	0.127
std FHR	20.8 [14.4 ; 29.0]	27.3 [10.8 ; 29.1]	0.760
mean MHR	94.4 [82.8 ; 100.9]	97.2 [79.9 ; 97.8]	0.760
std MHR	9.02 [6.66 ; 13.83]	8.17 [8.13 ; 21.71]	0.244
XApEn FHR	0.15 [0.06 ; 0.22]	0.15 [0.02 ; 0.20]	0.611
XApEn MHR	0.23 [0.13 ; 0.37]	0.16 [0.10 ; 0.34]	0.564
XSampEn	0.27 [0.21 ; 0.36]	0.23 [0.23 ; 0.36]	0.777
XFuzzEn	0.10 [0.08 ; 0.16]	0.10 [0.08 ; 0.15]	0.919
XPermEn	0.025 [0.005 ; 0.045]	0.014 [0.003 ; 0.055]	0.811
XCondEn FHR	1.33 [1.17 ; 1.45]	1.36 [1.26 ; 1.48]	0.448
XCondEn MHR	1.25 [0.96 ; 1.40]	1.12 [1.01 ; 1.40]	0.937
ApEn FHR sc1	0.22 [0.18 ; 0.24]	0.25 [0.19 ; 0.28]	0.178
ApEn FHR sc2	0.37 [0.30 ; 0.42]	0.41 [0.34 ; 0.48]	0.193
ApEn FHR sc3	0.45 [0.37 ; 0.53]	0.54 [0.46 ; 0.60]	0.053
ApEn FHR sc4	0.53 [0.42 ; 0.61]	0.61 [0.55 ; 0.70]	0.056
ApEn FHR sc5	0.56 [0.47 ; 0.67]	0.66 [0.60 ; 0.71]	0.111
ApEn FHR Ci	2.13 [1.75 ; 2.49]	2.43 [2.14 ; 2.78]	0.121
SampEn FHR sc1	0.11 [0.08 ; 0.14]	0.15 [0.14 ; 0.16]	0.053
SampEn FHR sc2	0.20 [0.15 ; 0.25]	0.27 [0.22 ; 0.30]	0.045
SampEn FHR sc3	0.29 [0.20 ; 0.34]	0.38 [0.35 ; 0.42]	0.017
SampEn FHR sc4	0.35 [0.25 ; 0.40]	0.48 [0.41 ; 0.53]	0.020
SampEn FHR sc5	0.41 [0.27 ; 0.47]	0.54 [0.45 ; 0.60]	0.031
SampEn FHR Ci	1.37 [0.98 ; 1.60]	1.83 [1.58 ; 1.99]	0.026
FuzzEn FHR sc1	0.059 [0.036 ; 0.076]	0.073 [0.015 ; 0.109]	0.627
FuzzEn FHR sc2	0.11 [0.07 ; 0.14]	0.13 [0.03 ; 0.20]	0.675
FuzzEn FHR sc3	0.16 [0.10 ; 0.22]	0.20 [0.05 ; 0.28]	0.726
FuzzEn FHR sc4	0.20 [0.12 ; 0.28]	0.26 [0.07 ; 0.36]	0.760
FuzzEn FHR sc5	0.24 [0.15 ; 0.32]	0.32 [0.09 ; 0.41]	0.726
FuzzEn FHR Ci	0.78 [0.47 ; 1.04]	0.99 [0.25 ; 1.36]	0.743

Continued on next page

Table A.5: Median, interquartile interval and p-value of the Mann-Whitney test for the penultimate 10 minutes before birth. (Continued)

PermEn FHR sc1	1.16 [1.11 ; 1.23]	1.17 [1.08 ; 1.30]	0.519
PermEn FHR sc2	1.92 [1.80 ; 1.97]	1.90 [1.77 ; 1.94]	0.611
PermEn FHR sc3	2.09 [2.01 ; 2.14]	2.02 [1.99 ; 2.08]	0.409
PermEn FHR sc4	2.21 [2.15 ; 2.25]	2.19 [2.15 ; 2.26]	0.991
PermEn FHR sc5	2.31 [2.25 ; 2.35]	2.31 [2.26 ; 2.38]	0.448
PermEn FHR Ci	9.70 [9.31 ; 9.88]	9.70 [9.37 ; 9.74]	0.812
cCondEn FHR sc1	0.20 [0.17 ; 0.22]	0.21 [0.15 ; 0.27]	0.709
cCondEn FHR sc2	0.36 [0.29 ; 0.40]	0.36 [0.26 ; 0.45]	0.643
cCondEn FHR sc3	0.44 [0.37 ; 0.54]	0.48 [0.35 ; 0.58]	0.760
cCondEn FHR sc4	0.52 [0.42 ; 0.65]	0.55 [0.41 ; 0.70]	0.692
cCondEn FHR sc5	0.58 [0.47 ; 0.70]	0.63 [0.45 ; 0.79]	0.709
cCondEn FHR Ci	2.09 [1.72 ; 2.53]	2.23 [1.61 ; 2.78]	0.627
DispEn FHR sc1	1.21 [1.15 ; 1.24]	1.18 [1.14 ; 1.25]	0.743
DispEn FHR sc2	1.31 [1.24 ; 1.37]	1.25 [1.23 ; 1.36]	0.627
DispEn FHR sc3	1.37 [1.30 ; 1.46]	1.30 [1.28 ; 1.44]	0.534
DispEn FHR sc4	1.43 [1.34 ; 1.53]	1.34 [1.33 ; 1.52]	0.643
DispEn FHR sc5	1.49 [1.40 ; 1.59]	1.40 [1.38 ; 1.59]	0.692
DispEn FHR Ci	6.82 [6.36 ; 7.17]	6.43 [6.40 ; 7.16]	0.709
BubbEn FHR sc1	0.22 [0.21 ; 0.23]	0.22 [0.20 ; 0.24]	0.675
BubbEn FHR sc2	0.36 [0.31 ; 0.39]	0.35 [0.31 ; 0.37]	0.519
BubbEn FHR sc3	0.44 [0.41 ; 0.47]	0.41 [0.40 ; 0.44]	0.325
BubbEn FHR sc4	0.51 [0.47 ; 0.53]	0.50 [0.47 ; 0.53]	0.955
BubbEn FHR sc5	0.56 [0.53 ; 0.58]	0.56 [0.53 ; 0.59]	0.435
BubbEn FHR Ci	2.10 [1.92 ; 2.18]	2.06 [1.94 ; 2.14]	0.692
AttnEn FHR sc1	3.42 [2.85 ; 4.08]	2.74 [2.63 ; 3.98]	0.396
AttnEn FHR sc2	3.73 [3.59 ; 3.86]	3.69 [3.57 ; 3.86]	0.991
AttnEn FHR sc3	3.33 [3.22 ; 3.43]	3.38 [3.24 ; 3.55]	0.549
AttnEn FHR sc4	3.01 [2.89 ; 3.15]	2.99 [2.88 ; 3.20]	0.955
AttnEn FHR sc5	2.77 [2.68 ; 2.94]	2.69 [2.65 ; 2.94]	0.579

Continued on next page

Table A.5: Median, interquartile interval and p-value of the Mann-Whitney test for the penultimate 10 minutes before birth. (Continued)

AttnEn FHR Ci	16.3 [15.8 ; 16.9]	16.2 [15.6 ; 16.7]	0.812
ApEn MHR sc1	0.58 [0.40 ; 0.71]	0.61 [0.37 ; 0.70]	0.955
ApEn MHR sc2	0.83 [0.62 ; 0.99]	0.86 [0.55 ; 1.04]	0.883
ApEn MHR sc3	0.90 [0.77 ; 1.10]	1.02 [0.67 ; 1.19]	0.675
ApEn MHR sc4	0.97 [0.83 ; 1.13]	1.11 [0.77 ; 1.18]	0.643
ApEn MHR sc5	1.00 [0.88 ; 1.11]	1.15 [0.83 ; 1.20]	0.504
ApEn MHR Ci	4.26 [3.54 ; 5.05]	4.76 [3.17 ; 5.26]	0.743
SampEn MHR sc1	0.44 [0.30 ; 0.61]	0.47 [0.28 ; 0.58]	0.991
SampEn MHR sc2	0.67 [0.50 ; 0.87]	0.71 [0.44 ; 1.05]	0.675
SampEn MHR sc3	0.78 [0.65 ; 0.99]	0.90 [0.56 ; 1.24]	0.611
SampEn MHR sc4	0.92 [0.75 ; 1.16]	1.05 [0.68 ; 1.29]	0.579
SampEn MHR sc5	0.99 [0.78 ; 1.21]	1.15 [0.76 ; 1.37]	0.490
SampEn MHR Ci	3.82 [3.08 ; 4.89]	4.28 [2.73 ; 5.38]	0.627
FuzzEn MHR sc1	0.15 [0.10 ; 0.22]	0.13 [0.09 ; 0.24]	0.919
FuzzEn MHR sc2	0.23 [0.16 ; 0.36]	0.21 [0.16 ; 0.36]	0.973
FuzzEn MHR sc3	0.30 [0.23 ; 0.42]	0.29 [0.22 ; 0.48]	0.973
FuzzEn MHR sc4	0.36 [0.28 ; 0.47]	0.36 [0.26 ; 0.56]	0.973
FuzzEn MHR sc5	0.41 [0.33 ; 0.53]	0.43 [0.31 ; 0.60]	0.937
FuzzEn MHR Ci	1.44 [1.11 ; 1.95]	1.42 [1.00 ; 2.23]	1.000
PermEn MHR sc1	1.30 [1.23 ; 1.36]	1.26 [1.17 ; 1.34]	0.282
PermEn MHR sc2	2.22 [2.11 ; 2.30]	2.19 [2.11 ; 2.23]	0.359
PermEn MHR sc3	2.34 [2.26 ; 2.44]	2.29 [2.21 ; 2.37]	0.293
PermEn MHR sc4	2.40 [2.31 ; 2.49]	2.40 [2.28 ; 2.45]	0.692
PermEn MHR sc5	2.43 [2.34 ; 2.50]	2.43 [2.30 ; 2.50]	0.830
PermEn MHR Ci	10.6 [10.3 ; 11.0]	10.6 [10.2 ; 10.9]	0.409
cCondEn MHR sc1	0.37 [0.30 ; 0.46]	0.40 [0.36 ; 0.46]	0.564
cCondEn MHR sc2	0.57 [0.48 ; 0.74]	0.64 [0.57 ; 0.71]	0.534
cCondEn MHR sc3	0.68 [0.61 ; 0.83]	0.75 [0.67 ; 0.83]	0.371
cCondEn MHR sc4	0.78 [0.66 ; 0.92]	0.86 [0.75 ; 0.98]	0.325

Continued on next page

Table A.5: Median, interquartile interval and p-value of the Mann-Whitney test for the penultimate 10 minutes before birth. (Continued)

cCondEn MHR sc5	0.84 [0.73 ; 0.97]	0.89 [0.82 ; 1.02]	0.371
cCondEn MHR Ci	3.22 [2.84 ; 3.91]	3.54 [3.18 ; 3.99]	0.371
DispEn MHR sc1	1.38 [1.29 ; 1.44]	1.39 [1.28 ; 1.43]	0.883
DispEn MHR sc2	1.53 [1.42 ; 1.65]	1.57 [1.40 ; 1.63]	0.973
DispEn MHR sc3	1.63 [1.49 ; 1.73]	1.68 [1.48 ; 1.74]	0.847
DispEn MHR sc4	1.68 [1.53 ; 1.79]	1.75 [1.54 ; 1.82]	0.692
DispEn MHR sc5	1.73 [1.57 ; 1.83]	1.74 [1.57 ; 1.84]	0.865
DispEn MHR Ci	7.98 [7.30 ; 8.46]	8.17 [7.27 ; 8.46]	0.865
BubbEn MHR sc1	0.24 [0.23 ; 0.25]	0.24 [0.22 ; 0.24]	0.201
BubbEn MHR sc2	0.52 [0.46 ; 0.56]	0.49 [0.46 ; 0.51]	0.272
BubbEn MHR sc3	0.58 [0.54 ; 0.62]	0.55 [0.51 ; 0.59]	0.359
BubbEn MHR sc4	0.60 [0.56 ; 0.62]	0.59 [0.55 ; 0.61]	0.396
BubbEn MHR sc5	0.61 [0.58 ; 0.62]	0.58 [0.54 ; 0.62]	0.519
BubbEn MHR Ci	2.54 [2.38 ; 2.65]	2.47 [2.32 ; 2.52]	0.178
AttnEn MHR sc1	3.64 [3.11 ; 3.94]	3.85 [3.29 ; 4.06]	0.462
AttnEn MHR sc2	3.17 [2.93 ; 3.35]	3.23 [3.08 ; 3.44]	0.504
AttnEn MHR sc3	2.80 [2.52 ; 3.01]	2.84 [2.57 ; 3.09]	0.692
AttnEn MHR sc4	2.59 [2.33 ; 2.83]	2.54 [2.31 ; 2.81]	0.795
AttnEn MHR sc5	2.49 [2.20 ; 2.66]	2.38 [2.09 ; 2.76]	0.883
AttnEn MHR Ci	14.5 [13.2 ; 15.5]	14.7 [14.0 ; 15.4]	0.743
SE lin FHR	1.43 [1.18 ; 1.74]	1.52 [1.40 ; 2.34]	0.178
SE bin FHR	1.18 [0.89 ; 1.27]	1.23 [0.96 ; 1.34]	0.564
SE lin MHR	1.43 [0.97 ; 1.74]	1.46 [1.29 ; 1.85]	0.564
SE bin MHR	1.03 [0.89 ; 1.19]	1.17 [1.02 ; 1.31]	0.171
TE lin MHR–FHR	1.36 [0.28 ; 3.64] E-03	1.08 [0.36 ; 3.34] E-03	0.812
TE bin MHR–FHR	0.00 [0.00 ; 1.83] E-02	1.17 [0.00 ; 2.66] E-02	0.336
TE lin FHR–MHR	1.45 [0.52 ; 3.46] E-03	2.08 [1.12 ; 9.65] E-04	0.034
TE bin FHR–MHR	0.00 [0.00 ; 0.00]	0.00 [0.00 ; 1.15] E-02	1.000

Table A.6: Median, interquartile interval and p-value of the Mann-Whitney test for the last 10 minutes before birth.

Measure	**Normal Fetuses Med [Q1;Q3]**	**Acidemic Fetuses Med [Q1;Q3]**	**p-value**
mean FHR	134.8 [119.8 ; 142.5]	118.0 [112.5 ; 130.8]	0.106
std FHR	23.8 [20.5 ; 28.5]	25.3 [15.2 ; 27.7]	0.830
mean MHR	98.7 [86.6 ; 104.5]	97.9 [88.1 ; 100.8]	0.595
std MHR	11.1 [7.8 ; 15.1]	13.9 [8.4 ; 21.0]	0.348
XApEn FHR	0.13 [0.05 ; 0.20]	0.11 [0.08 ; 0.19]	0.760
XApEn MHR	0.20 [0.08 ; 0.28]	0.11 [0.08 ; 0.29]	0.760
XSampEn	0.27 [0.21 ; 0.36]	0.25 [0.23 ; 0.38]	0.549
XFuzzEn	0.12 [0.09 ; 0.17]	0.12 [0.10 ; 0.16]	0.973
XPermEn	0.038 [0.022 ; 0.072]	0.038 [0.010 ; 0.065]	0.556
XCondEn FHR	1.34 [1.20 ; 1.45]	1.42 [1.32 ; 1.51]	0.138
XCondEn MHR	1.26 [1.15 ; 1.39]	1.18 [1.09 ; 1.36]	0.534
ApEn FHR sc1	0.24 [0.20 ; 0.27]	0.24 [0.23 ; 0.28]	0.519
ApEn FHR sc2	0.40 [0.35 ; 0.47]	0.41 [0.39 ; 0.48]	0.396
ApEn FHR sc3	0.50 [0.46 ; 0.57]	0.53 [0.50 ; 0.59]	0.314
ApEn FHR sc4	0.58 [0.50 ; 0.67]	0.62 [0.56 ; 0.69]	0.303
ApEn FHR sc5	0.62 [0.54 ; 0.71]	0.65 [0.56 ; 0.73]	0.435
ApEn FHR Ci	2.30 [2.04 ; 2.66]	2.44 [2.25 ; 2.76]	0.396
SampEn FHR sc1	0.12 [0.10 ; 0.16]	0.15 [0.14 ; 0.16]	0.072
SampEn FHR sc2	0.22 [0.18 ; 0.29]	0.27 [0.25 ; 0.30]	0.065
SampEn FHR sc3	0.30 [0.26 ; 0.41]	0.37 [0.35 ; 0.42]	0.072
SampEn FHR sc4	0.37 [0.32 ; 0.49]	0.48 [0.42 ; 0.54]	0.059
SampEn FHR sc5	0.44 [0.34 ; 0.58]	0.53 [0.44 ; 0.63]	0.096
SampEn FHR Ci	1.43 [1.21 ; 1.92]	1.81 [1.62 ; 2.04]	0.065
FuzzEn FHR sc1	0.078 [0.056 ; 0.098]	0.070 [0.043 ; 0.114]	0.991
FuzzEn FHR sc2	0.15 [0.11 ; 0.19]	0.13 [0.08 ; 0.21]	0.901
FuzzEn FHR sc3	0.22 [0.17 ; 0.28]	0.20 [0.12 ; 0.31]	0.991
FuzzEn FHR sc4	0.29 [0.22 ; 0.35]	0.26 [0.16 ; 0.42]	0.955
FuzzEn FHR sc5	0.33 [0.26 ; 0.41]	0.31 [0.20 ; 0.47]	0.955

Continued on next page

Table A.6: Median, interquartile interval and p-value of the Mann-Whitney test for the last 10 minutes before birth. (Continued)

FuzzEn FHR Ci	1.06 [0.81 ; 1.32]	0.96 [0.61 ; 1.52]	0.973
PermEn FHR sc1	1.17 [1.09 ; 1.24]	1.14 [1.11 ; 1.23]	0.919
PermEn FHR sc2	1.88 [1.81 ; 1.94]	1.89 [1.79 ; 1.92]	0.611
PermEn FHR sc3	2.08 [2.01 ; 2.13]	2.03 [2.00 ; 2.07]	0.409
PermEn FHR sc4	2.22 [2.17 ; 2.26]	2.19 [2.17 ; 2.26]	0.883
PermEn FHR sc5	2.31 [2.27 ; 2.34]	2.31 [2.29 ; 2.35]	0.579
PermEn FHR Ci	9.73 [9.30 ; 9.86]	9.51 [9.44 ; 9.82]	0.937
cCondEn FHR sc1	0.22 [0.20 ; 0.25]	0.21 [0.19 ; 0.26]	0.812
cCondEn FHR sc2	0.37 [0.34 ; 0.42]	0.39 [0.32 ; 0.47]	0.709
cCondEn FHR sc3	0.49 [0.45 ; 0.54]	0.50 [0.40 ; 0.59]	0.847
cCondEn FHR sc4	0.58 [0.52 ; 0.64]	0.58 [0.47 ; 0.73]	0.795
cCondEn FHR sc5	0.64 [0.58 ; 0.71]	0.64 [0.56 ; 0.79]	0.830
cCondEn FHR Ci	2.31 [2.11 ; 2.52]	2.32 [1.94 ; 2.84]	0.812
DispEn FHR sc1	1.21 [1.17 ; 1.23]	1.18 [1.13 ; 1.25]	0.709
DispEn FHR sc2	1.31 [1.28 ; 1.36]	1.30 [1.23 ; 1.38]	0.726
DispEn FHR sc3	1.40 [1.34 ; 1.44]	1.36 [1.29 ; 1.47]	0.643
DispEn FHR sc4	1.46 [1.41 ; 1.52]	1.43 [1.34 ; 1.54]	0.643
DispEn FHR sc5	1.52 [1.46 ; 1.58]	1.48 [1.39 ; 1.61]	0.627
DispEn FHR Ci	6.89 [6.69 ; 7.15]	6.78 [6.42 ; 7.24]	0.659
BubbEn FHR sc1	0.22 [0.20 ; 0.23]	0.21 [0.20 ; 0.23]	0.659
BubbEn FHR sc2	0.35 [0.32 ; 0.38]	0.36 [0.32 ; 0.36]	0.692
BubbEn FHR sc3	0.44 [0.40 ; 0.46]	0.42 [0.40 ; 0.43]	0.371
BubbEn FHR sc4	0.51 [0.48 ; 0.53]	0.50 [0.49 ; 0.53]	0.865
BubbEn FHR sc5	0.56 [0.54 ; 0.57]	0.56 [0.55 ; 0.58]	0.564
BubbEn FHR Ci	2.11 [1.94 ; 2.17]	2.03 [1.98 ; 2.13]	0.830
AttnEn FHR sc1	3.61 [3.08 ; 3.96]	3.00 [2.93 ; 3.97]	0.579
AttnEn FHR sc2	3.71 [3.60 ; 3.82]	3.77 [3.66 ; 3.82]	0.611
AttnEn FHR sc3	3.32 [3.20 ; 3.43]	3.38 [3.26 ; 3.43]	0.627
AttnEn FHR sc4	3.00 [2.88 ; 3.09]	3.01 [2.95 ; 3.08]	0.883

Continued on next page

Table A.6: Median, interquartile interval and p-value of the Mann-Whitney test for the last 10 minutes before birth. (Continued)

AttnEn FHR sc5	2.76 [2.69 ; 2.91]	2.75 [2.68 ; 2.81]	0.448
AttnEn FHR Ci	16.4 [15.9 ; 16.8]	16.0 [15.9 ; 16.8]	0.579
ApEn MHR sc1	0.58 [0.40 ; 0.68]	0.62 [0.41 ; 0.69]	0.830
ApEn MHR sc2	0.79 [0.60 ; 0.95]	0.83 [0.59 ; 1.00]	0.675
ApEn MHR sc3	0.88 [0.69 ; 1.02]	0.90 [0.71 ; 1.15]	0.564
ApEn MHR sc4	0.95 [0.75 ; 1.08]	0.94 [0.78 ; 1.13]	0.627
ApEn MHR sc5	0.98 [0.81 ; 1.08]	0.93 [0.83 ; 1.12]	0.675
ApEn MHR Ci	4.24 [3.15 ; 4.78]	4.22 [3.32 ; 5.08]	0.659
SampEn MHR sc1	0.46 [0.31 ; 0.55]	0.49 [0.31 ; 0.57]	0.812
SampEn MHR sc2	0.66 [0.49 ; 0.82]	0.71 [0.48 ; 0.98]	0.611
SampEn MHR sc3	0.82 [0.61 ; 0.97]	0.89 [0.59 ; 1.18]	0.549
SampEn MHR sc4	0.90 [0.71 ; 1.10]	1.06 [0.70 ; 1.19]	0.462
SampEn MHR sc5	0.98 [0.80 ; 1.17]	1.16 [0.78 ; 1.19]	0.534
SampEn MHR Ci	3.84 [2.85 ; 4.63]	4.32 [2.87 ; 5.10]	0.519
FuzzEn MHR sc1	0.17 [0.11 ; 0.24]	0.16 [0.10 ; 0.26]	0.901
FuzzEn MHR sc2	0.26 [0.18 ; 0.33]	0.24 [0.17 ; 0.38]	0.919
FuzzEn MHR sc3	0.34 [0.25 ; 0.43]	0.34 [0.22 ; 0.51]	0.830
FuzzEn MHR sc4	0.41 [0.30 ; 0.51]	0.42 [0.26 ; 0.59]	0.777
FuzzEn MHR sc5	0.46 [0.33 ; 0.56]	0.48 [0.31 ; 0.64]	0.643
FuzzEn MHR Ci	1.61 [1.18 ; 2.07]	1.64 [1.03 ; 2.37]	0.812
PermEn MHR sc1	1.34 [1.23 ; 1.41]	1.30 [1.22 ; 1.36]	0.371
PermEn MHR sc2	2.21 [2.12 ; 2.30]	2.23 [2.14 ; 2.24]	0.709
PermEn MHR sc3	2.33 [2.24 ; 2.44]	2.33 [2.21 ; 2.37]	0.659
PermEn MHR sc4	2.40 [2.30 ; 2.47]	2.41 [2.27 ; 2.44]	0.865
PermEn MHR sc5	2.42 [2.34 ; 2.49]	2.43 [2.31 ; 2.48]	0.847
PermEn MHR Ci	10.6 [10.4 ; 11.0]	10.7 [10.4 ; 10.8]	0.675
cCondEn MHR sc1	0.37 [0.30 ; 0.44]	0.45 [0.38 ; 0.48]	0.132
cCondEn MHR sc2	0.57 [0.48 ; 0.68]	0.70 [0.60 ; 0.72]	0.157
cCondEn MHR sc3	0.71 [0.59 ; 0.81]	0.80 [0.70 ; 0.84]	0.138

Continued on next page

Table A.6: Median, interquartile interval and p-value of the Mann-Whitney test for the last 10 minutes before birth. (Continued)

cCondEn MHR sc4	0.79 [0.66 ; 0.88]	0.89 [0.80 ; 0.95]	0.121
cCondEn MHR sc5	0.86 [0.72 ; 0.91]	0.94 [0.86 ; 1.00]	0.127
cCondEn MHR Ci	3.31 [2.79 ; 3.68]	3.77 [3.35 ; 3.98]	0.132
DispEn MHR sc1	1.37 [1.31 ; 1.45]	1.34 [1.28 ; 1.41]	0.659
DispEn MHR sc2	1.52 [1.43 ; 1.62]	1.50 [1.40 ; 1.60]	0.937
DispEn MHR sc3	1.59 [1.49 ; 1.71]	1.60 [1.47 ; 1.70]	0.865
DispEn MHR sc4	1.65 [1.55 ; 1.75]	1.68 [1.51 ; 1.75]	0.919
DispEn MHR sc5	1.69 [1.58 ; 1.81]	1.71 [1.55 ; 1.78]	0.883
DispEn MHR Ci	7.80 [7.35 ; 8.33]	7.85 [7.21 ; 8.24]	0.991
BubbEn MHR sc1	0.25 [0.23 ; 0.26]	0.24 [0.23 ; 0.25]	0.226
BubbEn MHR sc2	0.51 [0.46 ; 0.56]	0.52 [0.47 ; 0.52]	0.643
BubbEn MHR sc3	0.57 [0.53 ; 0.61]	0.57 [0.51 ; 0.59]	0.777
BubbEn MHR sc4	0.60 [0.56 ; 0.61]	0.60 [0.55 ; 0.60]	0.490
BubbEn MHR sc5	0.61 [0.58 ; 0.62]	0.57 [0.55 ; 0.61]	0.263
BubbEn MHR Ci	2.50 [2.38 ; 2.64]	2.52 [2.35 ; 2.57]	0.504
AttnEn MHR sc1	3.55 [3.34 ; 3.82]	3.84 [3.36 ; 3.91]	0.325
AttnEn MHR sc2	3.20 [2.89 ; 3.32]	3.07 [3.02 ; 3.40]	0.991
AttnEn MHR sc3	2.80 [2.51 ; 3.04]	2.69 [2.64 ; 3.06]	0.919
AttnEn MHR sc4	2.62 [2.34 ; 2.83]	2.46 [2.40 ; 2.81]	0.865
AttnEn MHR sc5	2.46 [2.24 ; 2.70]	2.29 [2.21 ; 2.79]	0.812
AttnEn MHR Ci	14.6 [13.6 ; 15.4]	14.4 [14.2 ; 15.1]	0.955
SE lin FHR	1.37 [1.26 ; 1.61]	1.57 [1.19 ; 2.04]	0.435
SE bin FHR	1.17 [1.03 ; 1.27]	1.17 [1.02 ; 1.24]	0.883
SE lin MHR	1.48 [1.03 ; 1.66]	1.47 [1.25 ; 1.68]	0.659
SE bin MHR	1.05 [0.92 ; 1.22]	1.15 [1.02 ; 1.29]	0.244
TE lin MHR–FHR	1.28 [0.46 ; 1.99] E-03	1.48 [1.01 ; 2.01] E-03	0.448
TE bin MHR–FHR	0.77 [0.00 ; 1.21] E-02	1.76 [0.17 ; 2.84] E-02	0.136
TE lin FHR–MHR	1.53 [0.64 ; 2.81] E-03	3.99 [1.62 ; 7.40] E-04	0.029
TE bin FHR–MHR	0.00 [0.00 ; 1.08] E-02	0.00 [0.00 ; 5.73] E-03	0.546

A.2 Generalised Linear Mixed Models results

Table A.7: Generalised Linear Mixed Models results considering entropy method and time fixed effects, and subject variability a random effect.

Measure	Model fit	Fixed effects coefficients (95% CIs)				Random effects
	AIC	Method' Estimate	Method' p-value	Time' Estimate	Time' p-value	Subject' Estimate
mean FHR	5021	-0.014	0.536	-0.0037	0.972	3.535
std FHR	5014	0.020	0.656	-0.0213	0.858	3.538
mean MHR	5027	-0.023	0.509	0.0375	0.746	3.538
std MHR	5023	0.071	0.496	-0.0354	0.767	3.530
XApEn FHR	5008	-0.257	0.857	0.0062	0.952	3.545
XApEn MHR	5012	-0.502	0.697	0.0008	0.994	3.538
XSampEn	5007	-0.035	0.993	0.0053	0.961	3.546
XFuzzEn	5009	-2.208	0.812	0.0191	0.872	3.545
XPermEn	5013	-5.709	0.726	0.0195	0.861	3.542
XCondEn FHR	5020	1.028	0.601	-0.0080	0.941	3.542
XCondEn MHR	5008	0.265	0.837	0.0019	0.986	3.546
ApEn FHR sc1	5007	-0.334	0.917	0.0035	0.974	3.546
ApEn FHR sc2	5007	0.013	0.996	0.0057	0.957	3.547
ApEn FHR sc3	5008	0.314	0.896	0.0074	0.944	3.547
ApEn FHR sc4	5008	0.368	0.871	0.0077	0.942	3.547
ApEn FHR sc5	5008	0.365	0.864	0.0085	0.936	3.547
ApEn FHR Ci	5007	0.045	0.929	0.0071	0.947	3.547
SampEn FHR sc1	5008	-0.613	0.873	0.0003	0.997	3.545
SampEn FHR sc2	5007	-0.169	0.950	0.0038	0.972	3.546
SampEn FHR sc3	5007	0.155	0.946	0.0074	0.945	3.547
SampEn FHR sc4	5007	0.235	0.907	0.0085	0.937	3.547
SampEn FHR sc5	5007	0.226	0.896	0.0090	0.933	3.547
SampEn FHR Ci	5007	0.022	0.963	0.0069	0.949	3.547
FuzzEn FHR sc1	5008	1.928	0.871	-0.0032	0.978	3.545
FuzzEn FHR sc2	5008	1.002	0.874	-0.0031	0.979	3.545
FuzzEn FHR sc3	5007	0.571	0.894	-0.0016	0.989	3.546
FuzzEn FHR sc4	5007	0.416	0.902	-0.0011	0.992	3.546

Continued on next page

Table A.7: Generalised Linear Mixed Models results considering entropy method and time fixed effects, and subject variability a random effect. (Continued)

FuzzEn FHR sc5	5007	0.306	0.917	-0.0001	0.999	3.546
FuzzEn FHR Ci	5007	0.115	0.898	-0.0014	0.991	3.546
PermEn FHR sc1	5026	2.082	0.596	0.0090	0.932	3.550
PermEn FHR sc2	5007	0.234	0.920	0.0052	0.960	3.548
PermEn FHR sc3	5008	0.404	0.881	0.0040	0.970	3.550
PermEn FHR sc4	5013	0.833	0.803	-0.0010	0.993	3.553
PermEn FHR sc5	5016	1.015	0.780	-0.0014	0.989	3.554
PermEn FHR Ci	5014	0.198	0.792	0.0020	0.984	3.554
cCondEn FHR sc1	5007	0.273	0.961	0.0053	0.960	3.547
cCondEn FHR sc2	5007	0.455	0.894	0.0037	0.972	3.546
cCondEn FHR sc3	5008	0.546	-4.881	0.0025	0.981	3.546
cCondEn FHR sc4	5010	0.658	0.783	0.0013	0.990	3.544
cCondEn FHR sc5	5011	0.695	0.750	0.0010	0.993	3.544
cCondEn FHR Ci	5009	0.135	0.821	0.0023	0.982	3.545
DispEn FHR sc1	5010	0.610	0.819	0.0066	0.950	3.548
DispEn FHR sc2	5009	0.479	0.839	0.0064	0.951	3.548
DispEn FHR sc3	5009	0.433	0.844	0.0064	0.951	3.548
DispEn FHR sc4	5008	0.362	0.861	0.0063	0.952	3.548
DispEn FHR sc5	5009	0.387	0.846	0.0063	0.952	3.548
DispEn FHR Ci	5009	0.090	0.842	0.0064	0.951	3.548
BubbEn FHR sc1	5020	8.594	0.658	0.0127	0.905	3.551
BubbEn FHR sc2	5007	-0.733	0.912	0.0061	0.953	3.545
BubbEn FHR sc3	5007	-0.048	0.995	0.0057	0.957	3.546
BubbEn FHR sc4	5009	1.478	0.855	0.0009	0.994	3.549
BubbEn FHR sc5	5012	2.443	0.772	-0.0015	0.989	3.550
BubbEn FHR Ci	5008	0.273	0.890	0.0036	0.972	3.548
AttnEn FHR sc1	5007	-0.030	0.959	0.0063	0.952	3.546
AttnEn FHR sc2	5028	0.715	0.629	0.0118	0.911	3.549
AttnEn FHR sc3	5012	0.426	0.788	0.0069	0.947	3.551

Continued on next page

Table A.7: Generalised Linear Mixed Models results considering entropy method and time fixed effects, and subject variability a random effect. (Continued)

AttnEn FHR sc4	5010	0.318	0.837	0.0074	0.944	3.550
AttnEn FHR sc5	5010	0.355	0.813	0.0079	0.940	3.550
AttnEn FHR Ci	5012	0.094	0.797	0.0060	0.955	3.552
ApEn MHR sc1	5007	-0.109	0.962	0.0047	0.965	3.546
ApEn MHR sc2	5007	0.141	0.937	0.0076	0.944	3.547
ApEn MHR sc3	5009	0.416	0.822	0.0112	0.917	3.547
ApEn MHR sc4	5012	0.614	0.753	0.0146	0.893	3.548
ApEn MHR sc5	5011	0.621	0.769	0.0134	0.901	3.548
ApEn MHR Ci	5008	0.074	0.855	0.0103	0.924	3.547
SampEn MHR sc1	5007	-0.195	0.935	0.0042	0.969	3.546
SampEn MHR sc2	5007	0.125	0.937	0.0076	0.943	3.547
SampEn MHR sc3	5008	0.300	0.836	0.0109	0.919	3.547
SampEn MHR sc4	5011	0.413	0.760	0.0142	0.896	3.547
SampEn MHR sc5	5010	0.370	0.777	0.0128	0.905	3.547
SampEn MHR Ci	5008	0.061	0.848	0.0105	0.922	3.547
FuzzEn MHR sc1	5013	-2.089	0.727	0.0204	0.856	3.544
FuzzEn MHR sc2	5011	-1.144	0.779	0.0177	0.875	3.545
FuzzEn MHR sc3	5008	-0.601	0.854	0.0139	0.902	3.545
FuzzEn MHR sc4	5007	-0.337	0.905	0.0112	0.922	3.546
FuzzEn MHR sc5	5008	-0.328	0.901	0.0119	0.918	3.546
FuzzEn MHR Ci	5009	-0.134	0.848	0.0146	0.898	3.545
PermEn MHR sc1	5015	-1.290	0.674	0.0212	0.848	3.541
PermEn MHR sc2	5007	0.022	0.992	0.0055	0.958	3.547
PermEn MHR sc3	5009	0.389	0.878	0.0058	0.956	3.550
PermEn MHR sc4	5024	1.365	0.728	0.0122	0.910	3.556
PermEn MHR sc5	5041	2.152	0.648	0.0204	0.856	3.553
PermEn MHR Ci	5009	0.099	0.869	0.0049	0.962	3.551
cCondEn MHR sc1	5015	1.649	0.674	0.0033	0.975	3.545
cCondEn MHR sc2	5017	1.311	0.629	0.0045	0.966	3.544

Continued on next page

Table A.7: Generalised Linear Mixed Models results considering entropy method and time fixed effects, and subject variability a random effect. (Continued)

cCondEn MHR sc3	5018	1.203	0.617	0.0041	0.969	3.544
cCondEn MHR sc4	5019	1.202	0.596	0.0034	0.974	3.543
cCondEn MHR sc5	5016	0.996	0.646	0.0040	0.969	3.544
cCondEn MHR Ci	5017	0.261	0.621	0.0038	0.971	3.544
DispEn MHR sc1	5008	0.514	0.871	0.0069	0.947	3.549
DispEn MHR sc2	5009	0.442	0.856	0.0079	0.940	3.549
DispEn MHR sc3	5010	0.548	0.811	0.0088	0.934	3.550
DispEn MHR sc4	5011	0.587	0.790	0.0094	0.929	3.550
DispEn MHR sc5	5011	0.585	0.786	0.0093	0.930	3.550
DispEn MHR Ci	5010	0.112	0.817	0.0086	0.935	3.550
BubbEn MHR sc1	5011	-5.288	0.768	0.0146	0.893	3.542
BubbEn MHR sc2	5009	-1.400	0.836	0.0073	0.944	3.543
BubbEn MHR sc3	5009	1.371	0.856	0.0074	0.944	3.549
BubbEn MHR sc4	5029	5.531	0.639	0.0164	0.880	3.551
BubbEn MHR sc5	5015	3.101	0.763	0.0079	0.940	3.553
BubbEn MHR Ci	5009	0.320	0.876	0.0058	0.955	3.550
AttnEn MHR sc1	5007	0.003	0.997	0.0056	0.957	3.547
AttnEn MHR sc2	5007	-0.010	0.993	0.0058	0.956	3.546
AttnEn MHR sc3	5010	-0.294	0.787	0.0144	0.895	3.543
AttnEn MHR sc4	5017	-0.536	0.629	0.0253	0.822	3.539
AttnEn MHR sc5	5017	-0.583	0.617	0.0267	0.813	3.538
AttnEn MHR Ci	5010	-0.062	0.791	0.0130	0.904	3.543
SE lin FHR	5009	0.229	0.784	0.0118	0.912	3.545
SE bin FHR	5012	0.566	0.705	-0.0048	0.964	3.542
SE lin MHR	5010	0.283	0.787	0.0004	0.997	3.546
SE bin MHR	5021	1.176	0.583	-0.0145	0.895	3.541
TE lin MHR–FHR	5011	-34.797	0.834	0.0039	0.970	3.544
TE bin MHR–FHR	5011	14.104	0.723	-0.0059	0.957	3.541
TE lin FHR–MHR	5007	-13.001	0.923	0.0047	0.964	3.546

Continued on next page

Table A.7: Generalised Linear Mixed Models results considering entropy method and time fixed effects, and subject variability a random effect. (Continued)

TE bin FHR–MHR	5007	-0.134	0.997	0.0056	0.957	3.546

Table A.8: Generalised Linear Mixed Models results considering entropy method a fixed effect, and subject variability and time random effect.

Measure	**Model fit**	**Fixed effects coefficients (95% CIs)**		**Random effects**	
	AIC	**'Method' Estimate**	**'Method' p-value**	**'Time' Estimate**	**'Subject' Estimate**
mean FHR	5021	-0.014	0.537	3.30E-05	3.535
std FHR	5013	0.016	0.679	1.76E-05	3.540
mean MHR	5021	-0.018	0.561	2.60E-05	3.538
std MHR	5019	0.056	0.540	2.94E-05	3.532
XApEn FHR	5008	-0.255	0.858	2.53E-05	3.545
XApEn MHR	5012	-0.504	0.693	2.05E-05	3.538
XSampEn	5007	-0.094	0.980	1.14E-05	3.546
XFuzzEn	5008	-1.493	0.854	3.19E-05	3.545
XPermEn	5011	-4.708	0.755	1.90E-05	3.542
XCondEn FHR	5019	0.992	0.602	1.61E-05	3.542
XCondEn MHR	5008	0.269	0.832	2.00E-05	3.546
ApEn FHR sc1	5007	-0.355	0.910	2.09E-05	3.546
ApEn FHR sc2	5007	-0.008	0.997	1.76E-05	3.546
ApEn FHR sc3	5007	0.292	0.903	2.01E-05	3.547
ApEn FHR sc4	5008	0.348	0.877	1.91E-05	3.546
ApEn FHR sc5	5008	0.338	0.872	1.14E-05	3.546
ApEn FHR Ci	5007	0.040	0.937	1.24E-05	3.547
SampEn FHR sc1	5008	-0.617	0.866	1.98E-05	3.545
SampEn FHR sc2	5007	-0.194	0.940	2.85E-05	3.546
SampEn FHR sc3	5007	0.115	0.959	1.48E-05	3.547
SampEn FHR sc4	5007	0.198	0.919	2.59E-05	3.547
SampEn FHR sc5	5007	0.191	0.909	1.76E-05	3.546

Continued on next page

Table A.8: Generalised Linear Mixed Models results considering entropy method a fixed effect, and subject variability and time random effect. (Continued)

SampEn FHR Ci	5007	0.014	0.975	2.02E-05	3.547
FuzzEn FHR sc1	5008	1.780	0.865	1.62E-05	3.545
FuzzEn FHR sc2	5008	0.924	0.869	1.90E-05	3.545
FuzzEn FHR sc3	5007	0.543	0.886	1.76E-05	3.546
FuzzEn FHR sc4	5007	0.400	0.893	1.41E-05	3.546
FuzzEn FHR sc5	5007	0.305	0.906	2.02E-05	3.546
FuzzEn FHR Ci	5007	0.110	0.890	2.25E-05	3.546
PermEn FHR sc1	5025	2.048	0.597	2.57E-05	3.550
PermEn FHR sc2	5007	0.238	0.918	2.99E-05	3.548
PermEn FHR sc3	5008	0.413	0.877	9.84E-06	3.550
PermEn FHR sc4	5013	0.827	0.800	2.54E-05	3.553
PermEn FHR sc5	5016	1.006	0.777	1.60E-05	3.554
PermEn FHR Ci	5014	0.199	0.790	2.01E-05	3.554
cCondEn FHR sc1	5007	0.293	0.959	1.83E-05	3.547
cCondEn FHR sc2	5007	0.471	0.889	1.90E-05	3.546
cCondEn FHR sc3	5008	0.555	0.839	3.58E-05	3.546
cCondEn FHR sc4	5010	0.663	0.780	1.43E-05	3.544
cCondEn FHR sc5	5011	0.698	0.747	1.48E-05	3.544
cCondEn FHR Ci	5009	0.137	0.817	2.66E-05	3.545
DispEn FHR sc1	5009	0.602	0.820	1.33E-05	3.548
DispEn FHR sc2	5009	0.473	0.841	1.43E-05	3.548
DispEn FHR sc3	5009	0.427	0.846	2.51E-05	3.548
DispEn FHR sc4	5008	0.356	0.862	1.48E-05	3.548
DispEn FHR sc5	5008	0.382	0.847	2.86E-05	3.548
DispEn FHR Ci	5009	0.089	0.843	2.51E-05	3.548
BubbEn FHR sc1	5019	8.181	0.664	7.80E-06	3.550
BubbEn FHR sc2	5007	-0.715	0.914	3.18E-05	3.545
BubbEn FHR sc3	5007	-0.012	0.999	8.61E-06	3.546
BubbEn FHR sc4	5009	1.493	0.849	1.25E-05	3.549

Continued on next page

Table A.8: Generalised Linear Mixed Models results considering entropy method a fixed effect, and subject variability and time random effect. (Continued)

BubbEn FHR sc5	5012	2.419	0.769	1.24E-05	3.550
BubbEn FHR Ci	5008	0.282	0.886	1.76E-05	3.549
AttnEn FHR sc1	5007	-0.025	0.965	2.46E-05	3.546
AttnEn FHR sc2	5027	0.690	0.632	3.61E-05	3.549
AttnEn FHR sc3	5012	0.419	0.790	1.92E-05	3.551
AttnEn FHR sc4	5009	0.307	0.840	2.37E-05	3.550
AttnEn FHR sc5	5010	0.343	0.816	7.80E-06	3.549
AttnEn FHR Ci	5012	0.093	0.797	1.22E-05	3.552
ApEn MHR sc1	5007	-0.128	0.954	1.40E-05	3.546
ApEn MHR sc2	5007	0.112	0.948	1.81E-05	3.547
ApEn MHR sc3	5009	0.371	0.835	1.41E-05	3.547
ApEn MHR sc4	5011	0.544	0.771	2.02E-05	3.547
ApEn MHR sc5	5010	0.555	0.784	1.48E-05	3.547
ApEn MHR Ci	5008	0.065	0.868	2.27E-05	3.547
SampEn MHR sc1	5007	-0.211	0.929	1.75E-05	3.546
SampEn MHR sc2	5007	0.098	0.949	1.40E-05	3.547
SampEn MHR sc3	5008	0.265	0.850	1.40E-05	3.547
SampEn MHR sc4	5010	0.367	0.778	1.77E-05	3.546
SampEn MHR sc5	5010	0.333	0.792	2.32E-05	3.546
SampEn MHR Ci	5008	0.053	0.862	2.52E-05	3.547
FuzzEn MHR sc1	5011	-1.677	0.760	1.61E-05	3.544
FuzzEn MHR sc2	5009	-0.898	0.810	2.32E-05	3.545
FuzzEn MHR sc3	5008	-0.440	0.883	2.53E-05	3.546
FuzzEn MHR sc4	5007	-0.222	0.931	2.53E-05	3.546
FuzzEn MHR sc5	5007	-0.210	0.929	2.85E-05	3.546
FuzzEn MHR Ci	5008	-0.097	0.878	1.48E-05	3.545
PermEn MHR sc1	5013	-1.084	0.708	1.76E-05	3.541
PermEn MHR sc2	5007	0.035	0.988	2.93E-05	3.547
PermEn MHR sc3	5008	0.385	0.878	3.00E-05	3.550

Continued on next page

Table A.8: Generalised Linear Mixed Models results considering entropy method a fixed effect, and subject variability and time random effect. (Continued)

PermEn MHR sc4	5022	1.262	0.729	7.86E-06	3.555
PermEn MHR sc5	5034	1.854	0.662	2.31E-05	3.553
PermEn MHR Ci	5009	0.100	0.867	1.14E-05	3.551
cCondEn MHR sc1	5015	1.656	0.673	1.77E-05	3.545
cCondEn MHR sc2	5017	1.314	0.628	2.02E-05	3.544
cCondEn MHR sc3	5018	1.207	0.616	2.09E-05	3.543
cCondEn MHR sc4	5019	1.205	0.594	1.49E-05	3.543
cCondEn MHR sc5	5016	0.999	0.645	9.81E-06	3.544
cCondEn MHR Ci	5018	0.262	0.619	2.70E-05	3.544
DispEn MHR sc1	5008	0.496	0.874	1.89E-05	3.549
DispEn MHR sc2	5008	0.419	0.861	1.62E-05	3.549
DispEn MHR sc3	5010	0.522	0.816	2.17E-05	3.549
DispEn MHR sc4	5010	0.557	0.796	3.01E-05	3.549
DispEn MHR sc5	5010	0.559	0.792	2.02E-05	3.549
DispEn MHR Ci	5009	0.107	0.822	1.48E-05	3.549
BubbEn MHR sc1	5010	-4.578	0.790	1.45E-05	3.543
BubbEn MHR sc2	5009	-1.360	0.840	1.70E-05	3.544
BubbEn MHR sc3	5008	1.316	0.860	9.93E-06	3.549
BubbEn MHR sc4	5026	5.080	0.646	2.54E-05	3.551
BubbEn MHR sc5	5014	3.018	0.764	2.55E-05	3.552
BubbEn MHR Ci	5008	0.317	0.876	1.04E-05	3.550
AttnEn MHR sc1	5007	0.002	0.998	8.64E-06	3.547
AttnEn MHR sc2	5007	0.002	0.998	2.34E-05	3.547
AttnEn MHR sc3	5009	-0.250	0.808	2.58E-05	3.543
AttnEn MHR sc4	5014	-0.442	0.664	1.35E-05	3.540
AttnEn MHR sc5	5014	-0.476	0.655	2.08E-05	3.539
AttnEn MHR Ci	5009	-0.054	0.808	3.43E-05	3.543
SE lin FHR	5009	0.209	0.797	3.42E-05	3.545
SE bin FHR	5012	0.548	0.704	4.15E-05	3.543

Continued on next page

Table A.8: Generalised Linear Mixed Models results considering entropy method a fixed effect, and subject variability and time random effect. (Continued)

SE lin MHR	5010	0.284	0.783	2.01E-05	3.546
SE bin MHR	5019	1.083	0.592	1.47E-05	3.541
TE lin MHR–FHR	5011	-35.263	0.831	1.25E-05	3.544
TE bin MHR–FHR	5011	13.486	0.723	9.97E-06	3.541
TE lin FHR–MHR	5007	-13.522	0.919	1.98E-05	3.546
TE bin FHR–MHR	5007	-0.039	0.999	2.49E-05	3.546

References

[1] A.A. Alaqeel. Hyporegenerative anemia and other complications of rhesus hemolytic disease: to treat or not to treat is the question. *Pan African Medical Journal*, 32:120, 2019.

[2] J.F. Alonso, M.A. Mañanas, S. Romero, M. Rojas-Martínez, and J. Riba. Cross-conditional entropy and coherence analysis of pharmaco-eeg changes induced by alprazolam. *Psychopharmacology*, 221:397–406, 2012.

[3] C. Antoine and B.K. Young. Fetal lactic acidosis with epidural anesthesia. *American Journal of Obstetrics and Gynecology*, 142(1):55–59, 1982.

[4] V. Apgar. A proposal for a new method of evaluation of the newborn infant. *Anesthesia & Analgesia*, 120(5):1056–1059, 2015.

[5] Y.-C.P. Arai, W. Ueda, T. Ushida, N. Kandatsu, H. Ito, and T. Komatsu. Increased heart rate variability correlation between mother and child immediately pre-operation. *Acta Anaesthesiologica Scandinavica*, 53(5):607–610, 2009.

[6] S. Asgari, F. Scalzo, and M. Kasprowicz. Pattern recognition in medical decision support. *BioMed Research International*, Vol. 2019:Article ID 6048748, 2019.

[7] R. Avci, D. Escalona-Vargas, E.R. Siegel, C.L. Lowery, and H. Eswaran. Coupling analysis of fetal and maternal heart rates via transfer entropy using magnetocardiography. In *2018 40th Annual International Conference of the IEEE Engineering in Medicine and Biology Society (EMBC)*, pages 1–4, Honolulu, HI, USA, 2018. IEEE.

[8] D. Ayres-de Campos, S. Arulkumaran, and FIGO Intrapartum Fetal Monitoring Expert Consensus Panel. FIGO consensus guidelines on intrapartum fetal monitoring: Physiology of fetal oxygenation and the main goals of intrapartum fetal monitoring. *International Journal of Gynecology and Obstetrics*, 131(1):5–8, 2015.

[9] D. Ayres-de Campos, J. Bernardes, A. Costa-Pereira, and L. Pereira-Leite. Inconsistencies in classification by experts of cardiotocograms and subsequent clinical decision. *British Journal of Obstetrics and Gynaecology*, 106(12):1307–1310, 1999.

[10] D. Ayres-de Campos, P. Sousa, A. Costa, and J. Bernardes. Omniview-SisPorto®3.5 – a central fetal monitoring station with online alerts based on computerized cardiotocogram+ST event analysis. *Journal of Perinatal Medicine*, 36(3):260–264, 2008.

[11] D. Ayres-de Campos, C.Y. Spong, E. Chandraharan, and FIGO Intrapartum Fetal Monitoring Expert Consensus Panel. FIGO consensus guidelines on intrapartum fetal monitoring: Cardiotocography. *International Journal of Gynecology and Obstetrics*, 131(1):13–24, 2015.

[12] H. Azami, P. Li, S.E. Arnold, J. Escudero, and A. Humeau-Heurtier. Fuzzy entropy metrics for the analysis of biomedical signals: Assessment and comparison. *IEEE Access*, 7:104833–104847, 2019.

[13] P.C.A.M. Bakker, G.J. Colenbrander, A.A. Verstraeten, and H.P. Van Geijn. The quality of intrapartum fetal heart rate monitoring. *European Journal of Obstetrics & Gynecology and Reproductive Biology*, 116(1):22–27, 2004.

[14] P.C.A.M. Bakker, P.H.J. Kurver, D.J. Kuik, and H.P. Van Geijn. Elevated uterine activity increases the risk of fetal acidosis at birth. *American Journal of Obstetrics and Gynecology*, 196(4):313.e1–313.e6, 2007.

[15] C. Bandt and B. Pompe. Permutation entropy: a natural complexity measure for time series. *Physical review letters*, 88(17):174102, 2002.

[16] O. Barquero-Pérez, R. Goya-Esteban, A. Caamano, C. Martín-Caballero, and J.L. Rojo-Alvarez. Fetal heart rate complexity measures to detect hypoxia. In *2015 Computing in Cardiology Conference (CinC)*, pages 133–136. IEEE, 2015.

[17] J.M. Barrett and F.H. Boehm. Documentation of recent fetal demise with simultaneous maternal and fetal heart rate monitoring. *Obstetrics & Gynecology*, 55(3 Suppl):28S–30S, 1980.

[18] J. Bernardes and D. Ayres-de Campos. Maternal heart rate analysis during labor. Has the time come for computerized analysis? *Acta Obstetricia et Gynecologica Scandinavica*, 91(12):1474, 2012.

[19] C. Bian, C. Qin, Q. Ma, and Q. Shen. Modified permutation-entropy analysis of heartbeat dynamics. *Physical Review E*, 85(2):021906, 2012.

[20] C.S. Bobrow and P.W. Soothill. Causes and consequences of fetal acidosis. *Archives of Disease in Childhood-Fetal and Neonatal Edition*, 80(3):F246–F249, 1999.

[21] A. Bokslag, M. van Weissenbruch, B.W. Mol, and C.J.M. de Groot. Preeclampsia; short and long-term consequences for mother and neonate. *Early human development*, 102:47–50, 2016.

[22] P.A. Bromiley, N.A. Thacker, and E. Bouhova-Thacker. Shannon entropy, renyi entropy, and information. *Statistics and Inf. Series (2004-004)*, 9:10–42, 2004.

[23] M.A. Busa and R.E.A. van Emmerik. Multiscale entropy: A tool for understanding the complexity of postural control. *Journal of Sport and Health Science*, 5(1):44–51, 2016.

[24] C. Carson. The effective use of effect size indices in institutional research. In *31st Annual Conference Proceedings*, volume 41, Portsmouth, NH, USA, 2012.

[25] A.M. Carter. Placental gas exchange and the oxygen supply to the fetus. *Comprehensive Physiology*, 5(3):1381–1403, 2011.

[26] M.C. Carter. Signal processing and display—cardiotocographs. *British Journal of Obstetrics and Gynaecology*, 100(s9):21–23, 1993.

[27] P. Castiglioni, G. Merati, G. Parati, and A. Faini. Sample, fuzzy and distribution entropies of heart rate variability: What do they tell us on cardiovascular complexity? *Entropy*, 25(2), 2023.

[28] L. Castro, M. Loureiro, T.S. Henriques, and I. Nunes. Systematic review of intrapartum fetal heart rate spectral analysis and an application in the detection of fetal acidemia. *Frontiers in Pediatrics*, 9:661400, 2021.

[29] R.V. Ceguerra, J.T. Lizier, and A.Y. Zomaya. Information storage and transfer in the synchronization process in locally-connected networks. In *2011 IEEE Symposium on Artificial Life (ALIFE)*, pages 54–61, Paris, France, 2011. IEEE.

[30] W. Chen, Z. Wang, H. Xie, and W. Yu. Characterization of surface EMG signal based on fuzzy entropy. *IEEE Transactions on Neural Systems and Rehabilitation Engineering*, 15(2):266–272, 2007.

[31] X. Chen, G. Xu, S. Zhang, X. Zhang, and Z. Teng. Building networks with a new cross-bubble transition entropy for quantitative assessment of mental arithmetic electroencephalogram. *Applied Sciences*, 12(21):11165, 2022.

[32] C.C. Chiu, S.J. Yeh, and T.Y. Li. Assessment of diabetics with various degrees of autonomic neuropathy based on cross-approximate entropy. In N. Osman, W. Abas, A. Wahab, and H. Ting, editors, *5th Kuala Lumpur International Conference on Biomedical Engineering 2011*, pages 266–269, Berlin, Heidelberg, 2011. Springer Berlin Heidelberg.

[33] D.Y. Chung, Y.B. Sim, K.T. Park, S.H. Yi, J.C. Shin, and S.P. Kim. Spectral analysis of fetal heart rate variability as a predictor of intrapartum fetal distress. *International Journal of Gynecology & Obstetrics*, 73(2):109–116, 2001.

[34] M. Costa, A.L. Goldberger, and C.-K. Peng. Multiscale entropy analysis of complex physiologic time series. *Physical review letters*, 89(6):068102, 2002.

[35] M. Costa, A.L Goldberger, and C.-K. Peng. Multiscale entropy analysis of biological signals. *Physical review E*, 71(2):021906, 2005.

[36] M. Costa, C.-K. Peng, and A.L. Goldberger. Multiscale analysis of heart rate dynamics: entropy and time irreversibility measures. *Cardiovascular Engineering*, 8(2):88–93, 2008.

[37] M. Costa, C.-K. Peng, A.L. Goldberger, and J.M. Hausdorff. Multiscale entropy analysis of human gait dynamics. *Physica A: Statistical Mechanics and its applications*, 330(1–2):53–60, 2003.

[38] D. Cuesta-Frau and B. Vargas. Permutation entropy and bubble entropy: Possible interactions and synergies between order and sorting relations. *Mathematical Biosciences and Engineering*, 17(2):1637–1658, 2020.

[39] A. Delgado-Bonal and A. Marshak. Approximate entropy and sample entropy: A comprehensive tutorial. *Entropy*, 21(6):541, 2019.

[40] J.A. DiPietro. Maternal stress in pregnancy: considerations for fetal development. *Journal of Adolescent Health*, 51(2 Suppl):S3–S8, 2012.

[41] H.S. Dweck, W. Huggins, L.P. Dorman, S.A. Saxon, J.W. Benton Jr, and G. Cassady. Developmental sequelae in infants having suffered severe perinatal asphyxia. *American journal of obstetrics and gynecology*, 119(6):811–815, 1974.

[42] S.J. Dwinnell, S. Coad, B. Butler, S. Albersheim, L.D. Wadsworth, J.K. Wu, and M.-F. Delisle. In utero diagnosis and management of a fetus with homozygous α-thalassemia in the second trimester: a case report and literature review. *Journal of Pediatric Hematology/Oncology*, 33(8):e358–e360, 2011.

[43] A. Ebrashy, O. Azmy, M. Ibrahim, M. Waly, and A. Edris. Middle cerebral/umbilical artery resistance index ratio as sensitive parameter for fetal well-being and neonatal outcome in patients with preeclampsia: case-control study. *Croatian medical journal*, 46(5):821–825, 2005.

[44] L. Faes. ITS – Matlab Tool for the computation of Information Dynamics. http://www.lucafaes.net/its.html, 2019. Accessed: 2023-01-20.

[45] L. Faes. ITS Toolbox: a Matlab toolbox for the practical computation of information dynamics [PowerPoint slides]. http://www.lucafaes.net/code/ITS_Toolbox_v2.1.pdf, 2019. Accessed: 2023-01-20.

[46] L. Faes, M. Gómez-Extremera, R. Pernice, P. Carpena, G. Nollo, A. Porta, and P. Bernaola-Galván. Comparison of methods for the assessment of nonlinearity in short-term heart rate variability under different physiopathological states. *Chaos*, 29(12):123114, 2019.

[47] L. Faes, A. Porta, and G. Nollo. Information decomposition in bivariate systems: theory and application to cardiorespiratory dynamics. *Entropy*, 17(1):277–303, 2015.

[48] L. Faes, D. Widjaja, S. Van Huffel, and G. Nollo. Investigating cardiac and respiratory determinants of heart rate variability in an information-theoretic framework. In *2014 36th Annual International Conference of the IEEE Engineering in Medicine and Biology Society*, pages 6020–6023, Chicago, IL, USA, 2014. IEEE.

[49] F. Faul, E. Erdfelder, A. Buchner, and A. Lang. Statistical power analyses using g* power 3.1: Tests for correlation and regression analyses. *Behavior research methods*, 41(4):1149–1160, 2009.

[50] L.A. Fleisher, S.M. Pincus, and S.H. Rosenbaum. Approximate entropy of heart rate as a correlate of postoperative ventricular dysfunction. *Anesthesiology*, 78(4):683–692, 1993.

[51] A.D. Fleming and M. Henn. Maternal-fetal oxygenation. In J.P. Phelan, L.D. Pacheco, M.R. Foley, G.R. Saade, G.A. Dildy, and M.A. Belfort, editors, *Critical Care Obstetrics*, chapter 10, pages 175–182. John Wiley & Sons, Ltd, 6 edition, 2018.

[52] M.W Flood. *The EntropyHub Guide: A user manual for the EntropyHub toolkit*. EntropyHub, 2021.

[53] M.W. Flood and B. Grimm. Entropyhub: An open-source toolkit for entropic time series analysis. *PLoS ONE*, 16(11):e0259448, 2021.

[54] L. Frassineti, A. Lanatà, B. Olmi, and C. Manfredi. Multiscale entropy analysis of heart rate variability in neonatal patients with and without seizures. *Bioengineering*, 8(9):122, 2021.

[55] K.B. Gan, E. Zahedi, and M.A.M. Ali. Transabdominal fetal heart rate detection using nir photopleythysmography: instrumentation and clinical results. *IEEE transactions on Biomedical Engineering*, 56(8):2075–2082, 2009.

[56] A. Georgieva, M. Moulden, and C.W.G. Redman. Umbilical cord gases in relation to the neonatal condition: the everest plot. *European Journal of Obstetrics & Gynecology and Reproductive Biology*, 168(2):155–160, 2013.

[57] J. Gierałtowski, D. Hoyer, F. Tetschke, S. Nowack, U. Schneider, and J. Żebrowski. Development of multiscale complexity and multifractality of fetal heart rate variability. *Autonomic Neuroscience*, 178(1-2):29–36, 2013.

[58] E. Giorgio, M.A. De Oronzo, I. Iozza, A. Di Natale, S. Cianci, G. Garofalo, A.M. Giacobbe, and S. Politi. Parvovirus b19 during pregnancy: a review. *Journal of Prenatal Medicine*, 4(4):63–66, 2010.

[59] R.F. Goldstein, R.J. Thompson Jr., J.M. Oehler, and J.E. Brazy. Influence of acidosis, hypoxemia, and hypotension on neurodevelopmental outcome in very low birth weight infants. *Pediatrics*, 95(2):238–243, 1995.

[60] H. Gonçalves, D. Fernandes, P. Pinto, D. Ayres-de Campos, and J. Bernardes. Simultaneous monitoring of maternal and fetal heart rate variability during labor in relation with fetal gender. *Developmental Psychobiology*, 59(7):832–839, 2017.

[61] H. Goncalves, T. Henriques-Coelho, A.P. Rocha, A.P. Lourenco, A. Leite-Moreira, and J. Bernardes. Comparison of different methods of heart rate entropy analysis during acute anoxia superimposed on a chronic rat model of pulmonary hypertension. *Medical Engineering & Physics*, 35(5):559–568, 2013.

[62] H. Gonçalves, P. Pinto, M. Silva, D. Ayres-de Campos, and J. Bernardes. Electrocardiography versus photoplethysmography in assessment of maternal heart rate variability during labor. *SpringerPlus*, 5(1):1079, 2016.

[63] H. Gonçalves, P. Pinto, M. Silva, D. Ayres-de Campos, and J. Bernardes. Toward the improvement in fetal monitoring during labor with the inclusion of maternal heart rate analysis. *Medical & Biological Engineering & Computing*, 54(4):691–699, 2016.

[64] H. Gonçalves, A.P. Rocha, D. Ayres-de Campos, and J. Bernardes. Internal versus external intrapartum foetal heart rate monitoring: the effect on linear and nonlinear parameters. *Physiological Measurement*, 27(3):307–319, 2006.

[65] H. Gonçalves, A.P. Rocha, D. Ayres-de Campos, and J. Bernardes. Linear and nonlinear fetal heart rate analysis of normal and acidemic fetuses in the minutes preceding delivery. *Medical & Biological Engineering & Computing*, 44(10):847–855, 2006.

[66] A. Grandpierre. Entropy and information of human organisms and the nature of life. *Frontier Perspectives*, 13(2):16–21, 2004.

[67] S. Guzzetti, S. Mezzetti, R. Magatelli, A. Porta, G. De Angelis, G. Rovelli, and A. Malliani. Linear and non-linear 24 h heart rate variability in chronic heart failure. *Autonomic Neuroscience*, 86(1-2):114–119, 2000.

[68] P. Hamelmann, R. Vullings, A. Kolen, J. Bergmans, J. van Laar, P. Tortoli, and M. Mischi. Doppler ultrasound technology for fetal heart rate monitoring: a review. *IEEE transactions on ultrasonics, ferroelectrics, and frequency control*, 67(2):226–238, 2019.

[69] A. Herbst and K. Thorngren-Jerneck. Mode of delivery in breech presentation at term: increased neonatal morbidity with vaginal delivery. *Acta Obstetricia et Gynecologica Scandinavica*, 80(8):731–737, 2001.

[70] A. Herbst, P. Wölner-Hanssen, and I. Ingemarsson. Risk factors for acidemia at birth. *Obstetrics & Gynecology*, 90(1):125–130, 1997.

[71] E.J. Herrick and B. Bordoni. *Embryology, Placenta*. StatPearls Publishing, Treasure Island (FL), 2022.

[72] K.-C. Hung. Medical pattern recognition: applying an improved intuitionistic fuzzy cross-entropy approach. *Advances in Fuzzy Systems*, Vol. 2012:Article ID 863549, 2012.

[73] J. Jiang and T. Nguyen. *Linear and generalized linear mixed models and their applications*, volume 1. Springer, 2007.

[74] A. Jubran. Pulse oximetry. *Critical Care*, 19:Article ID 272, 2015.

[75] E. Kafantaris, I. Piper, T.M. Lo, and J. Escudero. Augmentation of dispersion entropy for handling missing and outlier samples in physiological signal monitoring. *Entropy*, 22(3):319, 2020.

[76] C. Kähler, E. Schleußner, B. Grimm, A. Schneider, U. Schneider, H. Nowak, and H.J. Seewald. Fetal magnetocardiography: development of the fetal cardiac time intervals. *Prenatal Diagnosis*, 22(5):408–414, 2002.

[77] H. Kapaya, R. Williams, G. Elton, and D. Anumba. Can obstetric risk factors predict fetal acidaemia at birth? a retrospective case-control study. *Journal of Pregnancy*, 2018, 2018.

[78] V. Kapila and K. Chaudhry. *Physiology, Placenta*. StatPearls Publishing, Treasure Island (FL), 2021.

[79] A.H. Khandoker, F. Marzbanrad, A. Voss, S. Schulz, Y. Kimura, M. Endo, and M. Palaniswami. Analysis of maternal-fetal heart rate coupling directions with partial directed coherence. *Biomedical Signal Processing and Control*, 30:25–30, 2016.

[80] A.H. Khandoker, S. Schulz, H.M. Al-Angari, A. Voss, and Y. Kimura. Alterations in maternal-fetal heart rate coupling strength and directions in abnormal fetuses. *Frontiers in Physiology*, 10:482, 2019.

[81] A.H. Khandoker, M. Wahbah, R. Al Sakaji, K. Funamoto, A. Krishnan, and Y. Kimura. Estimating fetal age by fetal maternal heart rate coupling parameters. In *2020 42nd Annual International Conference of the IEEE Engineering in Medicine & Biology Society (EMBC)*, pages 604–607, Montreal, QC, Canada, 2020. IEEE.

[82] T. King and J. Parer. The physiology of fetal heart rate patterns and perinatal asphyxia. *The Journal of Perinatal & Neonatal Nursing*, 14(3):19–39, 2000.

[83] C.E. Kossmann. The normal electrocardiogram. *Circulation*, 8(6):920–936, 1953.

[84] F. Kovács, C. Horváth, A.T. Balogh, and G. Hosszú. Fetal phonocardiography—past and future possibilities. *Computer methods and programs in biomedicine*, 104(1):19–25, 2011.

[85] A.R. Laptook, S. Shankaran, N. Ambalavanan, W.A. Carlo, S.A. McDonald, R.D. Higgins, A. Das, and Hypothermia Subcommittee of the NICHD Neonatal Research Network. Outcome of term infants using apgar scores at 10 minutes following hypoxic-ischemic encephalopathy. *Pediatrics*, 124(6):1619–1626, 2009.

[86] X. Li, D. Zheng, S. Zhou, D. Tang, C. Wang, and G. Wu. Approximate entropy of fetal heart rate variability as a predictor of fetal distress in women at term pregnancy. *Acta Obstetricia et Gynecologica Scandinavica*, 84(9):837–843, 2005.

[87] J. Lim, J.Y. Kwon, J. Song, H. Choi, J.C. Shin, and I.Y. Park. Quantitative comparison of entropy analysis of fetal heart rate variability related to the different stages of labor. *Early human development*, 90(2):81–85, 2014.

[88] C. Liu, K. Li, L. Zhao, F. Liu, D. Zheng, C. Liu, and S. Liu. Analysis of heart rate variability using fuzzy measure entropy. *Computers in Biology and Medicine*, 43(2):100–108, 2013.

[89] C. Liu, C. Zhang, L. Zhang, L. Zhao, C. Liu, and H. Wang. Measuring synchronization in coupled simulation and coupled cardiovascular time series: A comparison of different cross entropy measures. *Biomedical Signal Processing and Control*, 21:49–57, 2015.

[90] J.T. Lizier, M. Prokopenko, and A.Y. Zomaya. A framework for the local information dynamics of distributed computation in complex systems. In *Guided self-organization: inception*, pages 115–158. Springer, 2014.

[91] J.A. Low, C. Panagiotopoulos, and E.J. Derrick. Newborn complications after intrapartum asphyxia with metabolic acidosis in the term fetus. *American Journal of Obstetrics and Gynecology*, 170(4):1081–1087, 1994.

[92] G. Lu and F. Yang. Limitations of oximetry to measure heart rate variability measures. *Cardiovascular Engineering*, 9(3):119–125, 2009.

[93] F. Maes, A. Collignon, D. Vandermeulen, G. Marchal, and P. Suetens. Multimodality image registration by maximization of mutual information. *IEEE Transactions on Medical Imaging*, 16(2):187–198, 1997.

[94] G. Manis, M.D. Aktaruzzaman, and R. Sassi. Bubble entropy: An entropy almost free of parameters. *IEEE Transactions on Biomedical Engineering*, 64(11):2711–2718, 2017.

[95] G. Manis, M. Bodini, M.W. Rivolta, and R. Sassi. A two-steps-ahead estimator for bubble entropy. *Entropy*, 23(6):761, 2021.

[96] G. Manis and R. Sassi. Relation between fetal hrv and value of umbilical cord artery ph in labor, a study with entropy measures. In *2017 IEEE 30th International Symposium on Computer-Based Medical Systems (CBMS)*, pages 272–277, Thessaloniki, Greece, 2017. IEEE.

[97] J.A.L. Marques, P.C. Cortez, J.P.V. Madeiro, V.H.C. de Albuquerque, S.J. Fong, and F.S. Schlindwein. Nonlinear characterization and complexity analysis of cardiotocographic examinations using entropy measures. *The Journal of Supercomputing*, 76(2):1305–1320, 2020.

[98] F. Marzbanrad, Y. Kimura, M. Endo, M. Palaniswami, and A.H. Khandoker. Transfer entropy analysis of maternal and fetal heart rate coupling. In *2015 37th Annual International Conference of the IEEE Engineering in Medicine and Biology Society (EMBC)*, pages 7865–7868, Milan, Italy, 2015. IEEE.

[99] F. Marzbanrad, Y. Kimura, M. Palaniswami, and A.H. Khandoker. Quantifying the interactions between maternal and fetal heart rates by transfer entropy. *PLoS one*, 10(12):e0145672, 2015.

[100] L.E. May, R.R. Suminski, A. Berry, M.D. Langaker, and K.M. Gustafson. Maternal physical activity mode and fetal heart outcome. *Early Human Development*, 90(7):365–369, 2014.

[101] P. McKnight and J. Najab. Mann-whitney u test. *The Corsini encyclopedia of psychology*, pages 1–1, 2010.

[102] T. McNanley and J. Woods. Placental physiology. Global library of women's medicine (ISSN 1756-2228), 2008.

[103] B. Moody, G. Moody, M. Villaroel, G. D. Clifford, and I. Silva. MIMIC-III Waveform Database (version 1.0). PhysioNet, 2020.

[104] M.M. Mukaka. A guide to appropriate use of correlation coefficient in medical research. *Malawi medical journal*, 24(3):69–71, 2012.

[105] I. Nunes, D. Ayres-de Campos, A. Ugwumadu, P. Amin, P. Banfield, A. Nicoll, S. Cunningham, P. Sousa, C. Costa-Santos, and J. Bernardes. Central fetal monitoring with and without computer analysis. *Obstetrics & Gynecology*, 129(1):83–90, 2017.

[106] American College of Obstetricians, Gynecologists, et al. ACOG Practice Bulletin No. 106: Intrapartum fetal heart rate monitoring: nomenclature, interpretation, and general management principles. *Obstet Gynecol*, 114:192–202, 2009.

[107] L. Omo-Aghoja. Maternal and fetal acid-base chemistry: a major determinant of perinatal outcome. *Annals of medical and health sciences research*, 4(1):8–17, 2014.

[108] S. Oudjemia, A. Zaylaa, J. Charara, and J. Girault. Delta-fuzzy similarity entropy to discriminate healthy from sick fetus. In *2013 2nd International Conference on Advances in Biomedical Engineering*, pages 1–4. IEEE, 2013.

[109] J. Parer, S. Katsuragi, S. Noda, and T. Ikeda. 178: Mechanism of reduction of umbilical arterial metabolic acidemia following application of a standardized rule-based fhr management schema. *American Journal of Obstetrics & Gynecology*, 206(1):S91–S92, 2012.

[110] S.Y. Park and S.S. Kim. An anesthetic experience with cesarean section in a patient with vasovagal syncope – a case report. *Korean Journal of Anesthesiology*, 59(2):130–134, 2010.

[111] S. Patel and S. Sharma. *Respiratory Acidosis*. StatPearls Publishing, Treasure Island (FL), 2021.

[112] S. Pincus. Approximate entropy (ApEn) as a complexity measure. *Chaos*, 5(1):110–117, 1995.

[113] S. Pincus and B.H. Singer. Randomness and degrees of irregularity. *Proceedings of the National Academy of Sciences*, 93(5):2083–2088, 1996.

[114] S.M. Pincus. Approximate entropy as a measure of system complexity. *Proceedings of the National Academy of Sciences*, 88(6):2297–2301, 1991.

[115] S.M. Pincus. Approximate entropy as a measure of irregularity for psychiatric serial metrics. *Bipolar disorders*, 8(5p1):430–440, 2006.

[116] S.M. Pincus, T. Mulligan, A. Iranmanesh, S. Gheorghiu, M. Godschalk, and J.D. Veldhuis. Older males secrete luteinizing hormone and testosterone more irregularly, and jointly more asynchronously, than younger males. *Proceedings of the National Academy of Sciences*, 93(24):14100–14105, 1996.

[117] S.M. Pincus and R.R. Viscarello. Approximate entropy: a regularity measure for fetal heart rate analysis. *Obstetrics and Gynecology*, 79(2):249–255, 1992.

[118] H. Pinto, R. Pernice, M.E. Silva, M. Javorka, L. Faes, and A.P. Rocha. Multiscale partial information decomposition of dynamic processes with short and long-range correlations: Theory and application to cardiovascular control. *Physiological Measurement*, 43(8):1440–1444, 2022.

[119] P. Pinto, J. Bernardes, C. Costa-Santos, C. Amorim-Costa, M. Silva, and D. Ayres-de Campos. Development and evaluation of an algorithm for computer analysis of maternal heart rate during labor. *Computers in biology and medicine*, 49:30–35, 2014.

[120] P. Pinto, C. Costa-Santos, D. Ayres-de Campos, and J. Bernardes. Computer analysis of maternal–fetal heart rate recordings during labor in relation with maternal–fetal attachment and prediction of newborn acidemia. *Journal of Maternal-Fetal and Neonatal Medicine*, 29(9):1440–1444, 2016.

[121] P. Pinto, C. Costa-Santos, H. Gonçalves, D. Ayres-De-Campos, and J. Bernardes. Improvements in fetal heart rate analysis by the removal of maternal-fetal heart rate ambiguities. *BMC pregnancy and childbirth*, 15(1):1–7, 2015.

[122] A. Porta, G. Baselli, D. Liberati, N. Montano, C. Cogliati, T. Gnecchi-Ruscone, A. Malliani, and S. Cerutti. Measuring regularity by means of a corrected conditional entropy in sympathetic outflow. *Biological cybernetics*, 78:71–78, 1998.

[123] A. Porta, L. Faes, A. Marchi, V. Bari, B. De Maria, S. Guzzetti, R. Colombo, and F. Raimondi. Disentangling cardiovascular control mechanisms during head-down tilt via joint transfer entropy and self-entropy decompositions. *Frontiers in Physiology*, 6:301, 2015.

[124] A. Porta, L. Faes, G. Nollo, V. Bari, A. Marchi, B. De Maria, A.C.M. Takahashi, and A.M. Catai. Conditional self-entropy and conditional joint transfer entropy in heart period variability during graded postural challenge. *PLoS One*, 10(7):e0132851, 2015.

[125] A. Porta, T. Gnecchi-Ruscone, E. Tobaldini, S. Guzzetti, R. Furlan, and N. Montano. Progressive decrease of heart period variability entropy-based complexity during graded head-up tilt. *Journal of applied physiology*, 103(4):1143–1149, 2007.

[126] A. Porta, S. Guzzetti, N. Montano, R. Furlan, M. Pagani, A. Malliani, and S. Cerutti. Entropy, entropy rate, and pattern classification as tools to typify complexity in short heart period variability series. *IEEE Transactions on Biomedical Engineering*, 48(11):1282–1291, 2001.

[127] A. Porta, E. Tobaldini, N. Montano, and T. Gnecchi-Ruscone. The strength of qt-rr coupling decreases during graded head-up tilt. In *2007 29th Annual International Conference of the IEEE Engineering in Medicine and Biology Society*, pages 5958–5961, Lyon, France, 2007. IEEE.

[128] A. Puertas, M. Navarro, P. Velasco, F. Montoya, and J.A. Miranda. Intrapartum fetal pulse oximetry and fetal heart rate decelerations. *International Journal of Gynecology & Obstetrics*, 85(1):12–17, 2004.

[129] I. Ramírez-Parietti, J.E. Contreras-Reyes, and B.J. Idrovo-Aguirre. Cross-sample entropy estimation for time series analysis: a nonparametric approach. *Nonlinear Dynamics*, 105(3):2485–2508, 2021.

[130] A. Rashkovska and V. Avbelj. Abdominal fetal ECG measured with differential ECG sensor. In *2017 40th International Convention on Information and Communication Technology, Electronics and Microelectronics (MIPRO)*, pages 289–291, Opatija, Croatia, 2017. IEEE.

[131] K.M. Rathbun and J.P. Hildebrand. *Placenta Abnormalities*. StatPearls Publishing, Treasure Island (FL), 2022.

[132] J.S. Richman and J.R. Moorman. Physiological time-series analysis using approximate entropy and sample entropy. *American Journal of Physiology-Heart and Circulatory Physiology*, 278(6):H2039–H2049, 2000.

[133] M. Rostaghi and H. Azami. Dispersion entropy: A measure for time-series analysis. *IEEE Signal Processing Letters*, 23(5):610–614, 2016.

[134] STAN S31 fetal heart monitor. Service Manual. In *Neoventa Medical*, Sweden, 2005.

[135] M.B. Sampson, N.A. Mudaliar, and A.S. Lele. Fetal heart rate variability: As an indicator of fetal status. *Postgraduate medicine*, 67(5):207–215, 1980.

[136] A. Sancho-Rossignol, Z. Schilliger, M.I. Cordero, S. Rusconi Serpa, M. Epiney, P. Hüppi, F. Ansermet, and D.S. Schechter. The association of maternal exposure to domestic violence during childhood with prenatal attachment, maternal-fetal heart rate, and infant behavioral regulation. *Frontiers in Psychiatry*, 9:358, 2018.

[137] P. Sarkar, S. Lobmaier, B. Fabre, D. González, A. Mueller, M.G. Frasch, M.C. Antonelli, and A. Etemad. Detection of maternal and fetal stress from the electrocardiogram with self-supervised representation learning. *Scientific reports*, 11(1):1–10, 2021.

[138] B.S. Schifrin. Electronic fetal monitoring–prevention or rescue? *Frontiers in pediatrics*, 8:503, 2020.

[139] C.E. Shannon. A mathematical theory of communication. *The Bell system technical journal*, 27(3):379–423, 1948.

[140] W. Shi, P. Shang, and A. Lin. The coupling analysis of stock market indices based on cross-permutation entropy. *Nonlinear Dynamics*, 79(4):2439–2447, 2015.

[141] M.G. Signorini, G. Magenes, S. Cerutti, and D. Arduini. Linear and nonlinear parameters for the analysis of fetal heart rate signal from cardiotocographic recordings. *IEEE Transactions on Biomedical Engineering*, 50(3):365–374, 2003.

[142] R.M. Silver. Implications of the first cesarean: perinatal and future reproductive health and subsequent cesareans, placentation issues, uterine rupture risk, morbidity, and mortality. *Seminars in Perinatology*, 36(5):315–323, 2012.

[143] T. Škorić. Automatic determination of cross-approximate entropy parameters for cardiovascular time series. In *2018 26th Telecommunications Forum (TELFOR)*, pages 1–8, Belgrade, Serbia, 2018. IEEE.

[144] T. Škorić, O. Sarenac, B. Milovanovic, N. Japundzic-Zigon, and D. Bajic. On consistency of cross-approximate entropy in cardiovascular and artificial environments. *Complexity*, 2017, 2017.

[145] P.W. Soothill, K.H. Nicolaides, and S. Campbell. Prenatal asphyxia, hyperlacticaemia, hypoglycaemia, and erythroblastosis in growth retarded fetuses. *Br Med J (Clin Res Ed)*, 294(6579):1051–1053, 1987.

[146] C.Y. Spong. Electronic fetal heart rate monitoring: another look. *Obstetrics & Gynecology*, 112(3):506–507, 2008.

[147] L. Sprik. The role of uterine NK cells in the etiology of preeclampsia. Master's thesis, Faculty of Science and Engineering, University of Groningen, 2016.

[148] T. Stampalija, M. Signaroldi, C. Mastroianni, E. Rosti, V. Signorelli, D. Casati, and E.M. Ferrazzi. Fetal and maternal heart rate confusion during intra-partum monitoring: comparison of trans-abdominal fetal electrocardiogram and doppler telemetry. *The Journal of Maternal-Fetal & Neonatal Medicine*, 25(8):1517–1520, 2012.

[149] M.J. Stout and A.G. Cahill. Electronic fetal monitoring: past, present, and future. *Clinics in Perinatology*, 38(1):127–142, 2011.

[150] G.M. Sullivan and R. Feinn. Using effect size—or why the p value is not enough. *Journal of graduate medical education*, 4(3):279–282, 2012.

[151] C.-K. Sun, C.-C. Liu, W.-M. Liu, H.-T. Wu, R.-M. Huang, and A.-B. Liu. Compatibility of pulse–pulse intervals with R–R intervals in assessing cardiac autonomic function and its relation to risks of atherosclerosis. *Tzu-Chi Medical Journal*, 32(1):41–46, 2020.

[152] E. Taricco, T. Radaelli, G. Rossi, M.S. Nobile de Santis, G.P. Bulfamante, L. Avagliano, and I. Cetin. Effects of gestational diabetes on fetal oxygen and glucose levels in vivo. *BJOG: An International Journal of Obstetrics & Gynaecology*, 116(13):1729–1735, 2009.

[153] M. Thomas and A. Joy. *Elements of information theory*. Wiley-Interscience, 2006.

[154] A. Topalidou, G. Tzagkarakis, and I.M. Healy. Utilising entropy analysis as a method to assess fetal wellbeing by extracting cardiotocography signals: 8332: Cost action birth conference: Lisbon. In *From Birth to Health: Towards sustainable childbirth: COST Action Birth Conference: Lisbon*, 2018.

[155] J.F. Valencia, A. Porta, M. Vallverdu, F. Claria, R. Baranowski, E. Orlowska-Baranowska, and P. Caminal. Refined multiscale entropy: Application to 24-h holter recordings of heart period variability in healthy and aortic stenosis subjects. *IEEE Transactions on Biomedical Engineering*, 56(9):2202–2213, 2009.

[156] R.C. Vannucci. Hypoxic-ischemic encephalopathy. *American journal of perinatology*, 17(03):113–120, 2000.

[157] C. Varon, L. Faes, D. Testelmans, B. Buyse, and S. Van Huffel. Information transfer between respiration and heart rate during sleep apnea. In *2016 Computing in Cardiology Conference (CinC)*, pages 845–848, Vancouver, BC, Canada, 2016. IEEE.

[158] J.R. Vergara and P.A. Estévez. A review of feature selection methods based on mutual information. *Neural computing and applications*, 24:175–186, 2014.

[159] P. Viola and W.M. Wells III. Alignment by maximization of mutual information. *International journal of computer vision*, 24(2):137–154, 1997.

[160] S. Von Steinburg, A. Boulesteix, C. Lederer, S. Grunow, S. Schiermeier, W. Hatzmann, K. Schneider, and M. Daumer. What is the "normal" fetal heart rate? *PeerJ*, 1:e82, 2013.

[161] J. Wang, J. Kim, W. Shao, S. Nam, and S.-C. Hong. Effect of oxytocin injection on fetal heart rate based on multifractal analysis. *Chaos, Solitons & Fractals*, 148:111045, 2021.

[162] Y. Wang and S. Zhao. *Vascular biology of the placenta*. Morgan & Claypool Life Sciences, San Rafael, CA, 2010.

[163] P.A. Warrick and E.F. Hamilton. Mutual information estimates of CTG synchronization. In *2015 Computing in Cardiology Conference (CinC)*, pages 137–139, Nice, France, 2015. IEEE.

[164] W.M. Wells III, P. Viola, H. Atsumi, S. Nakajima, and R. Kikinis. Multi-modal volume registration by maximization of mutual information. *Medical image analysis*, 1(1):35–51, 1996.

[165] K. Wilsterman and Z.A. Cheviron. Fetal growth, high altitude, and evolutionary adaptation: a new perspective. *American Journal of Physiology-Regulatory, Integrative and Comparative Physiology*, 321(3):R279–R294, 2021.

[166] B.J. Wylie and M.E. D'Alton. Fetomaternal hemorrhage. *Obstetrics & Gynecology*, 115(5):1039–1051, 2010.

[167] H.-B. Xie, Y.-P. Zheng, J.-Y. Guo, and X. Chen. Cross-fuzzy entropy: A new method to test pattern synchrony of bivariate time series. *Information Sciences*, 180(9):1715–1724, 2010.

[168] J. Yang, G.I. Choudhary, S. Rahardja, and P. Franti. Classification of interbeat interval time-series using attention entropy. *IEEE Transactions on Affective Computing*, 2020.

[169] L.A. Zadeh. Fuzzy sets. *Information and Control*, 8(3):338–353, 1965.

[170] M. Zanin, L. Zunino, O.A. Rosso, and D. Papo. Permutation entropy and its main biomedical and econophysics applications: A review. *Entropy*, 14(8):1553–1577, 2012.

[171] M.N. Zarmehri, L. Castro, J. Santos, J. Bernardes, A. Costa, and C.C. Santos. On the prediction of foetal acidaemia: a spectral analysis-based approach. *Computers in biology and medicine*, 109:235–241, 2019.

[172] R. Zavala-Yoe, R.A. Ramirez-Mendoza, and L.M. Cordero. Entropy measures to study and model long term simultaneous evolution of children in doose and lennox–gastaut syndromes. *Journal of Integrative Neuroscience*, 15(02):205–221, 2016.